JOURNAL OF THE Electrochemical Society

l. 103, No. 7 July 1956

AS PARTNERS
IN YOUR PROGRESS

OUR EXTENSIVE RESEARCH – is a *plus* factor!

Our extensive program in carbon and graphite research is conducted by highly qualified chemists, physicists and technicians.

The scope of their specialized knowledge is a significant *plus factor* in the reliability that distinguishes GLC electrodes, anodes and mold stock.

The high degree of integration between discoveries in our research laboratories, refinements in processing raw materials and improved manufacturing techniques is further assurance of excellent product performance.

ELECTRODE GLC® DIVISION

Great Lakes Carbon Corporation

GRAPHITE ELECTRODES, ANODES, MOLDS and SPECIALTIES

ADMINISTRATIVE OFFICE: 18 East 48th Street, New York 17, N. Y. PLANTS: Niagara Falls, N. Y., Morganton, N. C. OTHER OFFICES: Niagara Falls, N. Y., Oak Park, Ill., Pittsburgh, Pa. SALES AGENTS: J. B. Hayes Company, Birmingham, Ala., George O. O'Hara, Wilmington, Cal. SALES AGENTS IN OTHER COUNTRIES: Great Northern Carbon & Chemical Co., Ltd., Montreal, Canada; Great Eastern Carbon & Chemical Co., Inc., Chiyoda-Ku, Tokyo, Japan

Journal of the
Electrochemical Society

JULY 1956 VOL. 103 • NO. 7

CONTENTS

Editorial

Technical Papers

Current Affairs

Published monthly by The Electrochemical Society, Inc., Mount Royal and Guilford Aves., Baltimore 2, Md., combining the JOURNAL and TRANSACTIONS OF THE ELECTROCHEMICAL SOCIETY. Editorial offices: 216 West 102nd Street, New York 25, N. Y. Statements and opinions given in articles and papers in the JOURNAL OF THE ELECTROCHEMICAL SOCIETY are those of the contributors, and The Electrochemical Society assumes no responsibility for them. Nondeductible subscription to members $5.00; subscription to nonmembers $18.00. Single copies $1.25 to members, $1.75 to nonmembers. Entered as second-class matter November 15, 1947, at the Post Office at Baltimore, Md., under the act of August 24, 1912.

RAPID GERMANIUM RECTIFIERS

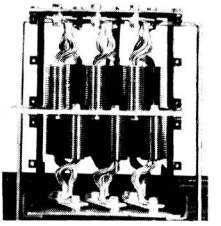

Hermetically Sealed Germanium Junctions

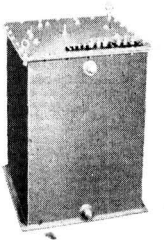

Oil Immersed, Motorized Continuously-Variable Inductor Control

THE *NEWEST* AND THE *ULTIMATE* IN PLATING POWER

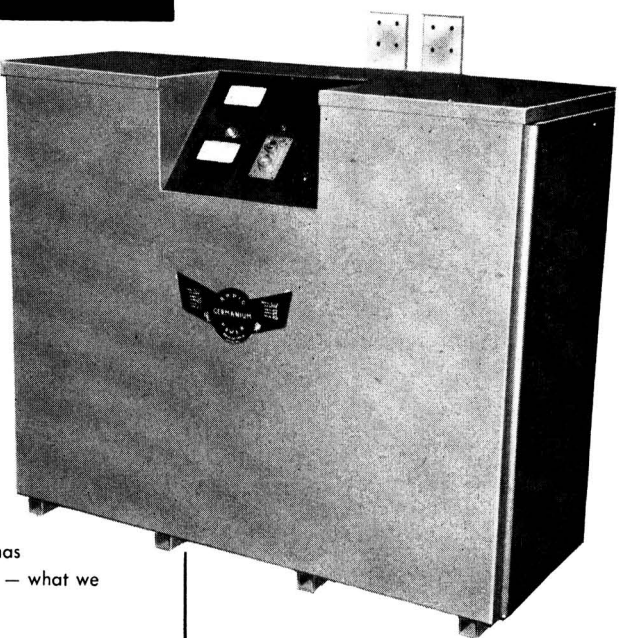

In keeping with our policy of continually supplying the plating industry with the ultimate in D.C. Plating Power, our research department has developed a series of GERMANIUM RECTIFIERS — what we believe to be the ultimate in Plating Power.

EFFICIENCY — 95% at full load.

VOLTAGE STABILIZATION — ± 1 volt from no load to full load.

COMPACT — require much less space than conventional units.

SEALED UNIT — corrosion is kept out.

LONG-LIVED — no aging or change in characteristics even after accelerated full load tests.

RAPID GERMANIUM RECTIFIERS are the power supplies of tomorrow—here today. Write for full details to Rapid Electric Co., 2881 Middletown Road, New York 61, N. Y. Ask for Bulletin G-1.

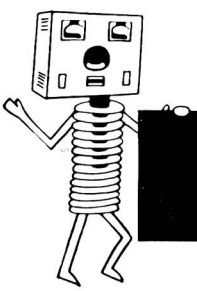

THE NAME THAT MEANS *"More Power to You!"*

RAPID ELECTRIC COMPANY

STACKPOLE
treated ANODES
stretch dollars

Nine times out of 10, Stackpole treated graphite anodes for chlorine cells result in a material cost saving by comparison with untreated anodes. They are priced a little higher—but they last a lot longer.

A test offers convincing proof of their greater efficiency in helping you get the most for your anode dollars.

Sizes and shapes available for all cells.

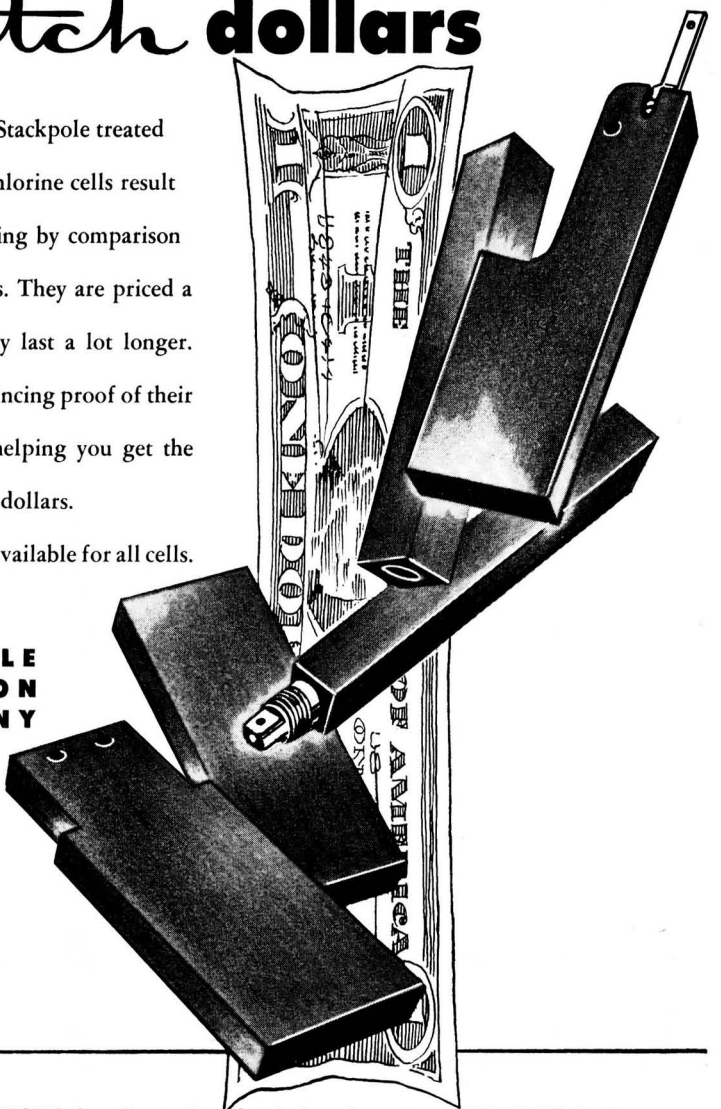

STACKPOLE CARBON COMPANY
St. Marys, Pa.

BRUSHES for all rotating electrical equipment • CONTACTS (carbon-graphite and metal powder types) • TUBE ANODES • CATHODIC PROTECTION ANODES • VOLTAGE REGULATOR DISCS • WATER HEATER and PASTEURIZATION ELECTRODES • BEARINGS • WELDING CARBONS MOLDS and DIES • SPECTROGRAPHITE • POROUS CARBON • SALT BATH RECTIFICATION RODS • SEAL RINGS • FRICTION SEGMENTS CLUTCH RINGS • ELECTRIC FURNACE HEATING ELEMENTS • PUMP VANES . . . and many others.

Transistorized telephone summons you with a musical tone

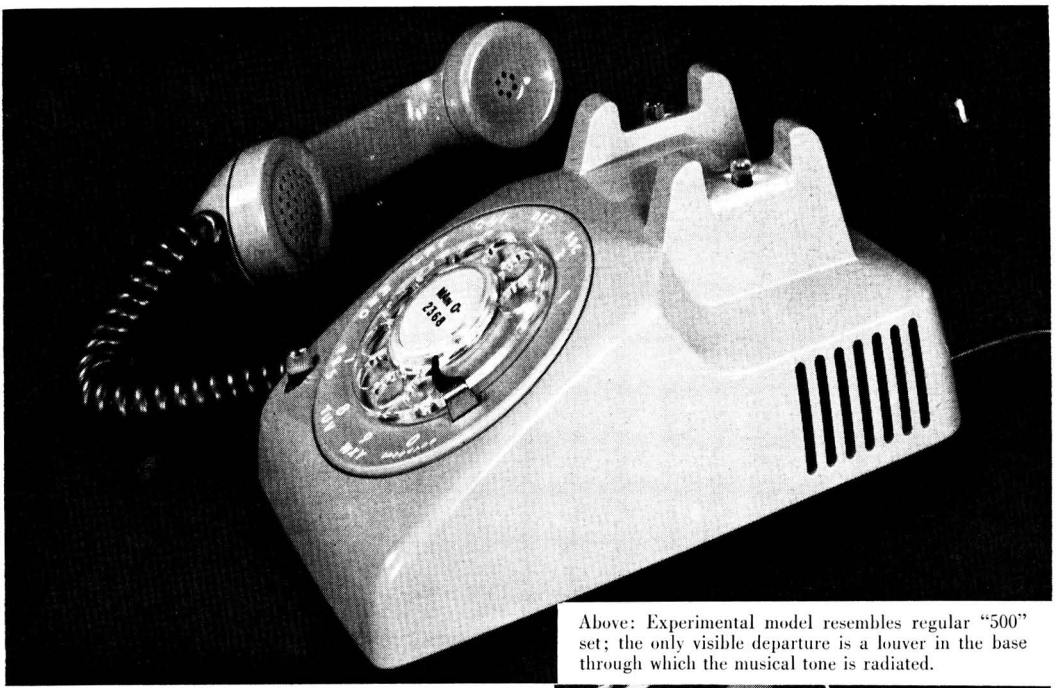

Above: Experimental model resembles regular "500" set; the only visible departure is a louver in the base through which the musical tone is radiated.

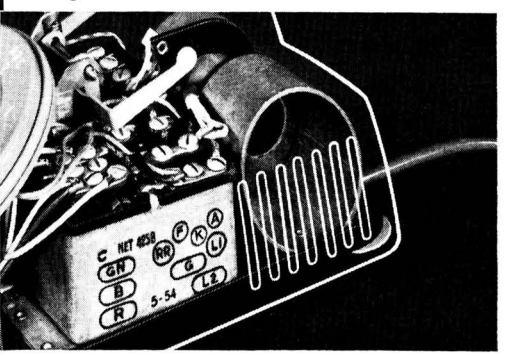

Bell scientists have developed a new musical tone device which may some day replace the telephone bell, if it meets technical standards and customers' approvals.

Because the musical tone equipment uses transistors, the tones will be transmitted with the same amount of power required to transmit a telephone conversation — considerably less than is needed to make a telephone bell ring.

The experimental telephone sets resemble the current "500" sets; the only external difference is a louver at the side of the base through which the tone is radiated by a small loudspeaker mounted inside the telephone's base.

Tests have shown that the musical tone can be heard at great distances. It stands out above general room noise and can be distinguished from such sounds as ringing of doorbells, alarm clocks, and home fire alarms.

This new low-power signaling technique is expected to play an important part in the electronic switching system now under development at Bell Laboratories.

Above: Bell ringer has been displaced by a small loudspeaker in transistorized telephone. Left: L. A. Meacham heads the team of engineers that developed the musical tone ringer. Mr. Meacham holds a B.S. in Electrical Engineering from the University of Washington. Class of '29. He became affiliated with Bell Labs a year after his graduation. In 1939 Mr. Meacham won the "Outstanding Young Electrical Engineer" award of Eta Kappa Nu.

BELL TELEPHONE LABORATORIES

World center of communications research and development

The Scientific Manpower Shortage

UNPRECEDENTED INDUSTRIAL DEVELOPMENTS and the defense and atomic energy programs have created an insatiable demand for graduating physicists, chemists, metallurgists, and engineers, while the lowered birth rate in the early 1930's and the attractive wages of today have decreased the number of students in advanced courses. News item: one school had 40 graduates, requests from 400 firms to interview them.

Many companies will have to do without the trained personnel they want and are prepared to pay for. For the present they must manage with temporary expedients. But, as long-range policy, it seems imperative to get more students into college science courses, and to keep the capable ones there for advanced degrees. Numerous plans are afoot to encourage the teaching of science from the high school up, and industries which need scientists are much concerned.

As mentioned in this space last month, many prospective graduate students must have financial support or paying positions if they are to continue. Teaching and research assistantships are the logical source of their income. Now the fact is that most universities are offering their teaching assistants a salary with less purchasing power than they could offer 30 years ago. Further, in those days, outside opportunities were not so plentiful or remunerative as now. In the early 1930's, a teaching assistantship literally kept a young man from starving. Today it may keep him back, financially, for a dozen years.

School assistantships have traditionally been regarded much as aids to the needy, with no necessity for anything above a subsistence level. The universities, never noted for their financial resources, have been pleased to have a low-paid staff for much of their routine teaching. In these times of national prosperity and also of national need, such attitudes should be reexamined. If the science student could anticipate a more normal financial existence while in graduate school, the advanced degree would become more popular. Also, those capable students who decide that the benefits of a Ph.D. are too remote might take a second look at the catalogue.

How can industry be of most assistance? Well, if 400 firms can descend on one school for its graduates, it seems reasonable that a much larger number of companies might form a nation-wide organization for the support of science in the colleges and universities. Such an effort should not be small-scale or niggardly. It is not a matter of a fund with a thousand small contributions, but a matter of convincing the entire scientific industry that it must invest a sizeable portion of each year's income as insurance for its own well-being and that of the nation.

While research assistantships and fellowships are highly desirable, especially when accompanied by grants to cover expenses other than salaries, a comprehensive program must not neglect the teaching aspect. The universities *must* be able to attract the best college graduates for their teaching staffs, and not just from their own localities, but from all over the country. They *must* offer the advantage of excellent graduate programs, including the opportunity to do quite independent basic research, not tied in any way to proposals, government contracts, or possible industrial application.

Finally, the professor must not be forgotten, with his salary in many cases little, if any, more than that of his graduating Ph.D. student.

—CVK

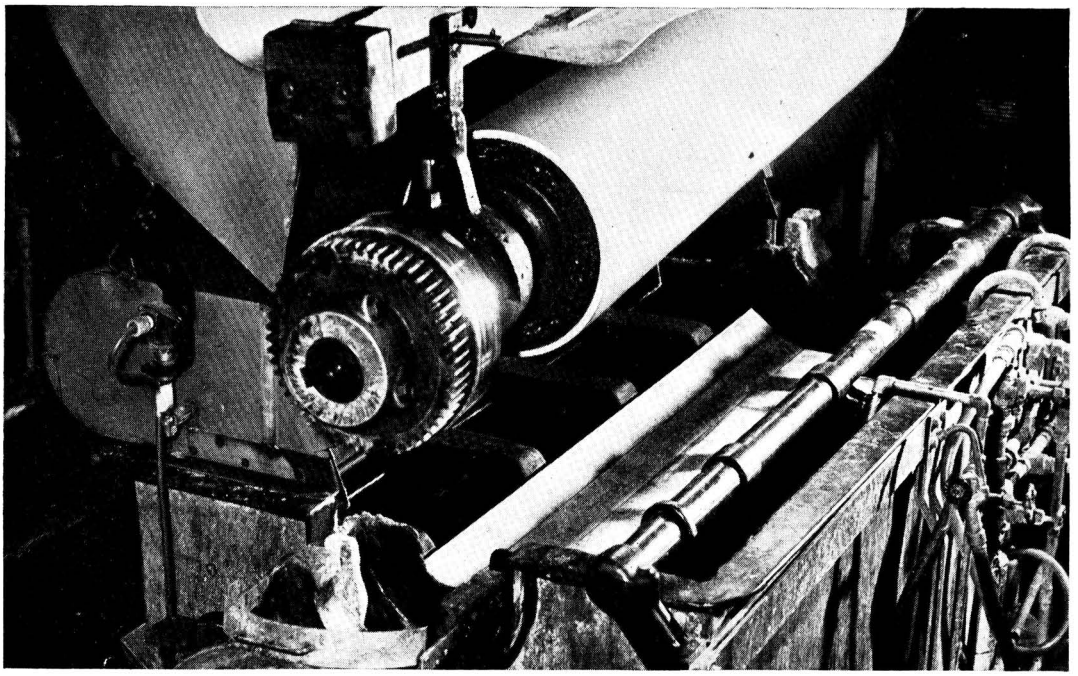

View of plating tank, drained to show location of the 67″ x 3″ x 1″ "Plus-4" Anodes.

Electroplating copper shells on rotogravure cylinders is simpler and faster with "Plus-4" Anodes

Triangle Publications, Inc., has an enviable reputation for high-quality 4-color gravure reproduction at high speed. Here are three of its leading magazines.

TRIANGLE PUBLICATIONS, INC., Philadelphia, made comparative tests, for a 22-month period, of "Plus-4" (Phosphorized Copper) Anodes in the electroplating of rotogravure cylinders.

The results were summarized by the Director of Triangle Publications' Research and Development Laboratories: "'Plus-4' Anodes give an improved copper printing surface with substantial savings in time, labor, and material—and our men like to use them."

Plating procedure: 1500-lb. steel rotogravure cylinders, 67″ long and 43″ in circumference, are cyanide-copperplated .0005″—then acid-copperplated .040″ to .080″. This surface is ground and polished and coated with immersion nickel. A .005″ copper Ballard shell is acid-plated over the nickel—the shell which is engraved and forms the printing surface. The nickel layer makes it possible to strip the outer shell off after printing. Another shell is then plated on the cylinder for the next job. The dense physical quality of the unchromed copper Ballard shell makes it possible to print 1,250,000 impressions from a single set of design cylinders.

For electroplating, the cylinders are placed horizontally in the acid-copper-plating solution ⅓ submerged, and rotated. The anodes lie parallel to the cylinder, 1½″ to 2″ away. Current density is 280 to 300 amps per sq. ft.

Solution balance: With other anodes, solution balancing to remove copper sulfate and add acid is necessary 20 to 22 times a year. With "Plus-4" Anodes, the solution has been balanced only 4 to 6 times a year. This not only made substantial savings in copper sulfate and acid, time, and labor—but also gave improved control of the plating process by minimizing cyclic changes in the solution.

Anode corrosion: When anodes corrode faster in length than width, low areas develop at the ends of the roll—and anodes must be scrapped. Scrap loss with other anodes has run 8 to 10%. "Plus-4" Anodes corrode so uniformly, however, that scrap was only 1 to 2%. They produce uniform deposits with less attention and checking.

Cathode deposit: With "Plus-4" Anodes the sharp reduction of copper lost as sludge and in copper sulfate dumped accounted for a 12 to 14% increase in cathode deposit.

See for yourself: Across the entire field of acid-copper electroplating—"Plus-4" Anodes are saving money, making work easier. Write today for details of how you can get a test supply of "Plus-4" Anodes sufficient to fill one tank. Address: The American Brass Company, Waterbury 20, Connecticut. In Canada: Anaconda American Brass Ltd., New Toronto, Ont. 56140

"PLUS-4" ANODES
(Phosphorized Copper)
an
ANACONDA®
product
made by
THE AMERICAN BRASS COMPANY
For use in Patent No. 2,689,216

The Nature of the Film Formed on Copper during Electropolishing

E. C. Williams and Marjorie A. Barrett

Metals Division Research Department, Imperial Chemical Industries Ltd., Kynoch Works, Birmingham, England

ABSTRACT

The thin film shown by Hoar and Farthing to exist on the surface of copper during electropolishing in orthophosphoric acid has been found, by electron diffraction methods, to be composed of a phosphate of copper. This evidence would appear to confirm the basic assumption of Elmore's theory of electropolishing of a limit to the solubility of copper in the boundary layer of electrolyte. Since the film is soluble in phosphoric acid in the absence of an applied potential, this limit is attributed to a decrease in hydrogen ion concentration at the anode surface during polishing.

Introduction

Elmore's theory (1) of the electropolishing of copper in aqueous solutions of orthophosphoric acid rests on the basic assumption that there is a limit to the solubility of the phosphate of the metal in this acid. The theory then develops with the argument that, because of this limit, concentration of copper ions in the electrolyte at the anode surface increases with current density up to a maximum value. Dissolution continues beyond this point only to the extent allowed by diffusion of copper ions into the bulk of the electrolyte from the boundary layer, and the rate of such diffusion is greatest at those parts of the surface where there are asperities and where the local current density is highest. Investigations by Edwards (2) have confirmed that the polishing, or smoothing action of anodic dissolution involves a diffusion control mechanism. Edwards, however, objects to Elmore's basic assumption for the reason, among others, that there is no well-defined limit to the amount of copper that can be dissolved anodically in phosphoric acid; he considers that solubility is governed by the availability of phosphate ions to accept the metal into solution in the form of an unspecified complex. According to this hypothesis the diffusion control mechanism refers to the migration of phosphate ions toward the anode rather than of copper ions in the opposite direction.

The purpose of the present communication is to report the identification by electron diffraction of a film of copper phosphate on the surface of electropolished copper, and to adduce it as evidence in favor of Elmore's theory. The existence of a thin, solid film on the surface of copper as it is being electropolished, and the subsequent disappearance of the film on switching off the current while a specimen is left immersed in the acid has been inferred by Hoar and Farthing (3) from the results of their mercury-drop experiment.

Jacquet and Jean (4) have evidence that copper surfaces after electropolishing in orthophosphoric acid are contaminated by traces of a compound containing phosphorus. Allen (5) examined electropolished copper surfaces by means of the cathodic reduction method and concluded that freshly prepared surfaces washed in distilled water and ethyl alcohol were contaminated with a substance which was not cuprous oxide and which he suggested was a phosphate. He found no evidence of contamination when specimens were washed in a 10% solution of orthophosphoric acid in water. Batashev and Nikitin (6) determined the composition of the electrolyte at different stages of electropolishing of copper in orthophosphoric acid, their results indicating the occurrence of secondary and tertiary phosphates of copper in solution.

Experimental Procedure

Small, rectangular-shaped specimens, approximately 2 cm x 3 cm and 3 mm thick, of annealed, oxygen-free, high-conductivity copper were prepared by mechanical polishing of one face, followed by preliminary electropolishing to remove the distorted and abrasive-contaminated surface layer. The apparatus for electropolishing consisted of two plates of copper approximately 3 cm^2, held horizontally and parallel to each other at a 3.5 cm distance apart and suspended by stiff copper wire from terminals in an insulating base, which rested on the rim of a 500 cc beaker containing the electrolyte. This arrangement permitted rapid withdrawal of the specimen, resting on the lower of the two plates, from the electrolyte. A 50% by-volume solution of orthophosphoric acid in water was used as electrolyte without agitation. Fresh solution was made up for each specimen and cooled to room temperature before use.

The current-voltage characteristic of the cell described above, given in Fig. 1, was determined with a previously electropolished specimen of copper as the anode by raising the voltage across the cell in steps and noting the steady value of the current at each step. Over a small range of voltage, indicated by the shaded region in Fig. 1, oscillations of current and voltage occurred. It is of interest to note that this graph was reproducible for previously electropolished specimens but not for specimens which had been abraded or mechanically polished.

Specimens were polished at various voltages for a standard time of 15 min. At the end of this period, the electrode assembly was quickly raised from the electrolyte and the specimen immediately washed by directing a jet of water from a wash-bottle on to its polished surface. The object of this immediate washing was to prevent any

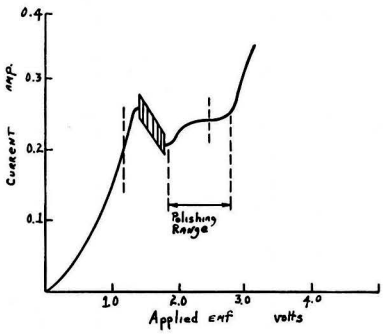

FIG. 1. Current-voltage characteristics of the cell used for electropolishing copper.

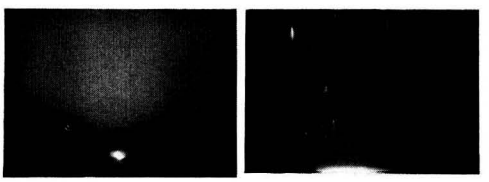

FIG. 2. (*left*) Diffuse scattering pattern from copper electropolished and immediately washed with water.

FIG. 3. (*right*) As Fig. 2, but specimen immersed in fresh solution of orthophosphoric acid after initial washing with water.

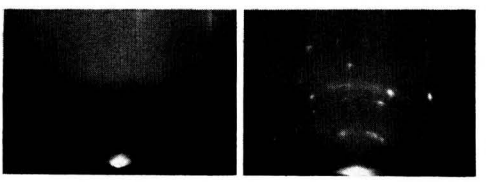

FIG. 4. (*left*) Pattern of cupric phosphate from water-washed specimen after heating to 450°C in vacuo.

FIG. 5. (*right*) Modified pattern of cupric phosphate from specimen washed with white spirits after heating to 900°C in vacuo.

change in surface condition through contact with the electrolyte in the absence of an applied voltage. In later experiments various organic liquids were tried as washing agents. All specimens were given a final washing in water and then rinsed, successively, in ethyl alcohol and acetone. Each specimen was mounted on the stage of an electron diffraction instrument while still wet with acetone, and in this way appreciable oxidation of the metal surface through exposure to the atmosphere was avoided.

RESULTS

Primary Observations

After electropolishing at all voltages in the polishing range, Fig. 1, and immediate washing with water, the surface was covered with an amorphous film as indicated by diffuse scattering of electrons, Fig. 2. Solubility of the film in phosphoric acid in the absence of an applied voltage is indicated by the pattern of Fig. 3 which refers to a specimen which was electropolished, immediately washed with water, and then immersed in a fresh solution of phosphoric acid for 1 min before final washing and drying. Reflections by individual crystals of copper are clearly visible in this pattern. In the case of diffraction by a surface on which there are numerous small and sharp asperities, such reflections appear as rounded spots, but they are elongated into vertical streaks in Fig. 3 because of the smoothness of the electropolished surface and the consequent restriction on the penetration of the diffracting crystals by the incident beam.

It is sometimes possible to crystallize amorphous substances by heating; this method was applied in the present instance in order to identify the film. A specimen which had been electropolished at point A of Fig. 1 and immediately washed with water was mounted on a hot stage so that it could be heated in the vacuum of the electron diffraction instrument. The temperature of the specimen was raised gradually, and the diffraction pattern kept under continuous observation. At 450°C a pattern of well-defined rings appeared, Fig. 4. The corresponding lattice spacings are in good agreement with those of cupric phosphate filed in the A.S.T.M. x-ray diffraction index. Lattice spacings and relative intensities are compared in Table I. The A.S.T.M. index attaches no formula to this pattern which differs in many respects from patterns for various basic and hydrated forms of cupric phosphate, e.g., $Cu_3(PO_4)_2 \cdot 3H_2O$.

In Fig. 4 there is evidence of diffraction by the underlying metal in the form of a few streaks similar to those in Fig. 3. No such streaks were observed for any specimen having an amorphous film which can be assumed, therefore, to have been of sufficient thickness to obscure the metal from the incident beam. The fact that diffraction was observed after crystallization but not before may be explained by granulation of the film, the metal being exposed in between the granules.

Since the amorphous film prevents diffraction by the metal, its thickness lies in a range with a lower limit of the order of 30Å. This figure is deduced from the glancing angle of the incident beam to the surface, which was approximately 0.5°, on the assumption that the surface is perfectly plane and smooth and that the thickness of film penetrated by a 50 kv electron beam without appreciable loss of energy through inelastic scattering is 1,000 Å. There are no means of estimating the upper limit which, however, must be below about 250 Å because, at this value, some effect on the optical reflectivity of the surface would be visible.

Further Experiments

The above results can be considered as establishing the structure and identity of a film on the surface of copper during electropolishing only if the assumption is correct that washing a specimen with water immediately on removal from the electrolyte preserves the surface condition unchanged. Doubt was cast on the validity of this assumption when it was observed that some specimens were stained with a bluish-white substance after washing and these also gave the halo diffraction pattern of Fig. 2.

TABLE I. *Comparison of diffraction data*

Cupric phosphate A.S.T.M. Card 1-0897		Water-washed specimen heated to 500°C		White spirits-washed specimen heated to 900°C		Unidentified pattern from etched specimen	
d, Å	*I/I*1	*d*, Å	*I/I*1	*d*, Å	*I/I*1	*d*, Å	*I/I*1
4.15	32	4.20	w	4.17	m		
3.76	32	3.90	vw			3.72	w
3.10	32	3.16	s	3.16	s	3.24	s
2.96	100	2.95	ms				
2.80	70						
2.69	8					2.72	s
2.58	60	2.56	ms	2.59	w		
2.42	40						
2.18	16	2.19	ms			2.29	s
2.06	32	2.09	mw				
1.98	24	1.91	mw	1.91	s	1.94	s
1.82	20	1.83	w			1.90	w
1.74	4	1.72	w			1.75	vw
1.69	8	1.67	w			1.71	m
1.65	16						
1.62	4	1.59	mw	1.62	s	1.62	mw
1.59	8	1.56	mw	1.58	m		
1.46	32	1.45	w			1.47	vw
1.44	32						
1.40	16	1.36	w	1.36	w	1.41	vw
1.31	8	1.30	w			1.30	w
1.25	4	1.24	w	1.23	m		
1.18	4	1.17	vw	1.18		1.20	vw
1.15	4	1.10	vw	1.10	m		
1.12	4	1.07	vw	1.04	w	1.09	w

Note: w = weak, m = medium, s = strong, mw = medium to weak, ms = medium to strong, vw = very weak.

Although it was found that staining could always be avoided by washing away the electrolyte adhering to the surface as rapidly as possible, the amorphous film on unstained specimens might still have been formed as a result of subsequent processes and not at all during electropolishing. In order to resolve this uncertainty ethyl alcohol, acetone, and white spirits or mineral spirits (a light petroleum distillate) were substituted for water in the initial washing.

Washing in either alcohol or acetone caused precipitation of a flocculent bluish-white substance in the liquid adhering to and running off the specimen, as well as pronounced staining of the surface. On washing with white spirits no precipitation or staining occurred, but the surface was covered with the amorphous film. This precipitate was probably copper phosphate of which the trihydrate, at least, is known to be insoluble in water and in alcohol. Precipitation on washing with alcohol or acetone is explained by the fact that these two liquids are only partially miscible with water, and on admixture with an aqueous solution have the effect of throwing out of solution any substance which they do not themselves dissolve. Washing with water can have the same effect, although in this case there is ultimately complete miscibility, because it is unlikely that the highly viscous layer of phosphoric acid with copper in solution will be uniformly and instantaneously diluted, and the condition of partial miscibility will obtain initially. White spirits is completely immiscible with water and it is therefore a justifiable assumption that its use for removing the residual electrolyte involves no danger of precipitation.

The experiment of heating on the electron diffraction hot stage in order to crystallize the amorphous film was repeated for a specimen washed with white spirits. The film did not crystallize at 750°C which was the highest temperature that could be attained on the hot stage. A similar specimen maintained for half an hour at 900°C in an evacuated silica tube gave the diffraction pattern of Fig. 5. This differs from the pattern of Fig. 4 as the comparison in Table I indicates, in that some reflections are absent, probably as a result of preferred orientation which is also manifest in the intensification of parts of some of the rings that are visible. There are also spots lying on the rings, some sharp and others diffuse, and arranged in horizontal rows in the manner of cross-grating patterns obtained with single crystals, and they are therefore probably due to one particularly large crystallite. A similar diffraction pattern was obtained by heating water-washed specimens to 900°C *in vacuo*.

These observations constitute strong evidence that the film first shown by Hoar and Farthing (3) to exist on the surface of copper during electropolishing in phosphoric acid is amorphous, and composed of a phosphate of copper. There is the possibility that the film initially consisted of some other substance, an oxide for example, which was transformed to phosphate when the specimen was removed from the solution. The experiments of Batashev and Nikiten (6) indicate, however, that the ultimate product of the anodic reaction, which they found by analysis of the solution, is copper phosphate $Cu(PO_4)_2$. The secondary phosphate $CuHPO_4$ is formed in the first 200 sec of electrolysis and is then converted to the tertiary phosphate. The appearance of this salt in solid form is therefore probable, if conditions are such that its solubility is limited. These conditions are considered later.

The difference between the temperatures of crystallization of films on specimens washed with water and white spirits remains to be explained. It is reasonable to suppose that washing with water, although not necessarily producing a visible stain on a specimen, results in slight precipitation of phosphate onto an existing amorphous film and the precipitated particles might well act as crystallization nuclei and thus lower the temperature for crystallizing the underlying amorphous material. There is possible evidence of such a microcrystalline deposit in two very faint but sharp diffraction rings superimposed on the diffuse scattering pattern of Fig. 2.

Secondary Observations

In the course of this investigation the surface condition of copper after anodic treatment in phosphoric acid at voltages below the polishing range was examined by the methods described above. The results are included here mainly as a matter of interest and for the sake of the record. At lower voltages, such as point B in Fig. 1, etching occurred and specimens gave a diffraction pattern, also recorded in Table I, which could not be identified. Diffraction rings were fairly sharp and of a width commensurate with a crystal size of at least 100 Å linear dimension, but

the substance was not considered to be in the form of a continuous film covering the surface because diffraction rings due to the metal were clearly visible for all specimens. The same diffraction pattern was obtained with specimens of copper which had been etched in a 50% by volume solution of nitric acid in water and also with specimens which had been brightened in a mixture of nitric and sulfuric acids and water in the volume ratios 6:3:1. It would appear, therefore, that the formation of this substance is not dependent on the presence of any particular anion, and it may be a hitherto unrecognized basic oxide of copper.

A common occurrence in electropolishing copper is the formation during the first few minutes of a visible, dark film which soon becomes detached and floats away leaving the surface bright. It is then slowly dissolved by the acid. In the present investigation it was observed that the film was formed on abraded or mechanically polished specimens, but never on those which had been previously electropolished. The nature of this film has never been made clear and in the practice of electropolishing it seems to be regarded as an agglomeration of oxide particles and detritus in the worked surface layer of the metal released by anodic dissolution. A transmission diffraction pattern of a piece of this film was identical with the A.S.T.M. pattern of cupric phosphate recorded in Table I, and it is suggested that the film is formed under the same conditions as are necessary to the formation of the invisible, amorphous film.

Discussion

The results of this investigation support Elmore's theory of electropolishing, since the presence of a film of phosphate on the anode under the correct conditions of current density for polishing indicates that there must be a limit to the amount of copper that can be taken into solution in the vicinity of the anode. A possible explanation of this limit is suggested by the observation that the film is soluble in phosphoric acid in the absence of an applied voltage. Edwards (2) has, in fact, mentioned that variations in the hydrogen ion concentration of the anolyte with current density may be a factor in polishing, and it can be concluded that a decrease in hydrogen ion concentration at the anode surface to a critical value corresponding to the minimum current density for polishing is responsible for limiting the solubility of copper phosphate.

Once this condition is established, the salt appears as a solid film which, however, does not continue to increase appreciably in thickness except in the case of abraded or mechanically polished specimens and then only in the initial stages, after which the bulk of it floats away leaving an invisible film. This fact suggests that a dynamic equilibrium is set up at the outer boundary of the film between the rate of diffusion of copper ions into the electrolyte, which is governed, as in Elmore's theory, by local variations in current density and the geometric form of the surface, and the rate of arrival of ions through the film from the metal. The crystalline film of phosphate formed initially on mechanically polished copper probably owes its much greater thickness to a slower rate of dissolution in the acid, but no reasons can be suggested for this difference. It may be related to the observed difference in structural state.

The acceptor hypothesis of Edwards has been adopted by Wagner (7) as the basis of a theoretical analysis of the diffusion-control mechanism. Wagner has rejected Elmore's postulate of a solubility limit to the salt of the metal because the wide variation in anode potential at constant current density is not compatible with a constant concentration of metal ions at the anode. This objection cannot be raised if, as is now apparent, the surface is covered with a layer of salt which is probably variable as regards thickness and conductivity. Wagner's analysis is, however, applicable to diffusion of copper ions away from the boundary layer of electrolyte because his particular solution to the general diffusion equation, when the sign of the entire expression is changed from + to − and when a constant is added, satisfies the boundary condition implicit in Elmore's theory equally well. The resulting expression for the concentration gradient normal to the surface is unchanged except in sign, which accords with diffusion of cations rather than of negative "acceptor" ions.

Hoar and Mowatt (8) have suggested that solid films formed on metal anodes cause dissolution of the metal to be uniform over the surface, and to be independent of variations in free energy due to anisotropy and structural discontinuities, because paths for diffusion of ions through the films are randomly distributed. Whereas it may well be true that the mobility of a cation in the film is independent of its original location in the structure of the metal, the present authors consider, in view of the weight of supporting evidence obtained by both Elmore and Edwards, that smoothing of the surface is primarily the result of a diffusion control mechanism operating in the boundary layer of electrolyte. Formation of a film, at least on copper in phosphoric acid, should be regarded as a subsidiary phenomenon which merely signifies the attainment of a solubility limit.

Manuscript received September 7, 1955.
Any discussion of this paper will appear in a Discussion Section to be published in the June 1957 Journal.

REFERENCES

1. W. C. Elmore, *J. Appl. Phys.*, **10**, 724 (1939).
2. J. Edwards, *This Journal*, **100**, 189*C*, 223*C* (1953).
3. T. P. Hoar and T. W. Farthing, *Nature*, **169**, 324 (1952).
4. P. A. Jacquet and M. Jean, *Compt. rend.* **230**, 1862 (1950); *Rev. Met.*, **48**, 537 (1951).
5. J. A. Allen, *Trans. Faraday Soc.*, **48**, 273 (1952).
6. K. P. Batashev and E. N. Nikitin, *Zhur. Priklad. Khim.*, **23**, 263 (1950).
7. C. Wagner, *This Journal*, **101**, 225 (1954).
8. T. P. Hoar and J. A. S. Mowatt, *Nature*, **165**, 64 (1950).

High Temperature Scaling of Nickel-Manganese Alloys

E. B. Evans, C. A. Phalnikar, and W. M. Baldwin, Jr.

Department of Metallurgical Engineering, Case Institute of Technology, Cleveland, Ohio

ABSTRACT

Scaling rates and scale compositions of nickel-manganese alloys were determined. All the alloys scaled according to the parabolic rate law between 600° and 1000°C. At any given temperature the scaling rate increased at low manganese concentrations, then levelled off at intermediate concentrations, approaching the scaling rate of manganese as the upper limit.

Both an external scale and a subscale were found after scaling, the scale composition being a function of alloy composition and temperature. Above a critical concentration of manganese (15% at 600°C to 60% at 1000°C), the external scale consisted exclusively of manganese oxides; the subscale was MnO. Below this critical concentration, complex external scales consisting of the oxides of both nickel and manganese were found along with subscales of either NiO or a solid solution of the monoxides (MnO + NiO). The spinel oxide ($NiO \cdot Mn_2O_3$) found in most of the complex scales was not associated with improved oxidation resistance. Schematic isothermal sections of the deduced Ni-Mn-O phase diagram were applied as an aid in interpreting the scaling behavior. It is concluded that none of the current theories of scaling of alloys describes the present case.

Scaling Behavior of Nickel

A summary of the crystal structures of nickel and its oxides and nitrides is given in Table I. The nickel-oxygen phase diagram is available (1).

Nickel oxidizes according to the parabolic rate law in the temperature range 600°–1200°C. Scaling constants reported by numerous investigators have been plotted on log K vs. $1/T$ coordinates in Fig. 1. All of the data—except those of the three latest studies (18–20)—cluster along a straight line. The scatter about this line has been attributed to the effect of those impurities most frequently found in commercial nickel, i.e., manganese and iron. Wagner (2) predicts that oxidation rates of metals such as nickel which form metal-deficit oxides are increased by additions of metals of higher valencies such as manganese. The markedly lower scaling constants obtained in the three latest studies cannot be explained with any definiteness. Moore and Lee (20) used preoxidized samples which may have affected their results. Gulbransen and Andrew (18) claim their results differ because the metal was exceptionally pure; however, it seems unusual that nickel of 99.9% purity has ten times the scaling resistance of nickel of 99.8% purity (carbonyl nickel). And, in fact, this is not true if the scaling constant at 750°C determined from their data is included in Fig. 1. (This point was not included in their plot of log K vs. $1/T$.) This point differs from the older work by a factor of two at the most. It may well be that better agreement could be obtained at still higher temperatures. However, it should be noted that Frederick and Cornet (19) also obtained lower rate constants using high purity carbonyl nickel.

Excluding the data of these latest studies, there is little difference in the scaling rate in an atmosphere of pure oxygen (P_{O_2} = 760 mm Hg) as compared with air (P_{O_2} = 152 mm Hg) for comparable grades of nickel. By Wagner's theory the scaling rate would be expected to increase with the one-fifth power (approximately) of the partial pressure of oxygen, so that the scaling rate at these two pressures should stand in the ratio of 0.738:1. The pressures used in the three latest investigations (P_{O_2} = 76, 100, and 152 mm Hg) were also close enough so that this factor is unlikely as a possible explanation for the wide discrepancy obtained in the scaling constants.

Scaling Behavior of Manganese

The known facts summarizing the structures of manganese and its oxides and nitrides are given in Table I.

The scaling behavior of manganese in air has been studied only once to date by Gurnick and Baldwin (40). They report that manganese oxidizes parabolically with time at a given temperature and that the parabolic constant adheres to a straight line in an Arrhenius plot (Fig. 2).

The scale formed on manganese from 400° to 1100°C consisted of an outer gray-black layer with a green interleaf between this layer and the metal, appearing at 600°C. Since x-rays revealed both Mn_3O_4 and MnO in the scale it was assumed that the black layer was Mn_3O_4 and the green layer was MnO. This assumption is particularly weak and a careful x-ray and metallographic study of the nature of the scale (to be described below) proved it to be in error. (This means, too, that Gurnick and Baldwin's discussion of the application of Valensi's theory to the scaling of manganese is in error.)

To study the nature of the scales, some Bureau of Mines electrolytic manganese was polished metallographically and heated in air to temperatures of 500°–1125°C for periods of over 100 hr in most cases. The scales were composed of two major layers.

At the lower temperatures (<825°C) the inner scale was green and x-rayed as MnO; the outer scale was grayish-black and x-rayed as Mn_2O_3 with some Mn_3O_4. Above 825°C the inner layer was black with a green interleaf next to the metal; the outer layer was still gray-black, but both x-rayed as MnO! Fig. 3*a* and 3*b* are photomicrographs of these two types of scales. They show, in addition to the major features just described, some secondary but

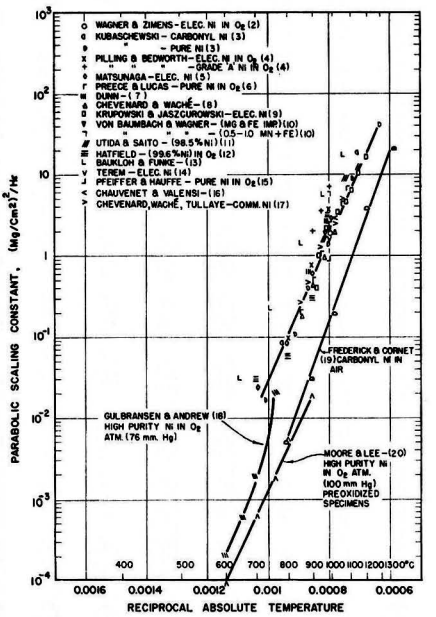

FIG. 1. Oxidation of nickel in air. Relationship between parabolic scaling constant and temperature.

important points of interest. In the outer MnO layer at 1000°C there is a dispersed precipitate that increases in quantity in moving outwardly to the exterior of the scale. It is presumed that this is Mn_3O_4 since some very weak diffraction lines of this phase were picked up in x-rays of the outer layer.[1] The photomicrograph of the scale formed at 1000°C also reveals a veneer outside of the outer MnO layer which glancing x-rays showed to be Mn_3O_4.

The outer Mn_2O_3-Mn_3O_4 layer occupied about 65% of the total scale thickness at low temperatures (600°C), but became relatively thinner as temperature went up until, at the critical temperature of about 825°C, it disappeared. As temperature was further increased, the outer layer of MnO first appeared in relatively thin layers, but increased gradually until at 1125°C it occupied over 80% of the scale thickness. These relationships are shown in Fig. 4. A point of interest is that the Mn_2O_3 layer disappears from the scale at about 825°C whereas its dissociation temperature in air is 940°C.

Since the MnO was found as a double layer above 825°C, the growth mechanism of the two layers was studied at 1000°C by scaling a specimen painted with a marker of zirconium oxide. Visual examination after scaling revealed the marker at the interface between the two MnO layers. This suggests that the outer MnO layer grows by diffusion of manganese ions outward and the inner MnO layer grows by diffusion of oxygen ions inward,[2] similar to the case of cobalt (6).[3]

Thickness measurements were also made of metal before and after scaling in the temperature range 800°–1125°C. Parabolic scaling constants calculated from the metal loss are entered in the Arrhenius plot of reaction rate in Fig. 2. (These constants were obtained by first calculating the loss in weight of metal from the metal thickness before and after scaling. It was assumed that the metal lost was combined with oxygen as oxides whose relative amounts were obtained from Fig. 4. The oxygen pickup could then be estimated and, assuming parabolic behavior, the scaling constants determined.) Fair agreement is found between these values and those obtained from the weight increase measurements of Gurnick and Baldwin, except at 1125°C where it is noted that the over-all scaling constant, K, determined by the metal loss method is greater than the extrapolated value of the weight increase method. This break in the straight line relationship of log K vs. $1/T$ cannot be ascribed to a change in scale composition since MnO is the predominate oxide above 825°C, and presumably the over-all scaling rate is determined by the growth of MnO. The transformation of manganese may be a factor since β-manganese transforms to α-manganese at 1060°–1100°C. Of equal note is the fact that no break in the Arrhenius curve is found at 825°C when the scales did change in composition.

Scaling Behavior of Nickel-Manganese Alloys

Nickel-manganese alloys form a series of solid solutions (26). The scaling behavior of a few nickel-rich alloys has been studied. These alloys oxidize according to the Pilling and Bedworth parabolic law. The scaling constant increases steadily with increasing manganese content up to 10 wt %, the maximum concentration studied (2, 42).

To study the scaling behavior of a much wider range of alloy compositions, six nickel-manganese alloys containing 3.7, 9.1, 20.4, 24.1, 34.8, and 46.6 wt % manganese were prepared. All the alloys were one-phase (alpha) with the exception of the 46.6% manganese alloy which showed a two-phase (alpha + theta) structure. The alloys were made by vacuum induction melting carbonyl nickel and electrolytic manganese in alundum crucibles. The ingots, about 1 in. in diameter and 4 in. long, were cropped and scalped to a $\frac{3}{4}$ in. square cross section, homogenized at 1750°F for 2 hr, hot rolled at 1650°F to $\frac{1}{8}$ in. thickness, scalped to $\frac{1}{16}$ in. thickness, and cold rolled to 0.040 in. strip. The ingots containing 34.8 and 46.6% manganese, respectively, were difficult to work and were processed by cropping, homogenizing at 1750°F for three days in a vacuum of 10^{-5} mm, and scalping (by grinding) to about a $\frac{3}{4}$ in. square bar. Samples approximately $\frac{1}{16}$ in. thick were obtained from the bars; 1-in. squares were cut from the cold rolled strip. Specimens were polished metallo-

[1] This Mn_3O_4 could conceivably appear either by a eutectoidal decomposition of MnO on cooling or by precipitation because of a decreasing solubility of oxygen in MnO as temperature is dropped. The latter cause seems more probable for the following reasons: (*a*) eutectoidal decomposition of MnO would give Mn_3O_4 and manganese; the latter was not detected; and (*b*) the dispersed Mn_3O_4 phase is in heaviest concentration at the exterior of the outer MnO layer where the oxygen content of the MnO is the highest.

[2] The growth mechanism at low temperatures could not be determined by this method since the scale formed was too thin.

[3] Carter and Richardson (41) report that only a single layer of CoO is formed; however, scaling studies by the authors (to be published soon) are in agreement with Preece and Lucas that a double layer of CoO is formed above 900°C.

TABLE I. *Crystal structure and stability of nickel and manganese and their respective oxides and nitrides*

Metal or compound	Crystal structure	Lattice a_o	Constant, Å c_o	Stability range, °C	Remarks
			Pure Metals (1, 21–26)		
Nickel	FCC	3.52		Up to 1455° (m.p.)	
Manganese	α BCC	8.89		Up to 680°	58 atoms to unit cell
	β BCC	6.30		680°–1100°	20 atoms to unit cell
	γ FCT	3.77	3.53	1100°–1138°	
	δ BCC	3.08		1138°–1245° (m.p.)	
			Oxides (6, 7, 10, 21, 27–38)		
NiO	NaCl-cubic	4.17		Up to 1575°	Green, gray, metal-deficit
	Rhombohedral	2.95	(α = 60°4.2′)	Unstable	
MnO	NaCl-cubic	4.43		Up to 1790° (m.p.)	Green, black, metal-deficit
Mn_3O_4	Spinel, tetr.	8.14	9.42	Up to 1580° (m.p.)	Black
Mn_2O_3	Cubic	9.41		Up to 940°	Black
MnO_2	Tetragonal	4.44	2.89	Up to 425°	Black
MnO_3	?			Unstable	Red, deliquescent
Mn_2O_7	?			Unstable at RT	Red, oily
			Nitrides (37, 39)		
Ni_3N	C.P. hexagonal			Up to 380°	
Ni_3N_2	Amorphous			Unstable	
Mn_4N	Cubic	3.80			
Mn_5N_2	Hexagonal			Up to 600°	
Mn_2N	Hexagonal				
Mn_3N_2	Tetragonal				

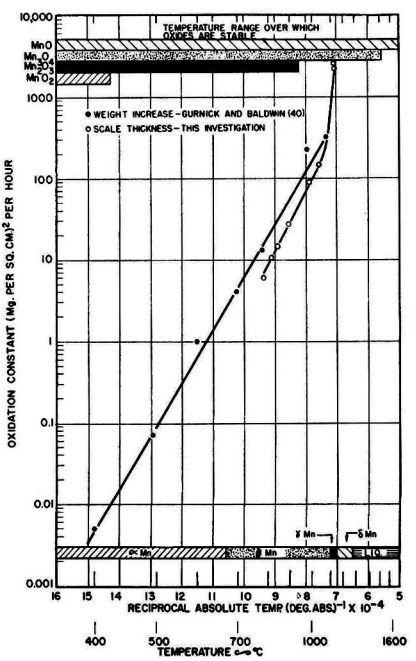

FIG. 2. Oxidation of manganese in air. Relationship between scaling constant, K, in Pilling and Bedworth's equation, $W^2 = Kt$, and temperature.

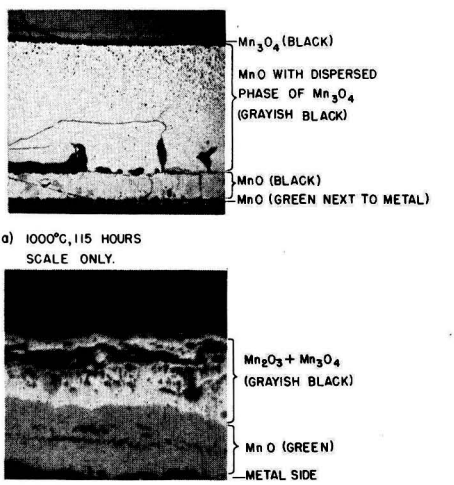

FIG. 3*a* and *b*. Microstructures of the scales formed on electrolytic manganese oxidized in air at the indicated temperatures and times. Unetched. *a*, 50× and *b*, 500× before reduction for publication.

graphically, washed in alcohol, dried, and scaled in air for various times in the temperature range 600°–1100°C. Each specimen was suspended into a resistance-wound vertical tube furnace by a fine nichrome wire from one arm of a magnetically damped chainomatic chemical balance (sensitivity 0.1 mg). Continuous weight measurements were taken from the moment the specimen was suspended and centered in the furnace.

All of the Ni-Mn alloys investigated formed a double-layered external scale. In addition, microscopic examination showed no alloy to be exempt from subscale formation. Wherever possible the external scale layers were

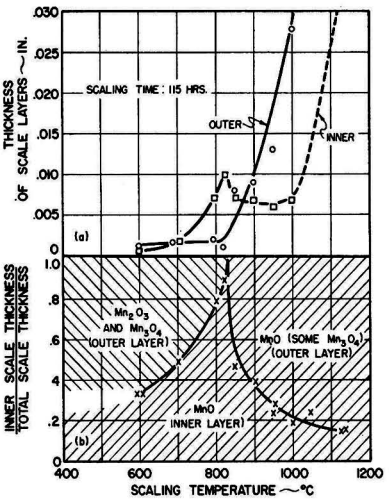

FIG. 4. Effect of temperature on the thickness and composition of the scale layers formed on manganese. The thickness of the individual layers was measured (with micrometers) directly and/or by difference of sample thickness before and after splitting off the layer in question. All scale layers individually x-rayed except those at 600°C.

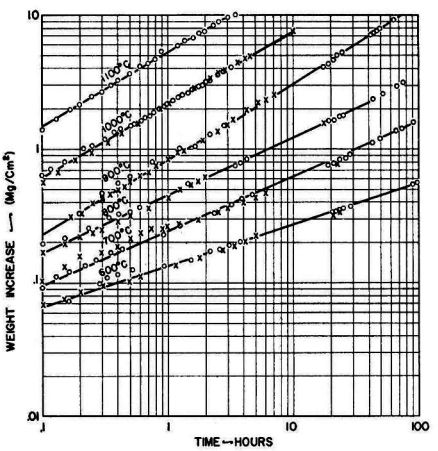

FIG. 5. Isothermal weight increase vs. time curves for 96:4 Ni-Mn alloy heated in air. (Crosses indicate duplicate runs)

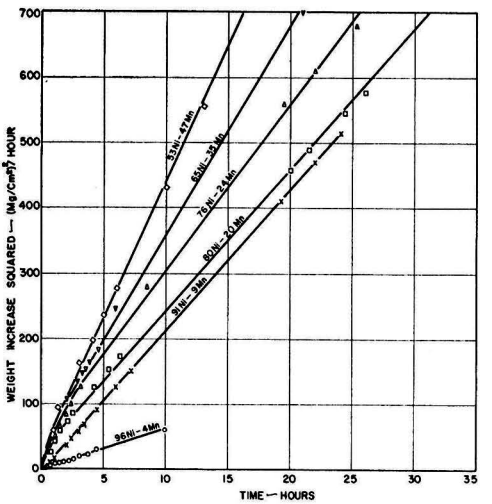

FIG. 6. Weight increase squared vs. time for Ni-Mn alloys heated in air at 1000°C.

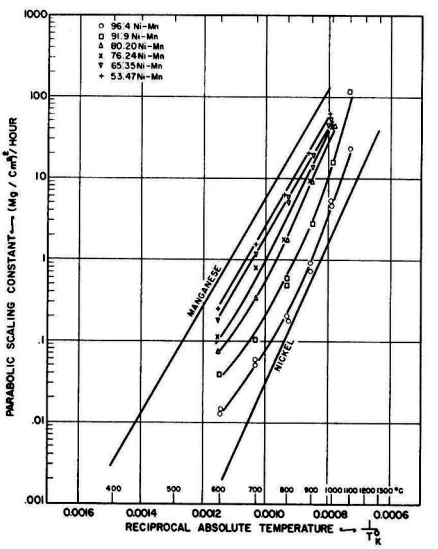

FIG. 7. Arrhenius plot of scaling rate for Ni-Mn alloys heated in air.

separated and x-rayed individually using powder samples. When the layers could not be separated, individual layers could be identified in some instances by x-raying the scale surface before and after grinding off the outer layer; otherwise, the total scale conglomerate was x-rayed using powder samples. To identify the subscale, glancing x-rays were used after the specimen was chipped and scraped clean of its external scale.

Some of the x-ray patterns contained diffuse diffraction lines of an NaCl structure whose lattice parameter was intermediate to that of MnO and NiO, indicating a variable composition of a solid solution of these oxides. Since both NiO and MnO are of the same crystal structure and since their respective cation diameters differ by only 15%, a complete series of solid solutions of these oxides is within the realm of possibility.[4] This point was checked by mixing equal proportions of the pure oxide powders, compacting a pellet, and heating the pellet at 1000°C for 50 hr in a vacuum of 10^{-5} mm mercury. X-rays of the powdered pellet revealed five sharp lines whose "d" values were intermediate to the five strongest lines of MnO and NiO,

[4] Rigamonte (43) reports that, when the difference in cation diameters does not exceed 13%, a continuous series of solid solutions is formed between oxides of divalent metals.

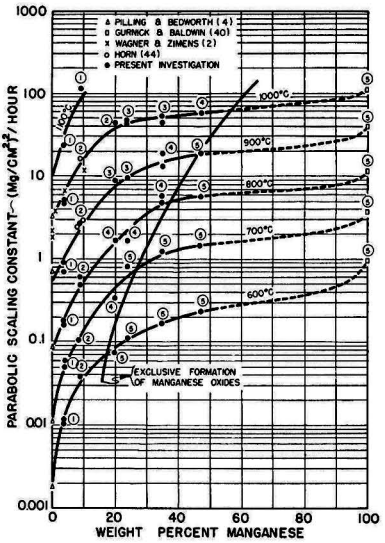

FIG. 8. Parabolic scaling constant vs. alloy composition for Ni-Mn alloys oxidized in air. Encircled numbers indicate scaling patterns (*see* text).

TABLE II. *Scaling patterns of* Ni-Mn *alloys*

Scaling pattern	Subscale	External scale	
		Inner layer	Outer layer(s)
1	NiO	NiO	Spinel
2	NiO	NiO, or A(NiO) and NiO	Spinel and Mn_2O_3[a]
3	A(NiO)	A(NiO) and spinel	Spinel and Mn_3O_4
4	A(MnO)	A(MnO)	Spinel and Mn_3O_4 and Mn_2O_3[a]
5	MnO	MnO[b]	Mn_3O_4 and Mn_2O_3[a]

[a] No Mn_2O_3 above 800°C since this oxide is not stable above this temperature.

[b] No nickel was detected in these scales by a Feigl spot test (45).

Note: Scales denoted "A" were solid solutions of the monoxides MnO and NiO. The oxide noted in parentheses was predominate. In all cases, x-rays of the metal surface after removing the external scale revealed not only the subscale oxide but also a face-centered cubic alloy phase. The composition of this phase was not determined, but from comparison with the "*d*" values of pure nickel and Ni-Mn alloys before oxidation was known to be high in nickel.

close to the MnO side. These oxides quite probably form a complete series of solid solutions.

RESULTS

Kinetics.—Weight increase vs. time data on a log-log scale for different isothermal runs (600°–1100°C) for one of the alloys are shown in Fig. 5.[5] The parabolic scaling law is essentially obeyed at all temperatures for all the alloys, although at the lower temperatures the reaction proceeded somewhat faster at the shorter times than at the

[5] Log-log plots of the data for the other alloys may be obtained from the authors.

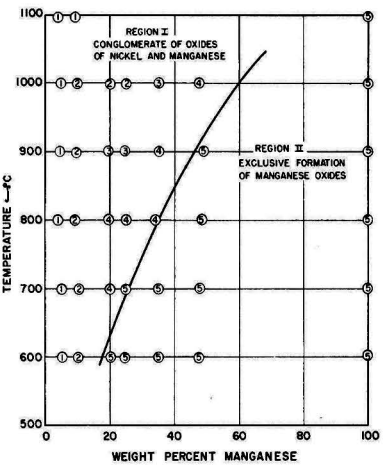

FIG. 9. Composition of scales formed on Ni-Mn alloys heated in air. Scaling patterns are given by encircled numbers.

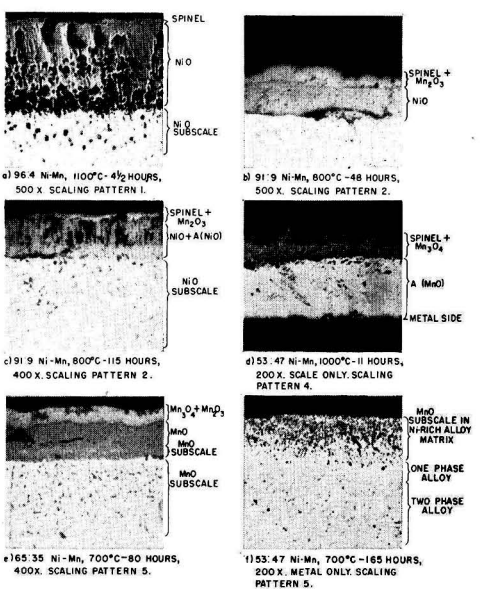

FIG. 10*a–f*. External scales and subscales on Ni-Mn alloys oxidized in air at the indicated temperatures and times. Unetched.

longer times. The parabolic scaling constants were obtained from the curves shown in Fig. 6.

An Arrhenius plot (Fig. 7) shows that the data for the 35 and 47% manganese alloys give straight lines, whereas the data for each of the other alloys follow a slight curve such that the activation energy increases with increasing temperature.

The parabolic scaling rates (log scale) are also plotted as a function of the alloying element (manganese) for constant scaling temperatures in Fig. 8. It is apparent that at each temperature the scaling rate increases con-

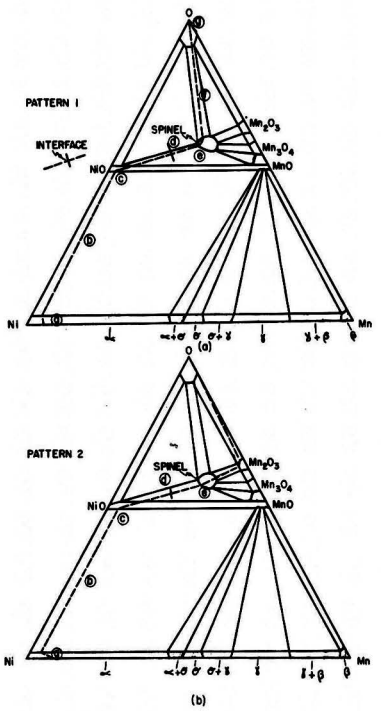

FIG. 11*a–b*. Schematic isothermal sections of the Ni-Mn-O equilibrium diagram showing the scaling patterns of Ni-Mn alloys.

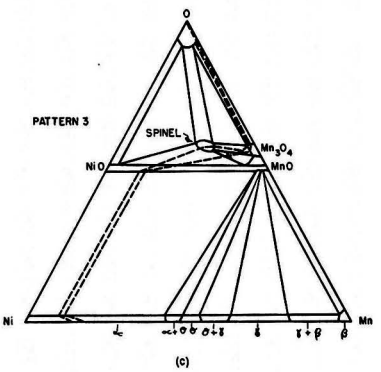

FIG. 11*c*. Schematic isothermal sections of the Ni-Mn-O equilibrium diagram showing the scaling patterns of Ni-Mn alloys.

tinuously with increasing additions of manganese, approaching the scaling rate of manganese as a limit.

Scale structure.—Scales were formed on the alloys in one of five different patterns listed in Table II, depending on alloy composition and temperature as shown in Fig. 9.[6]

Typical microstructures of most of these patterns are given in Fig. 10.

[6] In some cases the scaling pattern was also dependent on time at the scaling temperature; however, the patterns plotted in Fig. 14 pertain to the longer scaling times where steady state is assumed to hold. A complete record of the description and x-ray identification of the external scale and subscale formed on Ni-Mn alloys is on file at Case Institute of Technology (Doctor's Thesis by E. B. Evans).

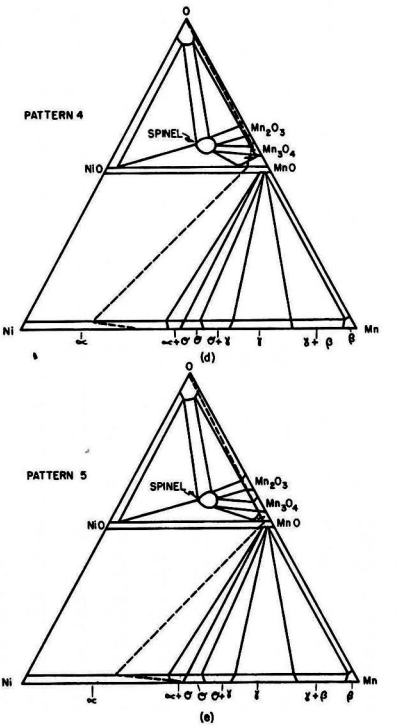

FIG. 11*d* and *e*. Schematic isothermal sections of the Ni-Mn-O equilibrium diagram showing the scaling patterns of Ni-Mn alloys.

DISCUSSION

The scaling patterns can be laid out with a fair degree of certainty in schematic isothermal sections of the ternary Ni-Mn-O phase diagram, Fig. 11, as an aid in visualizing the progressive changes in scaling behavior wrought by alloy composition. The application of phase diagrams to the rationalization of scaling behavior has been discussed in detail by Rhines (46).

The dotted paths shown in Fig. 11 were constructed as to satisfy the demands of the experimentally observed scale structures. (The path must place the compounds found in the various layers in their proper order; it must reveal a progressive oxygen gradient and still be compatible with the topology of the phase diagram.) Furthermore, as Rhines points out, one-phase and two-phase fields in the isothermal sections correspond to scale layers on the specimen, while three-phase fields in the diagrams correspond to interfaces. An exception in the case of the two-phase fields is that these areas correspond to interfaces rather than layers when the path follows a tie-line.

Pattern 1.—As Fig. 9 shows, Pattern 1 is found on relatively nickel-rich alloys only. The path thus starts on the Ni-Mn edge of the ternary diagram near the nickel corner (point *a* in Fig. 11*a*). According to Table II the inner layer

of the external scale is a NiO-rich monoxide. The path thus is drawn to this phase (point *c*) but the fact that a NiO-rich monoxide subscale is found (see Fig. 10*a*) indicates that the path crosses some tie-lines between the alpha phase and the monoxide phase (point *b*). The outer layer of the external scale according to Table II is spinel, hence the path is drawn through this one-phase region to indicate this fact (point *c*). Since the inner and outer layers have a sharp interface, the path between *c* and *e* must follow a tie-line between these two single phases (point *d*). The path then is carried out to the oxygen corner of the diagram (point *g*) along a tie-line between the spinel field and the oxygen field (point *f*) to indicate the sharp interface between the outer layer of spinel and the surrounding air. In some cases at low temperatures no subscale formation was observed although all other features of the pattern were retained.

Pattern 2.—According to Table II, Pattern 2 is similar to Pattern 1 except for the outer layer. Hence the path depicting this pattern, Fig. 11*b*, is the same as the path of Fig. 11*a* up to point *e*. The outer layer of Pattern 2 is given as Mn_2O_3 and spinel in Table II. Whether the Mn_2O_3 and spinel exist as separate layers or as a conglomerate in the outer layer could not be determined because of the thinness and brittleness of the scale layers. If the two oxides were separate layers, the path through the spinel-Mn_2O_3 field would follow a tie-line; otherwise, it would cross tie-lines in this zone. As in the case of Pattern 1, the subscale was not always observed at low temperatures. At 900°C and above, Mn_2O_3 did not appear in the outer layers (nor did it appear in the case of pure manganese) and Pattern 2 became the same as Pattern 1 except that the inner layer was much richer in manganese.

Pattern 3.—This pattern was observed only above 800°C where Mn_2O_3 was not to be found; therefore, the isothermal section was altered so as to exclude this oxide, Fig. 11*c*. Since the subscale consists of A(NiO) in a nickel-rich matrix while the inner scale contains A(NiO) and spinel, the path must cross these two-phase zones. Two choices are open for the path through the outer scale of spinel and Mn_3O_4: (*a*) the path may pass through the spinel zone, then follow a tie-line for some distance in the spinel-Mn_3O_4 zone before bending to the left in this zone, thus crossing the tie-line as shown in the upper path in Fig. 11*c*; or (*b*) the path may extend through the spinel-MnO-Mn_3O_4 field (which constitutes an interface), then cross the spinel-Mn_3O_4 field as shown in the lower path of Fig. 11*c*.

The latter path seems more likely in that it does not necessitate that the path first follows then diverges from a tie-line in a two-phase zone.

Pattern 3 shows a marked difference from Patterns 1 and 2 in that spinel is found in the inner as well as the outer layer. A feature common to these three patterns is that the inner layer consists of NiO or A(NiO).

Pattern 4.—The likely succession of zones traversed by the path that satisfies the requirements of this pattern is given in Fig. 11*d*. Since the subscale consists of A(MnO) in a matrix of nickel-rich alloy and the inner layer is composed of A(MnO) only, the path must cross this two-phase and one-phase area, respectively. The path through the outer layer(s) poses a problem. Since Mn_3O_4 and Mn_2O_3 with small amounts of spinel were found in the outer scale, more than one layer must be present but which could not be resolved under the microscope. The path drawn in Fig. 11*d* meets this demand in that it crosses a three-phase field denoting a sharp interface between the inner and outer layers, and it also passes through one- and two-phase fields which are compatible with the composition of the outer layers.

Pattern 5.—The only path that is compatible with this scaling pattern is shown in Fig. 11*e*. Here the 47% manganese alloy was chosen to illustrate this scaling behavior since it was the only two-phase alloy investigated and some interesting features are to be noted in the underlying metal, Fig. 10*f*. Between the two-phase alloy ($\alpha + \theta$) and the external scale, two layers were found as can be predicted from the isothermal section: (*a*) an α-layer next to the two-phase alloy matrix, and (*b*) an α-layer containing particles of MnO. Here enrichment of nickel and depletion of manganese in the alloy led to the α-layer between the two-phase MnO-α layer and the two-phase alloy matrix. Since the inner scale contains only MnO while the outer scale contains Mn_3O_4 and Mn_2O_3 (or only Mn_3O_4 above 825°C), the path must cross this one-phase and two-phase field, respectively. It must follow a tie-line between the two to indicate the sharp interface.

Scales formed on the alloys which followed this scaling pattern were similar in composition and structure to the scales formed on pure manganese at corresponding temperatures. The scaling behavior of pure manganese differs from Pattern 5 only in the absence of the subscale.

Patterns 4 and 5 have the common feature that the inner layer is a MnO-rich monoxide.

For all their differences in detail, all the patterns in Fig. 11 have a similar shape: instead of being straight lines from the original alloy composition to the oxygen corner of the ternary diagram they veer first to the nickel-rich side of a direct route and then to the manganese-rich side. This implies that the manganese ion diffuses outwardly at a much higher rate than the nickel ion. When the manganese content of the original alloy is high, the faster outward diffusion of manganese leads to the formation of manganese scales exclusively (Pattern 5). The minimum manganese content of the original alloy necessary for this to occur is drawn in as a solid line in Fig. 9. The fact that it runs as low as 15% at 600°C and as high as 60% at 1000°C indicates that the relative speed of the manganese ion over the nickel ion is greater at low temperatures.[7]

The scaling rate as a function of alloy composition has been depicted in Fig. 8 as increasing continuously with increasing manganese content. It should be pointed out, however, that horizontal breaks in the curve may possibly occur at high enough manganese concentrations where a two-phase alloy region is in equilibrium with the external scale, i.e., the two-phase alloy region immediately adjacent to the external scale. Thermodynamically, a two-phase region is a heterogeneous system at equilibrium

[7] A number of analyses have been proposed for predicting the minimum concentration of an alloy constituent necessary for the exclusive formation of its oxide (47, 48), but none of these applies here since they are based on assumptions that are not even closely approached in the present study.

wherein the activity of an element in the alloy is identical in the two phases. If the activity is a measure of the driving force of the oxidation reaction and equilibrium obtains, then the scaling rate and consequently the oxidation products should be the same over a two-phase field. It is not enough to say that this would hold true for alloys which are two-phase at the start of the scaling reaction, for as shown in the case of the 47% manganese alloy the metal surface is so depleted in manganese during the scaling reaction that a one-phase alloy and not a two-phase alloy was in equilibrium with the external scale. In any case, this behavior cannot be established with any definiteness for the case of the Ni-Mn alloys for the following reasons: (*a*) a prohibitive number of alloys would be required to describe the scaling behavior over that range of alloy compositions (say greater than 50% manganese) encompassing the one- and two-phase alloy regions, and (*b*) the expected change in scaling rate in this range is seen to be so small as to be within the realm of experimental error. However, preliminary results with Cu-Cr alloys indicate that the scaling rate is about the same for a number of different alloys lying in the broad two-phase field in this system. Further studies of the dependency of the scaling rate upon alloy composition in the one- and two-phase fields are underway for the case of Ni-Cr and Co-Cr alloys which show a very strong dependence of scaling rate upon alloy composition.

The increase in the scaling rate by small additions of manganese to nickel has also been found with small additions of chromium to nickel (or cobalt). This increase has been explained on the basis that trivalent manganese or chromium dissolves in the metal-deficit NiO (or CoO) and replaces some of the divalent nickel (or cobalt) ions (2), thus providing new cation defects for the diffusion of nickel (or cobalt) ions. Alternately, the rise in scaling constant with manganese additions may be attributed to the relatively greater mobility of the manganese ion over that of the nickel ion, since the inner layer was identified by x-rays as the bivalent monoxide, be it NiO, MnO, or a solid solution of the two. The fact that manganese effects a smaller increase in scaling constant at high temperatures than at low temperatures (see Fig. 8) may be consonant with the deduction noted above that the relative speed of the manganese ion *vis à vis* the nickel ion was not as great at high temperatures as it was at low temperatures. However, it should be pointed out that this alternate mechanism assumes that the same stoichiometry is maintained by the oxides. This assumption may not hold here. In the high temperature scaling of iron, for example, the "FeO" layer may contain as much as 30% trivalent iron ions. In any case, the present evidence is not adequate to distinguish between these two possible mechanisms.

Lastly, it is to be noted that although spinel was found in the scales at certain alloy compositions it did not effect any drop in scaling rate. This finding parallels that of Preece and Lucas (6) and Yearian (49) that spinels do not lead to low scaling rates in the Co-Cr, Fe-Cr and other analogous alloy systems.[8]

[8] The low scaling rate of nichrome has often (but erroneously) been attributed to the presence of spinel (2, 50, 51).

Conclusions

1. Nickel-manganese alloys scaled according to the Pilling and Bedworth parabolic law.

2. At a given temperature the scaling rate of Ni-Mn alloys increased with increasing additions of manganese which would seem to preclude their use as oxidation resistant components.

3. The composition of both the external and subscale found in these alloys was dependent on alloy composition and temperature. Above a critical concentration of manganese, the external scale consisted exclusively of manganese oxides and MnO subscale; below this critical composition complex external scales of the oxides of both nickel and manganese were formed along with a subscale of NiO or a solid solution of monoxides. The critical concentration of manganese was as low as 15% at 600°C, and as high as 60% at 1000°C.

4. The increase in scaling rate as manganese was added to nickel was due to (*a*) the faster mobility of the manganese ion, or (*b*) an increase in lattice defects in the monoxide introduced by manganese. The present evidence was not adequate to distinguish between these two mechanisms.

5. Spinel formation observed in most of the complex scales had no apparent beneficial effect on the scaling resistance.

Acknowledgments

The authors are especially indebted to the Office of Ordnance Research whose sponsorship made this work possible. They also wish to thank C. A. Barrett and F. Karpoff who performed some of the tests.

Manuscript received August 15, 1955.

Any discussion of this paper will appear in a Discussion Section to be published in the June 1957 Journal.

References

1. "Metals Handbook," Edited by Taylor Lyman, p. 1231, American Society for Metals, Cleveland, (1948).
2. C. Wagner and K. E. Zimens, *Acta Chem. Scand.*, **1**, 547 (1947).
3. O. Kubaschewski and O. von Goldbeck, *Z. Metallkunde*, **39**, 158 (1948).
4. N. B. Pilling and R. E. Bedworth, *J. Inst. Metals*, **29**, 529 (1923).
5. Y. Matsunaga, *Japan Nickel Rev.*, **1**, 347 (1933).
6. A. Preece and G. Lucas, *J. Inst. Metals*, **81**, 219 (1952).
7. J. S. Dunn and F. J. Wilkins, "The Oxidation of Non-Ferrous Metals," Section 4, p. 78, Review of Oxidation and Scaling of Heated Solid Metals, Dept. of Scientific and Industrial Research, London, His Majesty's Stationery Office (1935).
8. P. Chevenard and X. Waché, *Rev. Met.*, **45**, 121 (1948).
9. A. Krupowski and J. Jasczurowski, *ibid.*, **33**, 646 (1936).
10. H. H. von Baumbach and C. Wagner, *Z. phys. Chem.*, **B24**, 59 (1934).
11. Y. Utida and M. Saito, *Sci. Repts., Tohoku Imp. Univ.*, **13**, 391 (1925).
12. W. H. Hatfield, *J. Iron Steel Inst.*, **115**, 483 (1927).
13. W. Baukloh and P. Funke, *Korrosion u. Metallschultz*, **18**, 126 (1942).
14. H. N. Terem, *Bull. Soc. Chim.*, **6**, 664 (1939).
15. H. Pfeiffer and K. Hauffe, *Z. Metallkunde*, **43**, 364 (1952).
16. G. Chauvenet and G. Valensi, *Compt. rend.*, **205**, 317 (1937).

17. P. Chevenard, X. Waché, and R. De la Tullaye, *Bull. Soc. Chim.*, **11**, 41 (1944).
18. E. A. Gulbransen and K. F. Andrew, *This Journal*, **101**, 128 (1954).
19. S. F. Frederick and I. Cornet, *ibid.*, **102**, 285 (1955).
20. W. J. Moore and J. K. Lee, *Trans. Faraday Soc.*, **48**, 916 (1952).
21. C. D. Hodgman, ed., "Handbook of Chemistry and Physics," p. 370, Chemical Rubber Publish Co., Cleveland (1948).
22. B. F. Naylor, *J. Chem. Phys.*, **13**, 329 (1945).
23. Z. S. Basinski and J. W. Christian, *Proc. Roy Soc.*, **223**, 554 (1954).
24. D. Schlain and J. D. Prater, *J. (and Trans.) Electrochem. Soc.*, **94**, 58 (1948).
25. E. V. Potter, H. C. Lakens, and R. W. Huber, *Trans. Am. Inst. Mining Met. Engrs.*, **185**, 399 (1949).
26. W. Koster and W. Rauscher, *Z. Metallkunde*, **39**, 178 (1948).
27. S. Miyake, *Sci. Papers Inst. Phys. Chem. Research (Tokyo)*, **31**, 161 (1937).
28. P. W. Selwood, "Valence Inductivity and Catalytic Action," Pittsburgh International Conference on Surface Reactions, Corrosion Publishing Co., Pittsburgh, p. 49 (1948).
29. Y. Shimomura and Z. Nishiyama, *Mem. Inst. Sci. Ind. Research Osaka Univ.*, **6**, 30 (1948).
30. H. P. Rooksby, *Acta Cryst.*, **1**, 226 (1948).
31. M. J. Robin, *Compt. rend.*, **235**, 1301 (1952).
32. R. W. G. Wyckoff, "Crystal Structures," p. 253, Interscience Publishers, Inc., New York (1948).
33. M. LeBlanc and H. Sachse, *Z. Elektrochem.*, **32**, 58 (1926).
34. G. Valensi, *Compt. rend.*, **201**, 523 (1935).
35. R. L. Tichenor, *J. Chem. Phys.*, **19**, 796 (1951).
36. H. W. Foote and E. K. Smith, *J. Am. Chem. Soc.*, **30**, 1344 (1908).
37. C. J. Smithells, "Metals Reference Book," Interscience Publishers, Inc., New York (1955).
38. W. J. Moore, Rept. No. 1, AEC, Contract No. At(11-1)-250, Indiana University, May 1, 1953.
39. O. Kubaschewski and B. E. Hopkins, "Oxidation of Metals and Alloys," Academic Press, Inc., New York (1953).
40. R. S. Gurnick and W. M. Baldwin, Jr., *Trans. Am. Soc. Metals*, **42**, 308 (1950).
41. R. E. Carter and F. D. Richardson, *J. Metals*, **7**, 336 (1955).
42. L. Horn, *Z. Metallkunde*, **38**, 73 (1949).
43. R. Rigamonte, *Gazz. chim. ital.*, **76**, 474 (1946) (ASTIA AD No. 13051).
44. L. Horn, *Z. Metallkunde*, **36**, 142 (1933).
45. F. Feigl, "Spot Tests," p. 141, Elsevier Publishing Co., New York (1954).
46. F. N. Rhines, *Trans. Am. Inst. Mining Met. Engrs.*, **137**, 246 (1940).
47. C. Wagner, *This Journal*, **99**, 369 (1952).
48. L. S. Darken, *Trans. Am. Inst. Mining Met. Engrs.*, **150**, 157 (1942).
49. H. J. Yearian, "Investigations of the Oxidation of Chromium and Nickel-Chromium Steels," Purdue Research Foundation, Summary Technical Report to Office of Naval Research, Contract N7 onr-39419, June 1954.
50. K. Hauffe, "The Mechanism of Oxidation of Metals and Alloys at High Temperatures," in "Progress in Metal Physics," Vol. IV, pp. 71–104, Interscience Publishers, Inc., New York (1953).
51. K. Hauffe, *Z. Metallkunde*, **42**, 34 (1951).

Pitting Corrosion of 18Cr–8Ni Stainless Steel

M. A. Streicher

Engineering Research Laboratory, Engineering Department, E. I. du Pont de Nemours and Co., Inc., Wilmington, Delaware

ABSTRACT

I. Factors controlling pitting corrosion and laboratory methods used for its study are reviewed. An electrolytically accelerated test was developed for investigation of pit initiation. A controlled direct current was passed through a cell whose anode was the stainless steel specimen and whose electrolyte was the pitting solution. The number of pits formed depended on the current density, the steel specimen (composition and surface treatment), and the solution (composition and temperature).

II. The accelerated electrolytic pitting method described in Part I was used to determine the influence of alloying elements added to 18Cr-8Ni stainless steel on pit initiation in sodium chloride and bromide solutions. Reduction in carbon content, increase in nitrogen content of these steels, and alloying additions of molybdenum and silicon increased resistance to pit initiation. Grain boundaries, rather than nonmetallic inclusions, were primary sites of pit initiation during simple immersion or in the electrolytically accelerated test.

I. Development of an Accelerated Pit Initiation Method

Introduction

Pitting may be divided into two distinct steps: (*a*) pit initiation or surface breakdown, and (*b*) pit growth in depth and volume. Although the factors determining pit initiation are largely unknown, pit growth has been described in some detail in the literature.

The intensity of localized attack which leads to growth of deep pits results from several factors. The pit is the

anode, and the unaffected area surrounding the point of penetration is the cathode of a cell whose electrolyte is the corrosive solution. On metals covered by protective films, the surface area available for cathodic reactions is very large compared with that available for the anodic reaction, which takes place at breaks in the film. As a result, the current/unit area of cathode surface remains low, and large areas may be exposed to cathodic reaction accelerators in the solution, e.g., oxidizing agents which depolarize this reaction and thereby stimulate the anodic reaction. Anodic dissolution may also be stimulated by reduction of ferric to ferrous ions at cathodic areas (1).

The anodic current density is high, and enough metal is soon removed to form a depression in the surface, unless corrosion products stifle the reaction. In some cases, oxygen combines with metal ions produced by corrosion to form protective oxide films. However, if there is insufficient oxygen available, or if the oxides formed are not protective, the pit grows. A cavity is soon formed in which oxygen is not easily replenished and is, therefore, soon exhausted. Also, the corrosion current causes any chloride ions present to migrate to the anode (2). These ions tend to destroy the protective qualities of any films which may still be present and will acidify the solution in the pit. The combination of large cathodic and small anodic areas, oxygen exhaustion, chloride accumulation, and acid conditions produces an intensely localized form of attack.

Oxygen plays a dual role by its ability (*a*) to stifle the anodic reaction through film formation, and (*b*) to accelerate the cathodic process by removal of hydrogen and by regenerating ferrous to ferric ions. Both of these effects may be operative at the same time. The over-all result on the corrosion rate depends on whether anodic retardation or cathodic stimulation is dominant (3). For example, in a study of crevice corrosion on straight chromium (17% Cr) stainless steel in sea water (4) the amount of corrosion in the crevice (pit) was directly proportional to the size of the uncorroded (cathodic) area surrounding the crevice. Thus, as long as the amount of oxygen available/unit area of cathode exposed to flowing sea water was constant, the extent of stimulation depended only on the size of the cathodic area. In another investigation (5) pitting of Type 304 stainless steel in sodium chloride solutions exposed to the atmosphere was almost completely suppressed when oxygen was removed. Oxygen was acting as a cathodic stimulant. However, when the oxygen pressure was increased to 60 atm pitting was also retarded, because at this pressure the film-forming properties of oxygen became dominant.

Some Factors Affecting Pitting of Stainless Steels

Crevice conditions are especially severe in sea-water exposures where there is a high concentration of chlorides combined with severe attachment of barnacles and other marine organisms on the metal surfaces. Of all the standard AISI-300 series grades of stainless steels, Type 316 (Table I) is the most resistant, i.e., the addition of 2–3% molybdenum increases the sea-water pitting resistance of 18 Cr-8 Ni steels (6). The beneficial effects of molybdenum additions have also been observed by Smith (7) in his ferric chloride thermal convection test (described below). In addition, Type 302B stainless steel (18Cr-8Ni + 2.5% Si) was found superior in this test to regular 18 Cr-8Ni grades. An 18Cr-8Ni steel to which both silicon and molybdenum had been added, each in amounts of 2–3%, has been described by Riedrich (9). In a comparison of this steel with nickel, Monel, and an 18Cr-8Ni-2 Mo-1 Nb steel, Riedrich's steel showed the best pitting

TABLE I. *Analyses of stainless steels used in pitting tests (per cent by weight)*

Steel, AISI type	Code	Cr	Ni	C	N	Mo	Si	Mn	P	S	Nb	Ti	Cu	Al
304	EX-1	18.22	8.97	0.061			0.58	0.56	0.025	0.011				
304	ER-1	18.23	8.59	0.070			0.56	0.69	0.012	0.003				
304	ER-2	18.45	8.90	0.063			0.58	0.66	0.015	0.008				
304L	FK-4	18.30	11.02	0.020	0.033		0.37	1.06	0.018	0.014				
304L	FK-9	19.12	10.96	0.016	0.12		0.56	1.22	0.022	0.015				
302	GF-2	18.37	8.71	0.10			0.60	0.93	0.019	0.009				
302B	302B	18.79	9.19	0.060			2.49	0.38	0.01	0.012				
302B	302BP	17.30	8.62	0.14			2.71	1.44						
321	FF-7	17.83	9.21	0.061			0.79	1.25	0.028	0.023		0.31		0.041
347	EX-2	18.58	11.27	0.058			0.58	1.76	0.026	0.020	0.87			
347L	FE-6	17.14	11.00	0.016	0.029						0.33			
316	EW-5	17.93	13.50	0.031		2.47	0.31	1.77	0.023	0.006				
316	C-1	17.78	13.22	0.056		2.32	0.71	1.70	0.021	0.009				
316	C-2	17.80	12.52	0.055		2.28	0.58	1.53	0.017	0.005				
316L	FH-3	17.71	11.17	0.020	0.032	2.44								
316L	FH-1	17.85	11.34	0.027	0.13	2.25								
316L + Nb	FN-3	18.62	14.02	0.022	0.028	2.15					0.32			
316 + Si	SP-1	18.05	9.92	0.072	0.062	2.21	2.39	0.61	0.012	0.020			0.08	
316 + Si	SP-2	18.79	9.24	0.039	0.23	2.40	2.50	0.77					0.02	
316 + Si	SP-3	18.60	8.99	0.038	0.059	3.70	2.29	0.86					0.02	

Steel, AISI type	Cr	W	Fe	C	Si	Co	Mn	Cu	V	Mo	P	S	Ni
"Hastelloy" C*	16.38	4.55	5.18	0.06	0.43	1.58	0.58	0.09	0.27	16.77	0.017	0.006	Bal.
"Hastelloy" B	0.24		6.60	0.04	0.11		0.52		0.35	28.22			Bal.

* Nominal analysis.

resistance in solutions of acidified ferric chloride, iodine-alcohol, and mercurous chloride.

Nitrogen may increase the pitting resistance of stainless steels, e.g., a 23Cr-4Ni-0.3N steel showed greater resistance in 20% ferric chloride solution than did standard 18-8 stainless steel (10). It was also found that 0.24% N in 18Cr-8Ni stainless steel increased pitting resistance in ferric chloride solution (11). Nitrogen is 25–30 times more efficient than nickel as an austenitizer. In general, a single-phase austenitic structure is preferred in the 18 Cr-8Ni stainless steels because of its superior mechanical properties and corrosion resistance (8). Thus, it is possible that beneficial effects may be obtained when nitrogen is used as an addition agent, either for its own sake or to offset the ferrite-forming tendencies of other elements, such as silicon and molybdenum which may be added to increase corrosion resistance.

Pit Initiation Studies

Immersion Methods

In laboratory investigations of pitting corrosion the most difficult problem has been that of finding a controllable and reproducible pit initiation test. One of the most successful has been the "square drop" test (12–14) in which it was found that on iron corroding in potassium chloride solutions under oxygen-nitrogen mixtures, the probability of attack diminishes and the rate of corrosion increases with oxygen concentration. Certain types of nonmetallic inclusions were found to increase the probability of corrosion of low-carbon steels.[1]

The search for a satisfactory pit initiation technique has been a particularly acute problem in the case of pitting studies on stainless steels. Extensive efforts to solve this problem are described in the literature (19). Smith (7) used an apparatus for circulating by thermal convection a solution of ferric chloride and hydrochloric acid over the surface of the metal to be pitted in such a way that edge effects and crevice corrosion were avoided. As indicated above, he found that the addition of 3% molybdenum and, to some extent, silicon to 18Cr-8Ni steel reduced its tendency toward pitting. From metallographic observations of pitted surfaces, it was concluded that finer metallographic polishes reduce pitting attack and that factors other than microscopic inclusions were of primary importance in pit initiation. These were assumed to be cracks and pores in the protective film.

Objections were raised to the pitting test accelerated by acidified ferric chloride because it could not be used as an index of resistance of an alloy to attack by any solution other than ferric chloride. It was pointed out that the insolubility of ferric ion at *p*H 3 or higher makes vulnerable any theory that pitting of stainless steel in sea water, *p*H 8, is initiated by ferric chloride which might have been generated by iron or steel corroding in the vicinity (20).

[1] Mears and Brown (14) used the square drop technique and methods of pit isolation in studies of pitting on aluminum. Other techniques used for pitting research include radioactive tracers (16), radiography (17), and electrolytic pit initiation for studies of pit growth (18).

Electrolytic Methods

Many attempts have been made to produce controlled corrosion reactions electrolytically. Thus, Donker and Dengg (21) applied an external emf to a cell consisting of an iron anode and a silver cathode in solutions of various salts. A breakdown potential was reached at which there was a large increase in the current through the cell. The increase in cell current was caused by dissolution of the iron. This technique was used by Uhlig and Wulff (22), and, in modified form, by Brennert (23, 24) and by Mahla and Nielsen (25) for a study of the passivity of stainless steels. Measurements of breakthrough potentials were made in these investigations on relatively small areas from which edge effects were excluded. Breakthrough potential data and confirmatory immersion-corrosion data showed that no passivation treatment confers lasting protection to a stainless steel immersed in media which corrode unpassivated metal (25).

Experimental

The present investigation is concerned with factors producing breakdown of the passive surface. Simple immersion of the specimen in a given corroding solution was tried, but, as in previous investigations, most of the pitting attack took place at the edges of the specimen. An attempt was made to adapt the square drop method (15) to stainless steels. Again, practically all attack was at the edges, in this case at the edges of the wax coating. The pitting attack at the edge of the coating outlines the wax grid.

Because of difficulties with these pitting tests, electrolytic methods of acceleration were investigated, and a modified potential breakdown apparatus was constructed. In previous investigations the breakdown apparatus was used to determine the electrode potential at the breakdown of a relatively small area of stainless steel surface. In the modified apparatus (Fig. 1) a 25 cm² surface area was tested, and the primary measurement was the number of points of film breakdown, i.e., the number of pits initiated, rather than the potential at the breakdown.

A stainless steel specimen is made the anode of an electrolytic cell, and a platinized wire gauze, 6 cm in diameter, is the cathode. Gauze is used rather than sheet to allow hydrogen liberated during the test to rise through the horizontal mesh instead of forming large bubbles on the surface. The cathode is immersed in a porous cup to restrict diffusion of the alkaline catholyte into the solution

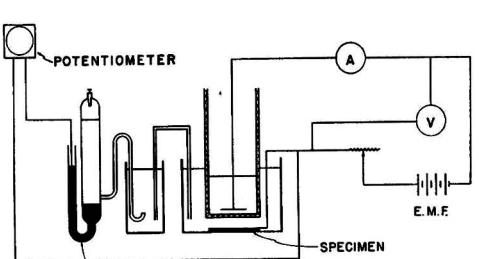

Fig. 1. Schematic diagram of electrolytic pitting apparatus

in which the steel is immersed. A crystallizing dish containing 1800 ml of electrolyte is set in a thermostated water bath.

Recording meters are used to measure the current through the cell and the voltage across the electrodes. Changes in the electrode potential between the specimen surface and the solution are measured against a calomel cell and are automatically recorded.

Characteristics of the Electrolytic Pitting Test

Preparation of specimens.—Specimens were cut from sheet stock 0.07 in. thick, in 2 in. squares. After removal of scale by grinding, stainless steel wires were spot-welded to one corner for electrical contact. Specimens were then suspended in a pickling bath containing 360 ml 65% nitric acid, 60 ml 48% hydrofluoric acid, and 60 ml 37% hydrochloric acid added to 3000 ml distilled water at 70°C (25). After about 20 min in this solution, Type 304 (18-8-S) stainless steel showed a characteristic flashing of the surface while a dark film, formed during the initial phases of pickling, dissolved, leaving a relatively uniform and bright surface. Electrode potential measurements made during this pickling process showed that no pronounced changes in potential accompanied the flashing phenomenon. There was only a gradual change in the direction of a more noble potential, probably indicating the progressive thickening of a passive film. Type 316 (18-8-S-Mo) stainless steel did not show flashing.

As soon as the surfaces were bright the specimens were removed from the pickling bath, rinsed with water, and immersed (when desired) in a passivating solution containing 180 ml 65% nitric acid and 15 g potassium dichromate in 3000 ml distilled water at 70°C for 30 min (25). On removal from this solution, specimens were rinsed and dried. When dry, the back, sides, and the wire were covered with a transparent plastic coating, Fig. 2. After the uncoated area was pitted, the coating was dissolved in acetone and the reverse side of the specimen was used for another pitting run, after a repetition of the chemical treatments and recoating.

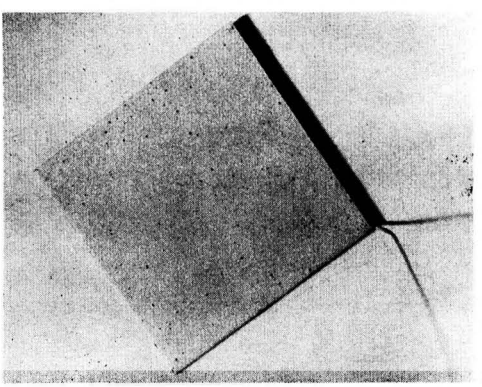

Fig. 2. Pitting test specimen. A stainless steel wire has been spot welded on the back of the specimen to make electrical contact. The wire, the edges, and the back of the specimen have been masked with a transparent insulating coating. The specimen is 5 x 5 cm and shows pits formed in the electrolytically accelerated test.

Testing procedure.—Runs to determine pitting resistance were made by placing a specimen (prepared as described in the previous section) at the bottom of a crystallizing dish containing 1800 ml of solution. The distance between the porous cup (containing the cathode) and the specimen was fixed, as well as the depth of immersion of the cup in the solution. The solution in the porous cup was of the same composition as that in the crystallizing dish, and its quantity did not affect the test as long as the cathode was covered. All solutions were renewed for every run.

By means of the slide wire, driven by a constant-speed motor, the external voltage across the specimen and the cathode was increased from zero to given voltage at the rate of about 2 v in 5 min. The electrode potential, voltage, and current were recorded on automatic instruments. As the external current was slowly increased, very faint pits appeared, which gradually increased in number and size. When the desired current density or voltage was reached, the slide wire motor was turned off and the voltage or current held constant for 5 min to enlarge any pits which may have just appeared.

Factors determining the number of pits.—As the voltage across the specimen and the cathode was gradually increased by the motor slide wire, the total number of pits increased. Since the current density was increasing at the same time, it was desirable to establish which of these elements, the potential difference across the cell or the current density, determined the pitting intensity (pits/cm²).[2] Two series of runs were made in 0.1*N* sodium chloride using sets of 18Cr-8Ni (Type 304) stainless steel specimens whose areas were 4–40 cm². In one series of runs the external emf was allowed to increase to 2 v and was then held constant for 5 min. In this way, since the exposed area varied for each specimen, different current densities were obtained on the surface being pitted. For the second series of runs a value of 5 ma/cm² was chosen as the maximum current density to be applied to all specimens. By multiplying the area of each specimen (cm²) by 5, the total current required (as registered on the milliammeter) was found. The voltage was allowed to increase in each run until the desired current was reached. Since the current is proportional to the voltage, various potential differences were produced across the cell while the maximum current density for each specimen remained constant.

At constant voltage.—If voltage across the cell is the determining factor in producing pits, then the number of pits per square centimeter will be constant, regardless of the area of the specimen, at a given potential difference across the cell. In a series of runs for which the voltage was increased from zero to a maximum of 2 v, while the area of the specimens was varied, the number of pits per square centimeter decreased with increasing specimen area. When the number of pits per square centimeter was plotted against the reciprocal of the area, a straight line

[2] The role of the single electrode potential is discussed below.

resulted. Therefore, at constant maximum voltage, the number of pits per square centimeter was inversely proportional to the area of the specimen. A plot of pits per square centimeter vs. current density (determined by dividing the maximum current at 2 v by the area of the specimen) also gave a straight line. Therefore, the number of pits formed is proportional to the current density on the specimen, and changes in cell geometry introduced by specimens of various sizes do not affect the pit initiation process.

At constant-current density.—To verify this effect of current density on pitting and to establish the effect, if any, of varying the maximum voltage across the cell, a second series of runs was made to a constant maximum current density. In Fig. 3 it is seen that the number of pits per square centimeter does not vary with voltage across the cell as long as the current density remains constant.

At constant area.—The effect of current density on the number of pits formed per square centimeter was studied on three types of 18Cr-8Ni stainless steels in both the pickled and the passivated condition. A series of specimens was exposed to 0.1*N* sodium chloride solutions at 25°C, while the current density was increased from zero to values ranging from 10 to 85 ma/25 cm². Data for a Type 304 stainless steel are given in Fig. 4. The linear relationship between current density and pits/25 cm² is apparent for both the passivated and the pickled condition. The parallel lines in Fig. 4 indicate the 68% tolerance limits. For the pickled specimens, 68% of all values fall within ±16 pits/25 cm² (or ± 0.65 pits/cm²) of the line and for the passivated, ±8.67 pits/25 cm² (0.34 pits/cm²). These values are typical. The fact that the lines do not go through the origin indicates that acceleration of pitting by chloride ions in this test is dependent on a certain minimum current density of the order of 0.4 ma/cm², below which no pitting occurs in the solutions used. From Fig. 4 it is seen that current densities of 60 ma/25 cm² or greater are desirable to bring out clearly the differences in pitting resistance between various steels and surface treatments. For this reason a maximum current density of 3 ma/cm² (75 ma/25 cm²) was chosen for all tests.

Effect of time.—To determine the effect of time and the quantity of electrical charge on the pitting intensity, two runs were made during which the same quantity of electricity was passed through the specimens at different current densities. From Fig. 4 it is seen that for pickled Type 304 stainless steel the pitting rate at 75 ma/25 cm² (specimen held for 5 min at maximum c.d.) is 140 pits/25 cm². A series of ten specimens of the same steel was run up to only 30 ma/25 cm² and held for 26 min. In this way, the total number of coulombs (current x time) was made the same in both runs. The average of the ten specimens from the 30 ma run was 77 pits/25 cm². Fig. 4 reveals that this is within 10% of the average at 30 ma for runs held only 5 min at this current density. Therefore, within the range studied, the number of pits formed is independent of the number of coulombs passing through the specimens or of the length of time for which the current density is held constant.

The assumption implicit in this check is that the average of ten pitting runs made with a certain maximum current density is comparable with the pitting intensity obtained from the lines of Fig. 4 which are based on data obtained over a range of maximum current densities. That this is a valid comparison is shown by data obtained on Type 347 stainless steel. From a plot for Type 347 steel similar to that of Fig. 3, it was found that in the passivated condition this steel may be expected to average 74 pits/25 cm² or 2.95 pits/cm² when a maximum current density of 3 ma/cm² is used. In two separate tests, run to a maximum current density of 3 ma/cm², the averages of two sets of ten specimens were 2.9 and 2.5 pits/cm². These values are in good agreement with the 2.95 pits/cm² obtained from a plot similar to Fig. 4.

In summary, the number of pits per unit of area found for a specific combination of steel and corrosive solution depends directly on the density of the current (ma/cm²) passing through the surface of the specimen and is independent of the voltage across the cell, the specimen area, the length of time of holding at constant current density, the total quantity of electricity passing through the cell,

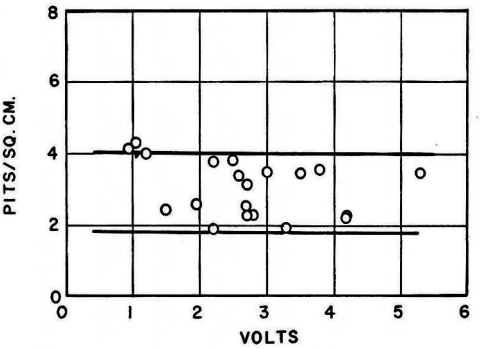

FIG. 3. Effect of voltage on the pitting intensity at constant current density (5 ma/cm²) on Type 304 stainless steel in 0.1*N* NaCl at 25°C.

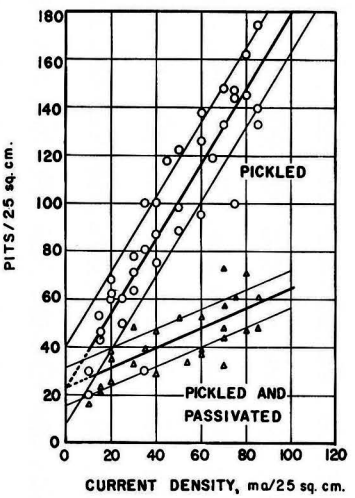

FIG. 4. Effect of current density on pitting of Type 304 stainless steel (EX-1) in 0.1*N* NaCl at 25°C.

the maximum electrode potential, or the prior appearance of pits.

The standard testing procedure derived from these experiments consists of increasing the current from zero to 3 ma/cm² and holding for 5 min at this current density to develop and reveal clearly any pits which may have just been initiated upon reaching the maximum current density. Only about 15 min is required to complete the test on one specimen, and the accelerating factor, the electrical current, is readily controlled. Thus, the modified test begins where the original Brennert test ends, i.e., when the first pit forms. In place of an electrode potential measurement, made at the initiation of the first pit, the number of pits formed on a relatively large surface area is used as a measure of resistance to pit initiation.

Reproducibility.—In order to obtain a measurement of the pitting resistance of a stainless steel, runs are made on ten specimens with the current increasing from zero to 3 ma/cm². At the completion of the runs, the total number of pits is counted and divided by the area of the specimen (usually about 25 cm²) to obtain the number of pits per square centimeter. The results of ten such runs are averaged to give a value, in pits per square centimeter, of the pitting resistance of that steel in a given corrosive solution at a controlled temperature. From a statistical study of typical data obtained on several types of steel at various temperatures in chloride solutions, it was found that 90% of the averages of ten such runs as described above will be within ±0.5 pits/cm² of the "true average," i.e., the average of an infinitely larger number of runs (confidence limits). Also, 95% of the time, 75% of the pits/cm² obtained in an individual run will be within ±1 pit/cm² of the average of ten runs (tolerance limits).

The data obtained from 70 comparable runs on Type 304 stainless steel in 0.1*N* sodium chloride solution fall on a symmetrical distribution curve. Efforts to reduce the tolerance limits by various methods of surface preparation, grinding, and pickling procedures, and by controlling the time between specimen preparation and testing were without success.

Electrode potential measurements.—As previously described, in the Brennert (23) method of electrolytic acceleration of the breakdown of passive surfaces, the electrode potential was used as a measure of the passivity of the surface toward a given corrosive solution. The potential measured was that of about 1 cm² of surface just before film breakthrough of the weakest point. The data obtained with the modified test and plotted in Fig. 4 indicate that in the region of low current densities (where, presumably, the weakest points break down) there is less distinction between various surface treatments than at higher current densities. One possible interpretation of this observation is that passivation, while reducing the number of weak points in the surface, is not effective in eliminating all types of the weakest points. Electrode potential measurements were also made in the present investigation to determine their relationship, if any, to the formation of pits.

Typical electrode potential data obtained during a regular run are plotted in Fig. 5. As the voltage across the specimen anode-platinum cathode was increased continuously from zero, there was a very rapid change in electrode potential of the specimen in the cathodic direction. During this period of rapid increase in electrode potential there was no measurable flow of current. This initial phase was terminated by a sudden leveling off of the electrode potential, which occurred despite continuing increases in the voltage across the cell. At this point current began to flow through the cell, indicating that electrochemical reactions, gas evolution, or pitting were taking place at the anode, and hydrogen was being evolved at the cathode. The electrode potential at which this sudden change occurred on pickled Type 316 stainless steel varied from 0.49 v to 0.64 v in three tests, and the voltages across the cell at this point were 0.6, 0.6, and 0.7 v. Further increases in voltage increased the current through the cell. Beginning at about 2.5 v (Fig. 5) the current increased linearly with increasing voltage. The slope of this line is the same for various specimens of a given steel in both the pickled and the passivated condition. The slope depends on the solution composition (specific conductance).

After current flowed through the cell, the electrode potential gradually changed in the cathodic direction in a somewhat irregular fashion. When pits formed the potential remained constant, or even decreased slightly. Then as the current through the cell increased, the potential increased again until another group of pits appeared, causing another leveling off or slight drop in electrode potential. This influence of the pits on the electrode potential was probably the reason for the observation, based on 50 runs, that the maximum potential reached at the end of the run is independent of the number of pits formed. However, there is some correlation between the maximum potential and the milliamperes per pit at the end of the run. On Type 304 stainless steel in 0.1*N* NaCl at 25°C the maximum potential changed 0.125 v when

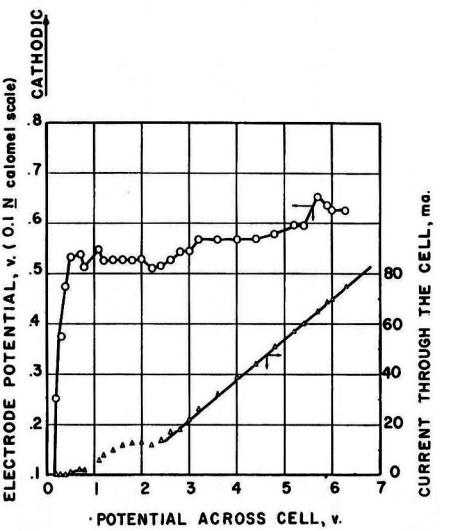

FIG. 5. Electrode potential of Type 316 stainless steel in the accelerated pitting test. Solution: 0.1*N* NaCl at 25°C; specimen: pickled only, 198 pits at end of run.

the calculated current density in the pits was increased from 0.3 to 1.8 ma/pit.

The weight loss per pit was inversely proportional to the total number of pits formed. Thus, when the total amount of electricity (coulombs = amp x sec) passing through the cell was constant (as in the case of repeat runs, given the steel and test solutions) the weight of metal dissolved was constant, and the amount removed from any one pit depended on the total number of pits. The size (depth and diameter) of pits formed during the electrolytic pitting test was essentially uniform on a given specimen when exposed to a certain solution. As the current density was increased continuously there was relatively rapid polarization of any pits that had been initiated. This increasing anodic polarization gradually resulted in complete passivity, i.e., the pits stopped growing. When this stage was reached, further increases in current density resulted in increases in electrode potential until another group of pits formed.

The electrode potential data obtained in a run using a steel which did not form any pits were similar to those of a run on a specimen which pitted readily (Fig. 5). The characteristics of the current-voltage curve were identical in both cases, and the electrode potential differed only in that, during the periods of current flow through the cell, the gradual change in the cathodic direction was more consistent and reached a maximum which was about 0.6 v higher than that given in Fig. 5. This again showed the influence of pit formation on the electrode potential. Pitting decreased the maximum potential at a given current density. At about 2.5 v across the cell the specimen surface became yellow, and soon thereafter gas bubbles appeared.

When the voltage across the cell was increased in discrete steps, rather than continuously, the electrode potential did not level off but dropped sharply in the anodic direction when current began to flow through the cell.

Electrochemistry of the pitting test.—As the potential across the specimen anode-platinum cathode is increased by application of an external emf while there is no current flow through the cell, a two-part layer forms on the specimen surface (26, 27). One layer, which is approximately a single anion in thickness, remains almost fixed to the solid surface. In this layer there is a sharp fall of potential. The second part extends some distance into the liquid phase and is diffuse. The distribution of positive and negative ions is not uniform since the electrostatic field of the anions at the surface results in preferential attraction of cations. The adsorption of anions on a (mercury) surface increases in the order $F^- < OH^- < Cl^- < Br^- < NO_3^- < I^- < ClO_4^- < CNS^-$ (Hofmeister or lyotropic series) (28). The least hydrated ions adsorb most readily on the metal surface. This double layer is electrically similar to a condenser of large specific capacity and causes a rapid change in electrode potential during the charging operation. The relation of anion adsorption on pit initiation is discussed in Part II. Increases in voltage across the cell eventually cause a flow of current and a considerably slower change in the electrode potential. The anodic processes responsible for current flow are usually assumed to take place in the order of greater oxidation potentials (26). In the case of a sodium chloride solution, oxygen (0.401 v) and chlorine (1.358 v) might be expected to be evolved in that order. However, it has been found that, on electrolysis of chloride solutions, chloride ions are discharged first and that evolution of oxygen soon follows, as the potential is changed in the more cathodic direction (26, 29). The order of anodic reactions depends on the concentrations of reactants and is probably related to the preferential adsorption of chloride ions during anodic polarization, which was found to prevent the formation of oxygen layers (30). Thus, in the electrolytic pitting test three reactions may take place on the anode: (*a*) discharge of chloride (halide), (*b*) evolution of oxygen, and (*c*) dissolution of metal, pitting.

During the current flow through the pitting cell, chloride ions migrate toward the specimen anode. This change in chloride-ion concentration in the solution surrounding the anode has been measured, confirming that the increase in concentration is proportional to the quantity of electricity (coulombs) passing through the cell (2). However, the change in chloride-ion concentration is not the controlling factor in acceleration of pit initiation in the test used in this investigation. It was shown above that pit initiation is not a function of the quantity of electricity passing through the cell, but only of the current density. Further support of this cause of pit initiation is given by the data on the effect of chloride-ion concentration (Part II) which showed that pit initiation actually decreases with increasing concentration of chloride ion in the pitting solution. Therefore, surface breakdown does not depend on the concentration of chloride ions in the solution around the specimen, but on the rate with which the chloride ions are brought to the surface. This is probably the determining factor in the adsorption, amount, and degree of surface coverage of the chloride ions on the stainless steel specimen.

II. Investigation of Variables in the Metal and in the Electrolyte Which Control Pit Initiation

Results of Pitting Tests

Pitting by various chlorides.—Nine different chloride salts were used for pitting tests on Type 304 stainless steel at 25°C. The solutions were 0.1*N* in chloride ion. All specimens were in the passivated condition and the standard testing procedure was used (*see* Part I). The chlorides tested and the results are given in Table II. Variation in pitting intensity among the various chlorides used was largely a function of the *p*H of these solutions. As the *p*H of the solution increased, the pitting intensity decreased. This was in agreement with other runs in which it was found that additions of sodium hydroxide to chloride solutions almost completely suppressed pit initiation. It was also in agreement with the results of other

TABLE II. *Effect of various chloride salts on pitting of stainless steel*

Steel, AISI-304 (ER-2) passivated; temp, 25°C; solution, 0.1*N* in chloride ion; standard test.

	*p*H	Pits/Cm²*
Chloride		
NaCl	6.22	3.4
$FeCl_2$	2.05	3.8
$CrCl_3$	3.14	4.5
$CuCl_2$	4.19	3.0
KCl	5.97	2.2
$CaCl_2$	6.90	3.2
$NiCl_2$	5.72	3.9
$MgCl_2$	6.20	2.3
LiCl	7.03	2.9
AISI-316		
NaCl	6.22	0.46
$FeCl_3$	2.05	1.3

* Average of 10 runs.

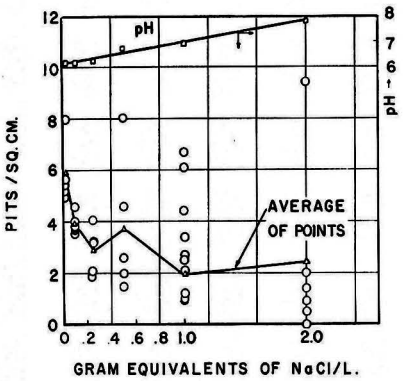

FIG. 6. Effect of concentration of NaCl on pitting of passivated AISI 304 steel (ER-2) at 25°C.

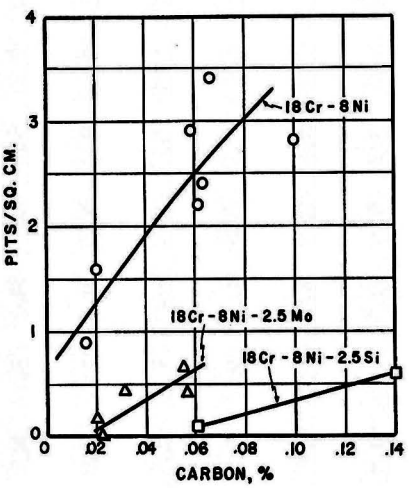

FIG. 7. Influence of carbon in stainless steels on pitting in 0.1*N* NaCl at 25°C in the standardized test. Specimens were pickled and passivated.

investigators (31–33) and with practical experience on the use of hydroxides to suppress chloride pitting of stainless steels. Thus, among the constituents of the solution, the chloride ion is the primary factor in the electrolytic pit initiation test, and the cationic member of the chloride salt plays only a minor role, if any.

Effect of chloride-ion concentration.—It was shown in Part I that the current density on the specimen rather than the quantity of electricity passing through the cell determined the number of pits formed per unit area. Since the quantity of electricity passing through the cell determined the chloride-ion concentration near the surface of the specimen, it was concluded that increasing the solution concentration would not appreciably affect pit initiation. To obtain further data on the effect of the chloride ion, tests were made in solutions 0.02–2*N* in sodium chloride. There was a tendency toward large numbers of pits in some runs, while the majority of specimens showed a definite decrease in pit initiation with increasing concentration of chloride ions (Fig. 6). On pickled Type 316 stainless steel (EW-5) the decrease was even more pronounced. The averages of ten runs were 7.3 pits/cm² at 0.1*N* sodium chloride and 0.92 pits/cm² in 1*N* sodium chloride.

The scatter in the data (Fig. 6) suggests that opposing factors are introduced as the chloride concentration is increased. Among those which contribute to a decrease in pit initiation are lower equivalent conductance and higher *p*H at higher chloride concentration. Increased adsorption of chloride ions at higher chloride concentrations may tend to increase pit initiation. These results on the effect of chloride concentrations on pit initiation are not expected to agree with studies of this effect based on weight-loss measurement, which include the results of pit initiation and growth. Uhlig (2) found an increasing weight loss with increasing concentration of chloride ions. The weight loss (total corrosion current) is a function of specific conductance, which increases rapidly with increasing concentration of sodium chloride.

Pitting of various grades of stainless steels in chloride solution.—To determine the influence on pit initiation of various alloying additions to the basic 18Cr-8Ni composition, all the more common types of the AISI-300 series steels and a number of special heats were submitted to the standardized, accelerated pitting test in 0.1*N* sodium chloride at 25°C. "Hastelloy" B and C were included for comparison.

Most alloys were tested in two conditions: pickled only, and pickled and passivated. Results are listed in Table III; some are plotted in Fig. 7.

In reference to Table III:

1. In every case the passivation treatment decreased pit initiation. The ratio (R) of the number of pits initiated in the pickled condition to that in the passivated condition may be used as a measure of the response of the steel to passivation. For the basic 18Cr-8Ni steels (304, 304L, 302, and 302B) this ratio is approximately 2.5.

Even though the pitting intensity of AISI-316 in the pickled condition is about the same as that of AISI-304, the response to passivation is much greater, $R = 15$. This ratio is 30 on the low-nitrogen, low-carbon, 18Cr-8Ni-Mo

(FH-3) steel. Thus, molybdenum additions do not change the basic (pickled) pitting resistance but greatly increase the response to passivation, especially on low-carbon steel.

This is in contrast to silicon additions, which considerably reduce pitting in the pickled condition but do not change the response to passivation.

2. In every case, decreasing the carbon content decreased pit initiation, Fig. 7. The basic 18Cr-8Ni curve includes AISI-302, 304, 304L, 321, 347, 347L. Addition of stabilizing elements, niobium in Type 347 and titanium in Type 321, did not affect pitting results. Since all steels were tested in the annealed condition (or in the case of Types 321 and 347 steels, the stabilized conditions), it may be concluded that carbon in solid solution (or in the form of titanium or niobium carbides) adversely affects pitting resistance. The nitrogen content of the steels used to obtain data for Fig. 7 was about 0.02%.

3. Steels containing higher amounts of nitrogen showed less pitting than those containing normal amounts of this element. The austenitic stainless steels normally contain about 0.02% nitrogen. A five to tenfold increase decreased pit initiation. This is in agreement with previously published results (10, 11) on stainless steels immersed in acidified ferric chloride.

4. These observations indicate that pitting resistance of the basic 18Cr-8Ni composition might be improved by additions of silicon, molybdenum, and nitrogen, and by keeping the carbon content as low as possible. An 18Cr-8Ni steel containing both molybdenum and silicon has already been described (9). The silicon and molybdenum contents were each limited to about 2.5% because of difficulties encountered in mechanical processing at higher percentages. Both of these elements are ferrite formers, and Riedrich's (9) steel contained 10–20% ferrite. A laboratory heat (SP-1) of this type of steel was prepared. It contained about 20% ferrite and did not pit in the accelerated laboratory test in the pickled or in the passivated condition at 25°C (Table III).

A second heat of 18Cr-8Ni-Mo-Si steel (SP-2) was made. Laboratory pitting results on low-carbon, high-nitrogen steels, described above, were considered in selecting the desired composition. The carbon content was reduced as much as possible (0.039%), and the nitrogen content was increased to 0.23%. The increase in nitrogen made the steel completely austenitic. As in the case of SP-1, there was no pitting in the accelerated laboratory test at 25°C.

Neither of these steels pitted in the accelerated test at 25°C, but under the more severe pitting conditions of sea-water exposure and immersion in ferric chloride, the high-nitrogen, low-carbon steel was definitely superior.

Effect of heat treatment on the pitting of stainless steels.— Stainless steels containing silicon were the most resistant to pit initiation in the accelerated pitting test. However, silicon in excess of about 1% increases the corrosion of annealed stainless steels in the standard, boiling 65% nitric acid test (36). In accordance with expectations, these steels (302B, SP-1, and SP-2) have nitric acid corrosion rates 2–40 times greater than the acceptable rate of 0.0015 in./mo (Table IV). The high rates were due to

TABLE III. *Pitting of various grades of stainless steels in 0.1N* NaCl *at 25°C (Influence of surface treatment)*

Steel, AISI type	Code	Description	Pits/cm²*		Ratio,
			Pickled	Pickled + passivated	Pickled/passivated
304	EX-1	C = .061	5.6†	2.2†	2.5
304	ER-2	C = .063	7.4	3.4	2.2
304L	FK-4	N = .033	4.5	1.6	2.8
304L	FK-9	N = .12		0.9	
302	GF-2	C = .10	6.3	2.8	2.2
302B	302B	Si = 2.5		0.1	
302B	302BP	Si = 2.7	1.5	0.6	2.5
321	FF-7	Ti = .31		2.4	
347	EX-2	Nb = .87		2.9	
347L	FE-6	C = .016		0.9	
316	EW-5	Mo = 2.47	7.3	0.46	15.8
316	C-1		6.6*	0.42	15.6
316	C-2			0.65	
316L	FH-3	N = .032	5.0	0.17	29
316L	FH-1	N = .13		0.0	
316L + Nb	FN-3	Mo = 2.15		0.0	
316 + Si	SP-1	Si = 2.4	0.0	0.0	
316 + Si	SP-2	N = .23	0.0	0.0	
"Hastelloy" B				0.0	
"Hastelloy" C				0.0	

* Average of 10 runs.
† Obtained from Fig. 4.

general corrosion, not intergranular attack. Since the object of the nitric acid tests is to detect susceptibility to intergranular corrosion, the lack of agreement between nitric acid corrosion rates and resistance to pit initiation was not surprising.

High rates on austenitic stainless steels in the nitric acid test are usually due to rapid intergranular attack on steels containing intergranularly precipitated chromium carbides (or other phases). Chromium carbides are precipitated most readily at about 1250°F (677°C) and greatly increase the nitric acid corrosion rate (Table IV, AISI-304 and 321).

Five different steels were tested in the accelerated, electrolytic pitting apparatus following a heat treatment of 1 hr at 1250°F (677°C). In two of these steels (AISI-304 and 321) large amounts of chromium carbide were precipitated at the grain boundaries. In two others no carbides were precipitated, because the carbon in the steel was very low (AISI-316L) or was held in combination with a stabilizing element (AISI-347). Results of pitting tests on heat-treated steels are given in Table V. On AISI-304 in the passivated condition there was essentially no difference (3.4 vs. 3.3 pits/cm²) between pit initiation of the annealed (carbon in solution) and the sensitized [1 hr 1250°F (677°C)] steel, containing large amounts of intergranularly precipitated chromium carbides.

Since all the chemically treated specimens were exposed to a pickling treatment which preferentially attacks the grain boundaries containing intergranularly precipitated chromium carbides, other methods of surface preparation were investigated. In place of chemical treatments, grinding on a 120-grit belt was used to prepare the surfaces for pitting. Even though the grain boundaries remained

TABLE IV. *Nitric acid corrosion rates of steels used for pitting tests*

Steel, AISI type	Code	Corrosion rate, in./mo	
		As-received	1 hr 1250°F, WQ
304	ER-2	0.00084	0.0276
304L	FK-4	0.00053	
302	GF-2	0.0010	
302B	302B	0.0139	
302B	302BP	0.0705	
316	EW-5	0.00081	0.00397
316L	FH-1	0.00090	0.0063
316 + Si	SP-1	0.00384	
316 + Si	SP-2	0.00321	
321	FF-7	0.00093	0.01239
347	EX-2	0.00068	0.00093
347L	FE-6	0.00063	

TABLE V. *Effect of surface preparation and heat-treatment on pitting of stainless steels in* 0.1*N* NaCl *at 25°C*

Steel, AISI type	Code	Pits/cm²*		
		Pickled	Passivated	Ground‡
304	ER-2	7.4	3.4	3.1
304†	ER-2†		3.3	5.0
316	EW-5	7.3	0.46	0.0
316†	EW-5†		0.76	
316L	FH-3	5.0	0.17	1.2
316L†	FH-3†	3.5	1.4	1.5
321	FF-7		2.4	3.9
321†	FF-7§		1.5	0.5
347	EX-2		2.9	6.7
347†	EX-2†		2.5	6.4

* Average of 10 runs.
† Heated 1 hr at 1250°F.
‡ Ground to 120-grit finish.
§ The amount of titanium added to this steel is insufficient to tie up all carbon. Thus, after heating for 1 hr at 1250°F there is extensive precipitation of chromium carbides at grain boundaries. This may explain in part the reduction in pit initiation following the (1 hr at 1250°F) heat treatment. After this heat treatment the amount of carbon left in solid solution may be unusually low. As shown in Fig. 7 there is a reduction in the number of pits/cm² when the carbon content in solid solution is reduced.

unattacked by this procedure, they were probably affected by the flowed metal layer formed during mechanical grinding. Also, the true surface area, and, therefore, the true current density during the test were altered to an unknown extent.

On some steels grinding increased pit initiation somewhat, while on others there was either no change, or a decrease, as compared with passivated specimens. The only exception was the AISI-316L steel on which pit initiation increased considerably in the "as-received" condition. However, even this steel showed no difference between passivated and ground specimens in the heat-treated condition [1 hr at 1250°F (677°C)]. So, this heat treatment did not influence pit initiation to any great extent under the present experimental conditions.

Effect of temperature on pit initiation.—To determine the effect of temperature on pit initiation, runs were made at 50° and at 70°C in 0.1*N* NaCl solution. Average results of ten runs at each temperature are plotted in Fig. 8 and 9.

Of particular interest is the large increase in pitting on Type 316 steel. This was investigated on three different heats and all showed a greater pit initiation at 50° and 70°C than any other AISI-300 series steel. The maximum displayed by one heat (EW-5) was checked by extra runs.

The addition of silicon to Type 316 stainless steel, as in SP-1 and SP-2, eliminated the large increase in pit initiation at higher temperatures. In general, the superiority of the steels containing silicon at 25°C held at higher temperatures also. However, both SP-1 and SP-2 steels pitted at temperatures above 25°C.

The decrease in pit initiation with increasing temperature found for AISI-304 steel was also observed for Type 302 stainless steel in which the number of pits per square centimeter changed from 2.8 at 25°C to 1.4 at 70°C.

The great variety of responses to pit initiation at elevated temperatures indicated that pitting data obtained for a certain stainless steel at one temperature could not be used to predict behavior for other steels or

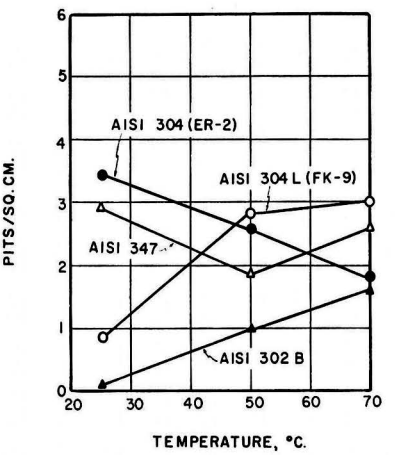

FIG. 8. Effect of temperature on pitting of 18Cr-8Ni steels in 0.1*N* NaCl.

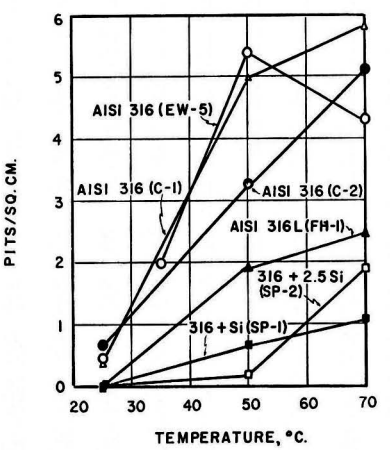

FIG. 9. Effect of temperature on pitting of 18Cr-8Ni-2.5Mo steels in 0.1*N* NaCl.

TABLE VI. *Effect of sodium nitrate on pitting of stainless steels in 0.1N* NaCl *at 25°C in the accelerated test*

Steel, AISI type	Condition	Pitting without inhibitor, pits/cm²	Minimum amount* of $NaNO_3$, g/l
304 (ER-2)	Pickled	7.4	0.60
304 (ER-2)	Passivated	3.4	0.40
316 (EW-5)	Pickled	7.3	0.25
316 (EW-5)	Passivated	0.46	

* Minimum amount of inhibitor required to suppress all pitting in the standard pitting test.

other temperatures. The versatility of temperature control possible in the accelerated, electrolytic test used in this study is one of its advantages over previously used accelerated tests, in which increased temperatures were used to produce accelerated corrosion. Some results on the effect of temperature on ferric chloride immersion tests are described below.

Inhibition of chloride pitting.—A number of pitting tests were made in 0.1*N* sodium chloride with sodium nitrate, a commonly used inhibitor for ferrous metals. Various amounts of sodium nitrate were added to determine the minimum amount of inhibitor required for suppression of all pitting in the standardized, electrolytic test. Results are listed in Table VI. The passivated specimens required less nitrate for inhibition than those that were pickled only. Also, the superior response of 18Cr-8Ni-2.5Mo (AISI-316 stainless steel) to passivating conditions was again evident. Even though in the pickled condition both AISI-304 and 316 pitted alike, the amount of nitrate required to suppress pitting on the pickled AISI-316 stainless steel was less than half the amount required for AISI-304 stainless steel.

The nitrate probably does not completely prevent breakdown of the surface but acts to heal rapidly and effectively all points which are beginning to break down and, thereby, prevents the formation of pits. Nitrate is consumed in the process of healing breaks in the protective film. Therefore, unless there is periodic replenishment, the initial addition of inhibitor merely delays the onset of corrosion (2, 37).

Protective film formation on corroding surfaces was observed on specimens which were scratched with a sharp instrument to produce a fresh surface. Two types of tests were made. In the first, SP-2 specimens were scratched in air before immersion in chloride solution (containing potassium ferrocyanide) for the accelerated, electrolytic test. There was no pitting or general corrosion in the scratches or on the unscratched surfaces during the test. In the second test, scratches were made while the steel was immersed in the chloride solution. Soon after the current was passed through the specimen, the scratch turned blue at about 0.3 ma/cm². However, as the current density was increased to about 1 ma/cm² the formation of blue ferri-ferro cyanide ceased, and what had formed earlier diffused away. Metallographic examination of the scratch after this test confirmed a small amount of general corrosion in the scratch.

Pit initiation by other halides.—To compare pitting properties of halogen salts, tests were made with the electrolytic apparatus in sodium fluoride, sodium bromide, and potassium iodide. Only the bromide salts pitted stainless steels so extensively that 0.01*N* solutions and a maximum current density of 2.3 rather than 3 ma/cm² were used for further tests.

TABLE VII. *Pitting of stainless steels in 0.01N* NaBr *at 25°C in the accelerated pitting test*

Steel, AISI type	Code	Pits/cm²*	
		0.01 *N* NaBr†	0.1 *N* NaCl
304	ER-2	6.4 (10)‡	3.4
304L	FK-9	3.4 (4)	0.9
304L	FK-4	3.2 (6)	1.6
316	EW-5	6.6 (10)	0.46
302B	302B	1.0 (9)	0.1
316 + Si	SP-1	1.8 (7)	0.0

* Passivated specimens.
† Maximum current density 2.3 ma/cm².
‡ Indicates number of specimens run.

Results of pitting tests in sodium bromide are listed in Table VII along with those obtained on the same steels in 0.1*N* sodium chloride. Even though the tests were made on passivated specimens, pit initiation on AISI-316 is the same as that on Type 304, in contrast to the behavior in 0.1*N* sodium chloride. It has been indicated that in bromide solutions the resistance to pit initiation of these two steels is identical (22). However, the weight loss on the 18Cr-8Ni-2.5Mo steel was lower than on 18Cr-8Ni steel (25) indicating that the steel containing molybdenum can heal more readily a surface breakdown. Weight-loss determinations give a measure of both pit initiation and pit growth and may, therefore, differ from pit initiation data.

As in the case of chloride solution, additions of about 2.5% silicon (302B, SP-1) to the 18Cr-8Ni and the 18Cr-8Ni-2.5Mo steels considerably increased the resistance to pit initiation in 0.01*N* bromide solution (Table VII).

Changes in pit initiation of AISI-316 steel with bromide ion concentration are shown in Fig. 10. An almost threefold increase in pit initiation was found but with practically no change in *p*H (cf. figure for chloride effect).

Pit initiation results with the various halides are generally in agreement with the Hofmeister series, i.e., the fluoride ion (no pitting) is the least readily adsorbed (most hydrated) and the bromide (greatest amount of pitting) is more readily adsorbed than the chloride. Also, nitrate ions, which inhibit pitting by chlorides, are more readily adsorbed than chloride ions. However, the iodide is even more readily adsorbed than any of the others, but does not pit in the accelerated test. It should be pointed out that adsorption of halide, while a necessary requirement for pit initiation, is only the first step in pit formation. Whether a pit forms depends on whether adsorption is followed by reaction between the surface and the halogen ion.

Correlation of results of electrolytic pitting test.—Total immersion tests of a number of stainless steels were made in 10% ferric chloride solutions for 72 hr and for 144 hr at 25°C and 50°C in order to compare with results of the accelerated pitting tests. Those steels which did not pit in the 72-hr periods also were immune to pitting after 144 hr. At 25°C, Type 316 stainless steel (passivated), "Hastelloy" C and the 316 + 2.5% Si (SP-2) steel did not

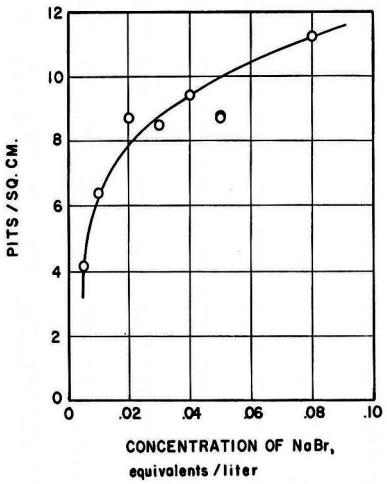

FIG. 10. Effect of concentration of NaBr on pitting of passivated AISI 316 (EW-5) steel in accelerated pitting test at 25°C. Maximum current density = 2.3 ma/cm².

pit (Cf. Table III and Fig. 8 and 9). At 50°C there was no pitting on the completely austenitic SP-2 alloy or "Hastelloy" C. Both AISI-304 and 316 steels pitted, but there were more pits on the Type 316 steel. The SP-1 steel which contained 10–20% ferrite pitted slightly at the stamped numbers.[3] These observations, even though based on a relatively brief exposure test in ferric chloride solution, nevertheless tend to confirm the results of the electrolytic test.

The 18Cr-8Ni steel containing 2.5% silicon (302B) showed relatively few pits, but these grew into enormous cavities underneath the surface. Thus, silicon, while decreasing pit initiation, could not be used alone to decrease pitting, but should be used together with molybdenum, which increased the response to passivation (film healing). The stabilized steels (AISI-321 and 347 steels) pitted more in ferric chloride than the other steels. This is in contrast to their behavior during simple immersion in sodium chloride, where they do not pit more than AISI-304 steel.

With sea-water exposure.—A set of 6 x 12 in. panels was completely immersed in sea water for 6 months.[4] During this period they were completely covered by a variety of marine organisms which produced severe crevice conditions. Only titanium, "Hastelloy" C, tantalum, and platinum are known to survive this type of exposure without attack. When the marine organisms were removed, it was found that "Hastelloy" C was unattacked, and the completely austenitic, high-nitrogen, low-carbon, silicon-modified Type 316 steel, SP-2, showed only minor edge attack on the two panels used. The samples resisted pitting in the order "Hastelloy" C, SP-2, SP-1, SP-3, AISI-316 stainless steel, AISI-304 stainless steel. These steels were then exposed for 6 more months with new nonmetallic washers mounted on them to render them more susceptible to crevice attack. The results of this second exposure confirmed those of the first 6 months. "Hastelloy" C was unattacked, and corrosion on the crevice on SP-2 was about one-half of that on AISI-316 stainless steel. Thus, the sea-water exposure tests confirm the results of the accelerated laboratory and the ferric chloride immersion tests, in that additions of silicon improve the pitting resistance of AISI-316 stainless steel and that low-carbon and high-nitrogen contents are also beneficial.

[3] A third heat of modified Type 316 steel, SP-3, containing about 50% ferrite, 3.7% Mo and 2.3% Si, was definitely less resistant to pit initiation than either SP-1 or SP-2.

[4] Exposure tests were made at the Harbor Island Marine Corrosion Test Station of the International Nickel Company.

METALLOGRAPHY OF PITTING

Previous investigators (19, 38) of the loci of pit initiation in stainless steel surfaces have come to the conclusion that depressions such as cracks, cusps, striations, and scarifications are the cause of pit initiation. Such depressions were thought to cause pitting by serving as minute reservoirs for the accumulation and stagnation of corrosive salt solution, which would result in a local electrolytic element (concentration cell). However, these depressions are not the sole cause, because steels which have been thoroughly pickled to remove depressions are still subject to pitting. Also, there is no relation between pitting and the number of nonmetallic inclusions (39). This is in agreement with the present investigation in which no correlation was found between the number of inclusions and the number of pits developed.[5]

Experimental methods.—Experiments were made in an effort to observe the loci of pit initiation. Such tests were difficult because the time required to form a pit was unpredictable and, once formed, pits grew so rapidly that it was almost impossible to observe the type of microstructure at which they originated. This was especially difficult on small-grained steels such as AISI 321 and 347. The pits had to be observed while they were smaller than one grain and on steels whose grain boundaries are readily etched. Therefore, this investigation on pit initiation was confined to AISI-304 stainless steel. In a few cases it was possible to observe pit initiation on polished surfaces during simple immersion. Other tests were made by observing portions of immersed surfaces while they were pitted electrolytically by making them anodic, as in the accelerated pitting test.

To observe the loci of electrolytic pit initiation, a stainless steel box was made with an open top and a window on one side. A polished stainless steel specimen was clamped about ¼ in. behind the window, the polished surface parallel to the window. This arrangement permitted observation of the immersed surface with a binocular microscope while the specimen was made anodic in chloride solution.

Two perpendicular lines were scratched on a polished surface to assist in the location of a specific area. Photomicrographs were then made of the polished surface in the four quadrants to locate nonmetallic inclusions. The specimen then either was immersed in chloride solution or electrolytically pitted in the box described above. As soon as pits were observed, the specimens were removed, dried, and photographed at the same magnification as before. By superimposing the two negatives, the relationship of pits to inclusions could be determined. The location of pits

[5] The free-machining, AISI-303 steel, which has numerous sulfide or selenide inclusions, is an exception.

FIG. 11. Electrolytically formed pit. Mechanically polished AISI 304 steel (annealed) pitted electrolytically in 0.1*N* NaCl and then electrolytically etched in nitric acid to bring out grain boundaries. 350× before reduction for publication.

in relation to grain boundaries was obtained by lightly etching a pitted surface to reveal the grain boundaries.

Results.—A characteristic pit formed electrolytically in chloride solution in the observation box is illustrated in Fig. 11. The large pit formed when the surface was penetrated in a small area, then grew rapidly into a large cavity underneath the surface. Progressive growth of the cavity caused further penetration of the surface from below. Part of the roof of the cavity then collapsed. The pit shown in Fig. 11 was formed by making the surface anodic. However, the morphology of pits formed by simple immersion was identical with that of pits formed electrolytically at low current densities.

Results of the metallographic techniques for study of pit initiation indicated that pits were formed primarily at grain boundaries in the metal surface. In Fig. 12 two photomicrographs are shown of polished Type 304 stainless steels which were immersed in ferric chloride solution. Pits formed at grain boundaries on both the annealed and heat-treated [1 hr at 1250°F (677°C)] specimens. Although some pits may have formed at inclusions, they were not preferred sites of attack. Whether the pits were formed by anodic treatment or by immersion, the majority were nucleated at grain boundaries. Only at the higher current densities and in the more aggressive pitting solutions (NaCl solutions to which HCl had been added) were larger numbers of pits nucleated in the interior parts of the grain surfaces. Thus, pits formed more readily at grain boundaries than on interior grain surfaces and appeared to be independent of the inclusions in stainless steels, except in the case of the steel (AISI-303) which contained large numbers of sulfide inclusions.[6]

[6] Because of the difficulty of reproducing the low-contrast prints, made from superimposed negatives which show the relation of pits to inclusions, none has been included in this paper.

These observations are supported by several other experimental results.

Effect of polishing.—In agreement with other results (7), resistance to pit initiation increased with the degree of mechanical polishing. Thus, a metallographically polished surface was more resistant to pitting than a belt-ground surface. During mechanical polishing, a layer of highly deformed metal was produced on the surface, which probably covered and obscured the grain boundaries. This view was given further support by the fact, observed in this study, that electropolishing produced a surface which was the most susceptible of all to pit initiation. In this case, metal was removed selectively from the surface by electrolytic action without the formation of a flowed metal layer to obscure grain boundaries.

Effect of heat treatment.—During heat treatment of 1 hr at 1250°F (677°C) of certain stainless steels large quantities of intergranular inclusions (chromium carbides), which frequently enveloped almost all grains, were formed. These intergranular "inclusions" did not affect appreciably pit

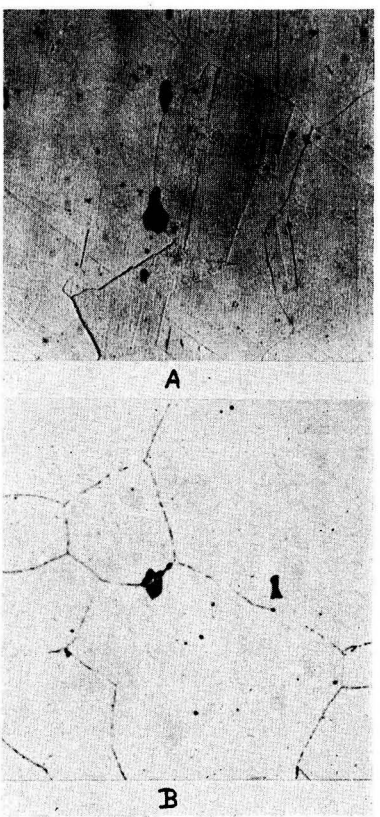

FIG. 12. Pits formed by simple immersion. Mechanically polished specimens of AISI 304 steel immersed 24 hr in 10% ferric chloride solution and etched electrolytically in oxalic acid to bring out grain boundaries. A, annealed—carbides in solid solution; B, sensitized—heated 1 hr at 1250°F to precipitate chromium carbides at grain boundaries. Note large inclusion near grain boundary which did not cause pit formation. 350× before reduction for publication.

initiation (Table V). However, in ferric chloride they accelerated pit growth along grain boundaries (40). The role of chromium carbides in pit initiation appeared no more significant than that of other nonmetallic inclusions in stainless steels, which have not been found to influence pit initiation.

Effect of grain-boundary etching.—When the grain boundaries on polished steels were electrolytically etched in nitric acid before electrolytic pitting in sodium chloride solution, pits formed almost entirely in the grain centers and only rarely at grain boundaries. Etching appeared to desensitize the grain boundaries toward pit initiation. This may explain the effect of pickling treatments by a titanium chloride, hydrochloric acid, sulfuric acid, and nitric acid on the pitting of stainless steels. The solution vigorously attacks stainless steels, but makes them more resistant to pitting in chloride solutions; Uhlig (38) stated that the steels became more resistant to pitting because mechanical depressions, adherent particles, and inhomogeneities were removed by pickling. Action of the pickling treatment on reducing pit initiation may also be assumed to involve desensitization of the main sites of pit initiation, i.e., the grain boundaries.

A further relationship between grain-boundary etching and pit initiation was shown by etching characteristics of the 18Cr-8Ni-2.5Mo-2.5Si steels. These steels (SP-1 and SP-2) were the most resistant to pit initiation and were also the most difficult to etch. The usual electrolytic etching reagents (oxalic acid and sodium cyanide) did not reveal the austenitic grain boundaries. Aqua regia solutions were required to bring out the grain structures.

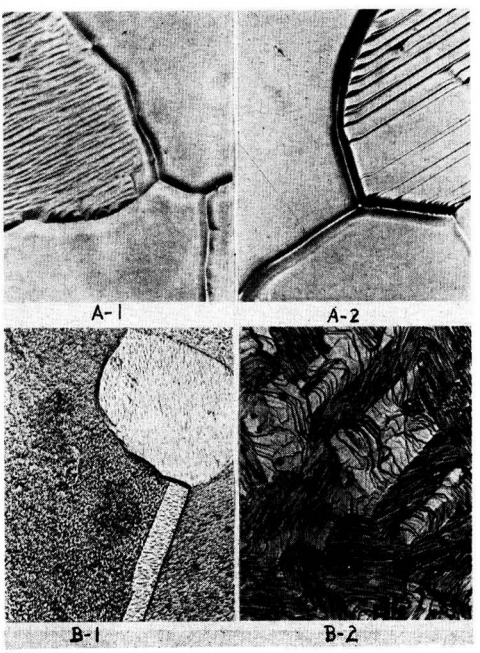

FIG. 13. Thermally etched stainless steels (etched by heating 24 hr at 2000°F in evacuated tube). A-1, AISI 304 (18Cr-8Ni); A-2, AISI 316 (18Cr-8Ni-2.5Mo); B-1, AISI 302B (18Cr-8Ni-2.5Si); B-2, SP-1 (18Cr-8Ni-2.5Mo-2.5Si). 1000× before reduction for publication.

Thermal-etch structures.—The pronounced influence of silicon on grain-boundary properties was further illustrated by the response of various stainless steels to thermal etching. Polished metal surfaces were etched by heating at high temperatures in controlled atmospheres or in vacuum. At elevated temperatures, structures were formed by surface diffusion which reflected the crystallographic characteristics of the grains and their boundaries. A relatively simple method was developed for thermally etching stainless steels. A polished stainless steel specimen was placed in a 12-in. long quartz tube which was heated to 400°C, evacuated to 5×10^{-5} mm Hg, and sealed. For thermal etching this tube was placed in a combustion tube furnace with the specimen in one end of the tube and the other end protruding 1–2 in. from the furnace to act as a condenser. The specimen was then heated at 1093°C for 24 hr and allowed to cool in the furnace. When cool, the tube was cracked open to remove the specimen.

Photomicrographs of four thermally etched stainless steels are given in Fig. 13. The 18Cr-8Ni (Type 304) and 18Cr-8Ni-Mo (Type 316) steels showed pronounced grooving at the grain boundaries. The angle at the bottom of these grooves varied with the orientation of the grains as well as the orientation of the boundary (41). The addition of about 2.5% Si, to give AISI-302B and the SP steels, completely eliminated all grooving at the grain boundaries, and in some cases produced pronounced steps between grains. Thus, there was a marked effect produced by silicon in these steels on the properties of their grain boundaries, which were the primary sites of pit initiation. It was demonstrated in a number of tests described above (Tables III and VII) that silicon additions to 18Cr-8Ni stainless steels increased the resistance to pit initiation. Thus, thermal etches provided further evidence for the primary role of grain boundaries in pit initiation.

Summary and Discussion

The present investigation showed that pitting resistance of 18Cr-8Ni stainless steels may be increased: (*a*) by increasing the basic resistance to pit initiation, and (*b*) by increasing the response to passivation, i.e., the ability to heal breaks in the protective films. Additions of silicon changed the properties of grain boundaries, which were the primary sites of pit initiation. Molybdenum additions to stainless steels did not change the grain-boundary properties, but greatly increased the ability of the steel to heal breaks in the protective film and to respond to oxidizing inhibitors. Lowering the carbon content increased the basic pitting resistance and also increased the response to passivation (Table III). The role of nitrogen in increasing pitting resistance was more difficult to determine. Nitrogen in its role as an austenitizer eliminated ferrite in the steels containing silicon and molybdenum and probably contributed to pit corrosion resistance in this way. The results on SP steels supported this conclusion. It has also been reported that 18Cr-8Ni-2.5Mo steels, containing ferrite, pit more readily than those which are completely austenitic (8). In addition, there is some evidence that increasing

the nitrogen content of completely austenitic steels improves pitting resistance (Table III).

The improvement in pitting resistance (initiation and growth) of 18Cr-8Ni stainless steels produced by individual use of silicon or nitrogen additions or removal of carbon was relatively small. However, when used in combination (molybdenum, silicon, and nitrogen additions, and removal of carbon) the resulting austenitic alloy (SP-2) was superior to the regular 18Cr-8Ni-2.5Mo (Type 316) steel, even in sea water.

The unique physical and chemical properties of grain boundaries have been revealed in a large variety of measurements (42). They are frequently preferred sites for the accumulation of impurities, for precipitation of new phases from solid solution, for adsorption, and for chemical attack. The boundary represents a transition from one crystal lattice to another. Such transition regions have a high density of lattice imperfections, i.e., dislocations, which are sites of preferential chemical attack (43, 44). These imperfections probably influence the structure and properties of any films formed on them. Thus, the portions of the protective film over the imperfections probably also contain structural imperfections, which are more susceptible to breakdown than other portions of the surface.

On exposure of a stainless steel surface to chloride solutions there probably is preferential adsorption (especially at grain boundaries) of chloride ions, which tends to exclude adsorption of film healing oxygen, as in the case of platinum surfaces (30). At certain imperfections in the protective film, occurring primarily at grain boundaries, cations from the metal can diffuse through the film more readily than at other points (45, 46).

This diffusion process may also be accelerated if chloride ions become imbedded in the lattice of the protective film; these chloride ions would then prevent the formation of protective oxides (47). Thus, chloride ions may contribute in several ways to the breakdown of protective films and may also prevent the healing of such points of breakdown by excluding oxygen and by decreasing the *p*H of the solution adjacent to the surface. In acid solution, solid corrosion products, which might serve to plug any points of film penetration, become soluble (48).

The enhanced self-passivating property of 18Cr-8Ni stainless steel containing molybdenum has also been demonstrated by a reverse of the breakdown method. In this technique, electrode potential measurements are made on stainless steels which have been activated by chemical pickling (35, 49, 50) or mechanical scratching (51) to determine whether or not, and the rapidity with which, passivity is reestablished in a given solution. It was found that molybdenum additions to stainless steels greatly increase the rate at which passivity is restored. In the present investigation it was concluded in agreement with others (35, 49, 51) that passivity is restored by a protective film which is a product of the reaction between the corroding metal and some constituent of the potentially corrosive solutions. The temperature of the corroding solution greatly influences the capacity for self-passivation. This is shown by the results on the influence of molybdenum on pit initiation at temperatures between 35° and 70°C. The beneficial effects of molybdenum, observed at room temperature, are lost at higher temperatures.

This dynamic view of passivity is supported by the fact that certain inhibitors are consumed, even though the metal being inhibited does not corrode appreciably. At numerous points of incipient breakdown in the surface the inhibitor reacts with the metal ions diffusing through nonprotective areas to form protective films before actual pits are formed.

ACKNOWLEDGMENT

The author wishes to thank Mr. F. L. LaQue, Vice President, and Dr. T. P. May, The International Nickel Company, New York, N. Y., for arranging the sea-water exposure tests and Mr. J. L. Sheppard and Mr. S. J. Kucharsey for their assistance with the experimental work.

Manuscript received September 14, 1955. This paper was prepared for delivery before the Pittsburgh Meeting, October 9 to 13, 1955.

Any discussion of this paper will appear in a Discussion Section to be published in the June 1957 JOURNAL.

REFERENCES

1. R. H. BROWN AND R. B. MEARS, *Trans. Faraday Soc.*, **35,** 467 (1939).
2. H. H. UHLIG, *Trans. Am. Inst. Mining Met. Engrs.*, **140,** 442 (1940).
3. R. B. MEARS AND R. H. BROWN, *This Journal*, **97,** 75 (1950).
4. O. B. ELLIS AND F. L. LAQUE, *Corrosion*, **7,** 362 (1951); *see also* E. WYCHE, L. R. VOIGHT, AND F. L. LAQUE, *Trans. Electrochem. Soc.*, **89,** 149 (1946).
5. F. G. FRESE, *Ind. Eng. Chem.*, **30,** 83 (1938).
6. International Nickel Co., "Nickel Topics," **4,** [2], 7 (1951).
7. H. A. SMITH, *Metal Progr.*, **33,** 596 (1938).
8. S. P. ODAR AND H. A. SMITH, *Trans. Am. Inst. Mining Met. Engrs.*, **135,** 526 (1939).
9. G. RIEDRICH, *Metallwirtschaft*, **21,** 407 (1942).
10. W. TOFAUTE AND H. SCHOTTKY, *Arch. Eisenhüttenw.*, **14,** 71 (1940); *see also* H. BENNEK, **15,** 515 (1942).
11. H. H. UHLIG, *Trans. Am. Soc. Metals*, **30,** 947 (1942).
12. U. R. EVANS AND R. B. MEARS, *Proc. Roy. Soc.*, **146A,** 153 (1934).
13. R. B. MEARS, *Iron Steel Inst. (London) Carnegie Schol. Mem.*, **24,** 69 (1935).
14. R. B. MEARS AND R. H. BROWN, *Ind. Eng. Chem.*, **29,** 1087 (1937); *Trans. Electrochem. Soc.*, **74,** 495 (1938).
15. R. B. MEARS AND U. R. EVANS, *Trans. Faraday Soc.*, **31,** 527 (1935).
16. P. M. AZIZ, *This Journal*, **101,** 120 (1954).
17. H. A. LIEBHAFSKY AND A. E. NEWKIRK, *Corrosion*, **9,** 432 (1953).
18. R. MAY, *J. Inst. Metals*, **32,** 65 (1953).
19. J. WULFF, H. A. SMITH, AND H. H. UHLIG, Progress Reports to the Chemical Foundation, Massachusetts Institute of Technology No. I-VI (1936-38).
20. W. A. WESLEY AND C. H. LINDSLEY, *Metals and Alloys*, **8,** 335 (1937).
21. H. J. DONKER AND R. A. DENGG, *Korrosion u. Metallschutz*, **3,** 217, 241 (1927).
22. H. H. UHLIG AND J. WULFF, *Trans. Am. Inst. Mining Met. Engrs.*, **135,** 494 (1939).
23. S. J. BRENNERT, *J. Iron Steel Inst. (London)*, **135,** 101 (1937); *also Korrosion u. Metallschutz*, **13,** 379 (1937).
24. U. R. EVANS, "Metallic Corrosion, Passivity and Protection," p. 21, Ed. Arnold & Co., London (1946).
25. E. M. MAHLA AND N. A. NIELSEN, *Trans. Electrochem. Soc.*, **89,** 167 (1946).

26. S. Glasstone, "Textbook of Physical Chemistry," pp. 1016, 1221, D. Van Nostrand Co., New York (1947).
27. O. Stern, *Z. Elektrochem.*, **30**, 508 (1924).
28. D. C. Grahame, *Chem. Rev.*, **41**, 441 (1947).
29. A. Hickling, *Trans. Faraday Soc.*, **41**, 333 (1945).
30. B. Ershler, "Discussions of the Faraday Society on Electrode Processes," No. 1, p. 269, Gurney and Jackson, London (1947).
31. L. Cavallaro and C. Bighi, *Metallurgia ital.*, **44**, 361 (1952).
32. J. W. Matthews and H. H. Uhlig, *Corrosion*, **7**, 419 (1951).
33. H. H. Uhlig and M. C. Morrill, *Ind. Eng. Chem.*, **33**, 875 (1941).
34. K. Bungardt, *Stahl u. Eisen*, **70**, 582, 589 (1950).
35. W. G. Renshaw and J. A. Ferree, *Corrosion*, **7**, 353 (1951).
36. M. H. Brown, W. B. DeLong, and W. R. Myers in "Symposium on Evaluation Tests for Stainless Steels," STP-93, A.S.T.M. p. 103-120 (1949).
37. E. M. Mahla and N. A. Nielsen, Unpublished results.
38. H. H. Uhlig, U. S. Pat., 2,172,421, Sept. 12, 1939.
39. E. E. Thum, "Book of Stainless Steels," p. 693, American Society for Metals, Cleveland (1935).
40. N. A. Nielsen, Unpublished results.
41. B. Chalmers, R. King, and R. Shuttleworth, *Proc. Roy. Soc.*, **A193**, 465 (1948).
42. R. King and B. Chalmers, "Progress in Metal Physics I," pp. 127-62, Interscience Publishers Inc., New York (1949).
43. R. Gevers, S. Aurelinckx, and W. Dekeyser, *Naturwissenschaften*, **39**, 448 (1952).
44. W. T. Read, "Dislocations in Crystals," p. 158, McGraw-Hill Book Co., New York (1953).
45. J. V. Petrocelli, *Trans. Electrochem. Soc.*, **97**, 10 (1950).
46. T. P. Hoar and U. R. Evans, *This Journal*, **99**, 212 (1952).
47. E. J. W. Verwey, *Philips Tech. Rev.*, **9**, 46 (1947); "Proceedings of the International Symposium on the Reactivity of Solids," Part II, p. 844. Elanders Boktryckeri, Gothenburg (1952).
48. T. P. Hoar, "Discussions of the Faraday Soc. on Electrode Processes," No. 1, p. 299, Gurney and Jackson, London (1947).
49. L. Guitton, *Metal Treatment*, **14**, [53], (1948).
50. H. H. Uhlig, *Trans. Am. Inst. Mining. Met. Engrs.*, **140** 387 (1940).
51. G. V. Akimov and G. B. Clark, *Compt. rend. acad. sci. U.R.S.S.*, **45**, 379 (1944).

A Study of Whisker Formation in the Electrodeposition of Copper

P. A. van der Meulen and H. V. Lindstrom

Ralph G. Wright Laboratory, Rutgers University, New Brunswick, New Jersey

ABSTRACT

Under certain conditions the electrolysis of acid copper sulfate between copper electrodes leads to formation of long filaments, or "whiskers," of copper on the cathode. Certain additives in the electrolyte are capable of overcoming the tendency toward abnormal growth and act to give smooth copper deposits. Possible mechanisms involved in electrolytic copper filament formation and its prevention are discussed, and a reasonable hypothesis to explain the process is suggested.

Introduction

In commercial copper electrorefining with acid copper sulfate electrolyte the current density is usually around 2.0 amp/dm^2 (18 amp/ft^2). This leads to copper deposits which tend to give nodules or trees unless smoothing agents are added. If the current density is quite low (0.05-0.10 amp/dm^2) and if the electrolyte is quite pure, a fairly smooth deposit is obtained. Under some conditions the deposits at these low current densities show abnormalities which do not occur at higher current densities and may, therefore, be considered characteristic of low current operation. These abnormalities are manifested as fine filaments or "whiskers" of copper on the cathode. Only a small part of the copper deposited electrolytically appears in the form of whiskers. In one case this amounted to about 5% of the total, the other 95% forming a fairly smooth deposit. Calculation reveals that copper deposition at the tip of the whisker takes place nearly a thousand times as fast as on the smooth part of the cathode. At higher current densities these growths appear to form nodules or spikes.

Most of the references in the literature on the subject of metal whiskers relate to filaments formed on metals in dry environments. Wakelin (1) reported the appearance of whiskers on heated copper and has given a review of the subject. Compton, Mendizza, and Arnold (2) described whisker growths on metal surfaces used in telephone communications equipment. In the field of copper electrodeposition from acid copper sulfate baths, copper whiskers were described by Gollop (3) who stated that very low current densities and absence of motion of cathode or electrolyte are needed before filaments can grow. Turnbull (4) described the appearance of copper spikes on cathodes in large electroforming baths which contain chloride and which are operated at higher currents.

This paper reports a study of the growth of fine copper filaments on copper cathodes in acid copper sulfate cells operated at low current densities. Two types of whiskers

grew under these conditions. One, grown in the presence of chlorides, is a straight needle-like filament which may have the appearance of a single crystal. The other, grown in the presence of cationic surface-active agents, appears as a polycrystalline filament which is a twisting hair of varying diameter.

Experimental

The Experimental Cell

Results of work in open beakers were not reproducible. It was suspected that whiskers could not accumulate enough copper to grow to visible size in beaker experiments because they dissolved in the oxygen-containing electrolyte. To test the dissolution tendency of copper under these conditions, copper strips were partially submerged in acid copper sulfate solution open to the air. It was noted that copper dissolved fairly rapidly at the air-electrolyte interface. However, if antioxidants (such as tertiary butyl cresol) were added to the electrolyte, the rate of loss of copper at this interface was very low.

To control all factors which might affect copper filament formation, a closed glass cell was constructed. High purity copper electrodes could be inserted and tightened to give a glass-to-copper contact. The cell volume was about 30 ml, but cells two and three times as large gave identical results. Fig. 1 shows the parts in proper relative positions before assembling.

The control electrolyte consisted of reagent grade copper sulfate pentahydrate (120 g/l), reagent grade sulfuric acid (72 g/l), and reagent grade hydroxylamine sulfate (5 g/l). The presence or absence of the hydroxylamine sulfate had no effect on whisker manifestation. However, it did give finer grain deposits and was included to insure smooth control cathodes for purposes of comparison. The electrolyte was at equilibrium with air prior to its addition to the cell. The cell was then sealed with a glass stopper so that the electrolysis was performed without further contact with air. In no instance could filaments be formed with the control electrolyte alone. When filament-generating substances were present in the electrolyte, whisker formation took place to a maximum extent if nitrogen gas was used to sweep the cell and its contents prior to electrolysis. If the cell and its contents were treated with oxygen gas to saturate the electrolyte prior to electrolysis, practically no whiskers formed. This was an indication that whiskers in their early stage probably dissolve in the electrolyte with the aid of oxygen and are prevented from growing. If the cells which had been treated with oxygen were allowed to run longer at the usual current or were run at somewhat higher currents, some whisker formation did take place. It is likely that the oxygen is depleted, then the filaments grow.

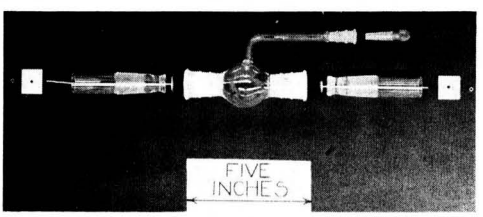

Fig. 1. Glass cell and copper electrodes used in this work to grow copper filaments electrolytically.

Filaments Generated by Chlorides

Chlorides have been used for many years as addition agents in copper electroplating baths utilizing acid copper sulfate. This halide reportedly removes silver as silver chloride and keeps the codeposition of antimony and bismuth with copper to a minimum. The concentration used in practice varies from 10 to 50 mg/l as chloride ion. A comprehensive study of the effect of chlorides on copper deposition was made by Winkler and co-workers (5, 6). They showed that chloride ions in acid copper sulfate have no effect on electrode processes below a definite minimum concentration (9 mg/l at 25°C), corresponding to the solubility of cuprous chloride in their electrolyte. Their work was concerned with electrode appearance and polarization, so they did not mention whisker formation. They operated at about 2 amp/dm², much too high for filament formation at low chloride levels, according to the present work.

Here chloride was added as the calcium and sodium salts and as hydrochloric acid; all were effective in growing filaments. Only hydrochloric acid was used after preliminary experiments had shown that chloride ion is the essential constituent. It was found that whiskers would grow at 25°C from electrolyte containing chloride in the range from 5–15 mg/l. Above this level a coating of white cuprous chloride formed on the cathode. The optimum appeared to be 10 mg/l which corresponds to the 9 mg/l mentioned above (5, 6). The most effective current densities for whisker formation, utilizing chloride at 10 mg/l, were in the range of 0.05–0.20 amp/dm². Under these conditions whiskers develop in about 48 hr. At higher values the filaments became branched, changed into trees, or collapsed into nodules. Fig. 2 is a photograph of the whisker type brought about with chloride at 10 mg/l. The filaments are straight and needle-like with a sharp point and have the appearance of single crystals.

At first the chloride experiments were not reproducible.

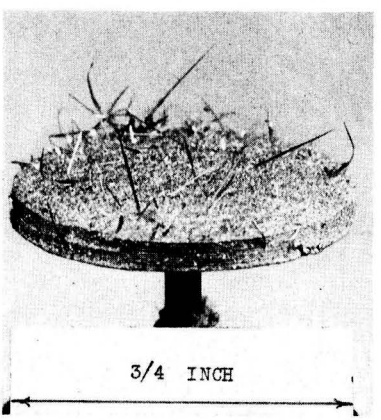

Fig. 2. Copper filaments grown with chloride at 10 mg/l using a current of 0.07 amp/dm².

Under apparently identical conditions, some cells might produce whiskers and others not. The cause of these variations was traced eventually to the presence of suspended particles in the electrolyte. If the electrolyte with chloride present was filtered through an ultrafine filter[1] prior to use, the variability disappeared almost completely and essentially no filaments would form. The effect of suspended particles was confirmed by adding such materials as carbon black, clay, or silica to the filtered electrolyte. Invariably such additions increased whisker formation by chloride ion and gave satisfactory reproducibility. The presence of these added particles did not bring about filament growth in the absence of chloride. It seems to be clear that dust and foreign material present in supposedly pure chemicals play an important role in the whisker formation brought about by chloride ion.

Filaments Generated by Cationic Surface-Active Agents

Copper filaments, of a type different from those grown with chloride, could be formed on the cathodes in the presence of cationic surface-active agents in the electrolyte. Except for substituting surface-active agents for chloride, all operating conditions were the same. These filaments were polycrystalline and grew in a twisting fashion. They were fine hairs elongated to a considerable extent, in contrast to the relatively short, thick needles formed in the presence of chloride. Fig. 3 is a photograph of filaments formed with cetyl trimethyl ammonium bromide as the generating substance. Similar filaments were grown with cetyl dimethyl ethyl ammonium bromide and cetyl pyridinium bromide. No whisker formation was possible with tetramethyl ammonium bromide. These surface-active agents, being cationic, may migrate to the cathode, and this fact probably may play a large role in filament formation. Various anionic and nonionic surface-active agents did not produce whiskers on the cathode. Suspended particles were shown to play a role here as well as in the case of chloride, because solutions containing cetyl trimethyl ammonium bromide filtered through an ultrafine glass filter did not produce filaments.

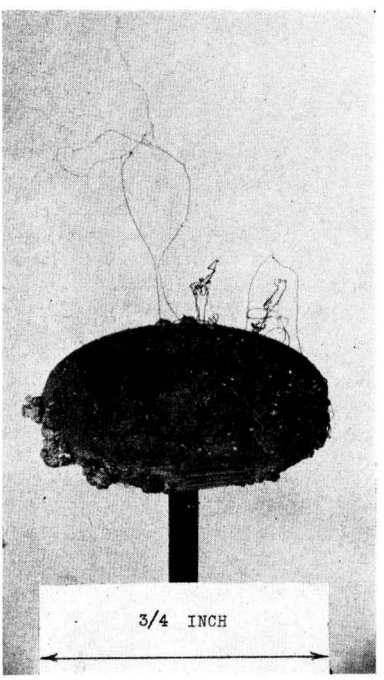

FIG. 3. Copper filaments grown with cetyl trimethyl ammonium bromide at 100 mg/l.

[1] Bacteria Filter Apparatus No. 68235, Emil Greiner Co.

Certain cationic polysoaps, described by Strauss and Gershfeld (7), are also capable of producing hairlike filaments. In this case, however, the whiskers are shorter and quite brittle in comparison to the wire-like and ductile filaments produced in the presence of cetyl trimethyl ammonium bromide. One of Strauss' polysoaps (polymerized vinyl pyridine partially quaternized with lauryl bromide and labeled G 147) gave reproducible results and was studied in detail. In this instance, passage through the ultrafine filter prior to electrolysis did not prevent the formation of filaments. This is very likely due to the fact that dispersed G 147 polysoap is not filtered out but still has a particle size capable of aiding whisker growth. This is in addition to its action as a cationic surface-active agent.

The cationic surface-active agents described here bring about whisker formation most readily at concentrations from 20 to 100 mg/l in electrolyte.

Cathode Potentials

The influence of various whisker-forming agents, in a concentration of 100 mg/l, on the cathode potential was studied in a glass electrolytic cell operating at 0.07 amp/dm^2. These potentials were measured by the use of a calomel half-cell dipping into an electrolyte reservoir connected to the cell by means of a glass tube of small bore, the tip of which was placed almost in contact with the cathode surface. Readings were made with a L&N Type K potentiometer. Observed increases in cathode potential are given in Table I. The whisker promoters, cetyl pyridinium bromide, cetyl trimethyl (or dimethyl ethyl) ammonium bromide, and the quaternized polysoaps give large increases and therefore may have a strong tendency to form a film on the cathode. Materials which did not promote whiskers show small increases to indicate a lesser tendency to form a cathode film. The effect of chloride at 100 mg/l was included, even though this level is too high for filament formation by chloride. It indicates that the chloride mechanism probably differs from the surface-active agent mechanism. It might be noted here that it was possible to obtain chloride whiskers at 100 mg/l by the use of higher currents (0.50 amp/dm^2). Some relationship exists between chloride level and current density as far as whisker formation is concerned. Thick spikes of copper in large electroplating baths do occur under conditions of commercial operation where the chloride level and current density are both higher than in the cells under discussion.

TABLE I. *Relation between cathode potential and filament formation*

Additive (100 mg/l)	Increase in cathode potential (mv)	Filament formation
Cetyl pyridinium bromide	225	Good
Cetyl trimethyl ammonium bromide	251	Good
Cetyl dimethyl ethyl ammonium bromide	254	Good
Tetramethyl ammonium bromide	1	None
Polysoap G146 (Strauss)	224	Good
Polysoap G147 (Strauss)	270	Good
Polysoap G254 (Strauss)	224	Fair
Polyvinyl pyridine (Strauss) (not quaternized)	23	Poor
Chloride ion (HCl)	27	Good at higher current

Influence of Various Factors on Filament Formation

It has been shown above that filaments of copper grow most readily when the proper generating agent (chloride or cationic surface-active agent) is present, when the current density is low, and when oxygen is absent. Other factors have little, if any, bearing on the formation of whiskers. Although high purity copper was used in these experiments, it was found that whiskers would grow also on impure copper cathodes. When the standard electrolyte was diluted to one-half and to one-fourth concentration with distilled water prior to use, filaments grew as readily as in the more concentrated solution. Whiskers grew regardless of the position of the electrodes. The general manifestation was the same whether the electrodes were vertical or horizontal, or whether the cathode was the upper or lower electrode. When the cells were rotated slowly and continuously during the electrolysis the whiskers gave way to nodules.

Prevention of Whisker Growth

A search was made for materials which could be added to the electrolyte to prevent formation of whiskers by polysoap G 147, which was chosen as a standard filament generator. Results are given in Table II. Cystine and thiourea prevent filament formation if added just prior to cell operation. However, they are unstable in the electrolyte and lose their effectiveness. The successful smoothing action of pure phenazine and of the phenazine dyes (Safranine T and Neutral Red) indicates a unique ability of the phenazine grouping to stop whisker growth. When the phenazine group of safranine is opened to give an indamine molecule (by the use of Toluylene Blue dye) whisker growth is unhampered. Both of the nitrogen atoms in the center of the phenazine molecule appear to be necessary for effective smoothing action. When one of these nitrogen atoms is replaced by oxygen, sulfur, or carbon (by selecting, respectively, Brilliant Cresyl Blue, Thionin, and Acridine) the smoothing action is lost.

Safranine dyes continue to prevent whisker formation after prolonged aging of the electrolyte at room temperature. Dye preparations of Safranine T (Du Pont 125%) in a concentration of 20 mg/l in electrolyte have been effective after an aging period of four months. The chromophoric nature of the dye undergoes a change, however, after such storage. The absorption spectrum of freshly prepared Safranine T in electrolyte shows a single peak at 5200Å, but on standing the 5200Å peak decreases in height and a new peak appears at 4400Å. Since the smoothing action is dependent on the phenazine group, and the phenazine group itself has no dye properties, a change of color does not necessarily indicate a loss of smoothing action.[2]

TABLE II. *Effect of additives on "whisker" formation by Polysoap G147 (100 mg/l)*

Additive	Concentration of additive (mg/l)	Smoothing action on cathode
Anionic detergent (Sodium lauryl sulfate)	100	Poor
Nonionic detergent (Polyoxyethylated nonylphenol)	100	Poor
Aniline	100	Poor
Phenylhydrazine	25	Poor
Nitrobenzene	25	Poor
Azoxybenzene	25	Poor
Cresol Indophenol	25	Poor
Chrysoidine Y	25	Poor
Ethylene Diamine	25	Poor
Malonic ester	25	Poor
Methionine	100	Poor
Cystine (freshly added)	50	Excellent
Cystine (after 30 days at 25°C in electrolyte)	50	Poor
Thiourea (freshly added)	50	Excellent
Thiourea (after 30 days at 25°C in electrolyte)	50	Poor
Bismarck brown Y	100	Poor
Zambesi black VD	100	Poor
Supranol brown RL	100	Poor
Safranine T (freshly added)	20	Excellent
Safranine T (after 4 months at 25°C in electrolyte)	20	Excellent
Neutral red	20	Excellent
Phenazine	20	Excellent
Brilliant cresyl blue	20	Poor
Thionin	20	Poor
Acridine	20	Poor
Toluylene blue	20	Poor

TABLE III. *Cathode potentials brought about by mixtures of polysoap and smoothing agents*

Electrolyte additive (G147 Polysoap 100 mg/l) (smoothing agents 20 mg/l)	Cathode potential (mv)
G147 Polysoap alone	273
Cystine alone	37
Cystine plus G147 Polysoap	250
Thiourea alone	33
Thiourea plus G147 Polysoap	276
Safranine alone	70
Safranine plus G147 Polysoap	78
Neutral Red alone	58
Neutral Red plus G147 Polysoap	85
Phenazine alone	12
Phenazine plus G147 Polysoap	82

[2] Patents have recently been issued for the use of safranine dyes to assure smooth electrolytic copper deposits from acid baths in the electroplating industry (8, 9). These came to the authors' attention after the completion of this work.

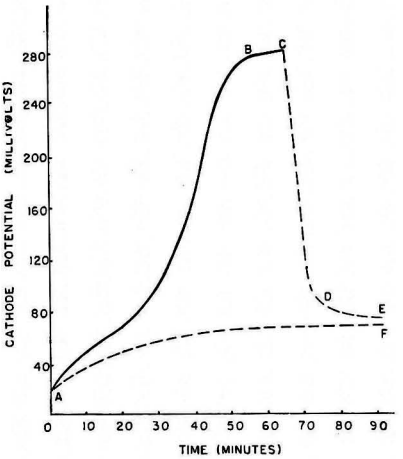

FIG. 4. Influence of additives on the copper cathode potential in a closed cell operating at 0.07 amp/dm². Curve ABCDE shows the increase in cathode potential due to the addition of polysoap, and its reduction by Safranine T. At A, 100 mg/l of polysoap G147 was added to the cell, and measurements of cathode potential were made at intervals. The potential rose to 270 mv in about 60 min (B), and remained constant. At (C), 20 mg/l of Safranine T was added. The cathode potential dropped sharply to a value of 80 mv (D), and then remained practically constant (E). Curve AF shows the effect of the addition of 20 mg/l of Safranine T to the cell when no polysoap is present. The cathode potential value rises to about 75 mv.

Under the conditions of the experiments, whisker-producing agents raise the copper cathode potential more than 200 mv (Table I). Table III gives the copper cathode potentials brought about by whisker-preventing agents and also shows the effect of these agents on the high potentials brought about by the whisker-forming agent G 147. Addition of a phenazine dye alone raises the cathode potential to a relatively moderate extent (70 mv), and reduces the rise in cathode potential brought about by whisker-producing agent G 147. Fig. 4 shows that this reduction is sufficient to bring the potential down to the level produced by the dye alone. This nullification may well be involved in the smoothing action of safranine dyes. With the smoothing agents cystine and thiourea, a reduction of the high potential does not take place.

Undoubtedly the action of fiber-generating agents begins with adsorption of the substance on the copper cathode. The large increase of the cathode potential brought about by cetyl trimethyl ammonium bromide indicates strong adsorption. The whisker-forming chloride ion is also adsorbed on copper metal as was shown when typical Freundlich adsorption isotherms were obtained utilizing finely divided copper powder[3] as adsorbent in pure water as solvent. The whisker-preventing agent Safranine T was also strongly adsorbed on copper metal. The dye probably displaces whisker-forming agents, and this results in a reduced cathode potential. Nullification of a high cathode potential does not necessarily have to enter into whisker-prevention, but when it does, there is likely to be a more effective smoothing action.

[3] Supplied by U. S. Metals Co., Carteret, N. J.

DISCUSSION

The results of the experimental work described above lead to a reasonable hypothesis to explain the whiskering process. The generating substance forms a film on the cathode and interferes with the normal deposition of the copper. In the case of chloride this film is cuprous chloride and in the case of the cationic surface-active agent this film is the oriented molecule held tightly to the copper cathode because of the surface-active grouping and because of its positive charge. During copper electrodeposition, these films are responsible for an increase in potential between the cathode and the solution. Certain areas may be bare for shorter or longer periods of time. These spots have a relatively higher current density and copper tends to deposit on them more readily than on the rest of the surface. However, the presence of these bare spots alone does not account for whisker growth. Suspended particles are also necessary. These probably adsorb copper sulfate. When such a particle with its adsorbed copper sulfate layer settles on a bare spot on the copper surface, there will be a rapid deposition at this spot and a fiber starts. The particle will be carried away from the cathode on top of the depositing copper, but will continue to furnish a convenient path for supplying copper from the solution to the growing fiber. Obviously the particle can continue most effectively in an unstirred solution. The sides of the fiber will be coated with a film in the same manner as the cathode proper. Lateral growth of the fiber is, therefore, inhibited. The tip of the fiber is free from such a film because copper is depositing selectively at this point faster than film-forming substance can get to the growing surface. In the acid solution, dissolved oxygen tends to dissolve the fine whiskers before they grow very long. If oxygen is removed, or if antioxidants are present, whisker growth is facilitated. The strong adsorption tendency of some smoothing agents on copper undoubtedly aids smoothing action. The apparently specific action of safranine dyes, as opposed to azo dyes, etc., has been shown to involve the phenazine grouping. Both of the nitrogen atoms of this phenazine appear to be necessary, since substitution of oxygen, sulfur, or carbon for one of these nitrogen atoms results in a loss of smoothing action.

ACKNOWLEDGMENTS

The authors wish to acknowledge the assistance of Dr. Y. E. Lebedeff of the Central Research Laboratory of the American Smelting and Refining Company for valuable suggestions and helpful discussions.

This investigation was sponsored by the Naval Ordnance Laboratory, Silver Spring, Maryland, and was carried out under Bureau of Ordnance Contract NOrd 14075.

Manuscript received October 24, 1955.

Any discussion of this paper will appear in a Discussion Section to be published in the June 1957 JOURNAL.

REFERENCES

1. R. J. WAKELIN, *Bull. Inst. Metals*, I (20), 186 (1953).
2. K. G. COMPTON, A. MENDIZZA, AND S. M. ARNOLD, *Corrosion*, 7, 327 (1951).

3. H. Gollop, *Bull. Inst. Metals*, II (1), 7 (1953).
4. J. G. M. Turnbull, *ibid.*, II (3), 19 (1953).
5. W. H. Gauvin and C. A. Winkler, *This Journal*, **99**, 71 (1952).
6. L. Mandelcorn, W. B. McConnell, W. Gauvin, and C. A. Winkler, *ibid.*, **99**, 84 (1952).
7. U. P. Strauss and N. L. Gershfeld, *J. Phys. Chem.*, **58**, 747 (1954).
8. H. Brown, H. Woods, and R. A. Fellows (Udylite Corp., Detroit, Mich.), U. S. Pat. No. 2,707,166, April 26, 1955.
9. E. W. Hoover and H. Woods (Udylite Corp., Detroit, Mich.), U. S. Pat. No. 2,707,167, April 26, 1955.

Deposition of Titanium from Titanium-Oxygen Alloys on Copper, Iron, and Mild Steel

S. T. Shih,[1] M. E. Straumanis, and A. W. Schlechten

Department of Metallurgy, University of Missouri School of Mines and Metallurgy, Rolla, Missouri

ABSTRACT

The presence of some oxygen was found to be beneficial in coating titanium on other metals in a fused alkali chloride bath. An improved method of titanizing was developed by controlling the amount of oxygen by the use of prepared titanium-oxygen alloys or of titanium fines of known oxygen content as a source of titanium. The object to be coated with titanium was embedded in a mixture of NaCl or KCl and the alloy, and was heated in helium for several hours at about 850°C for copper objects, and about 1000° for those of iron and mild steel. The thickness of the coating depends primarily on temperature and secondarily on time, oxygen content of the alloy, and composition of the bath. The same bath can be used repeatedly. The coatings adhere well to the base metals and protect them from corrosion. Deformation within the elasticity limits of the base metal does not affect the quality of the coating.

Introduction

Previous work has shown that copper, iron, or nickel pieces can be coated with titanium, if they are embedded in titanium powder, covered with salt, and heated in air, or if the piece of metal and a piece of titanium were put adjacent to each other and heated in a salt bath in presence of air. Titanium corroded (1) while the other metal was covered with titanium (2). However, if the process was carried out in vacuum, good coatings were not obtained. This suggests that the presence of air was helpful to the production of the coating. Indeed, later work showed that one of the main corrosion products of titanium in a fused salt bath was a titanium-oxygen alloy containing 9–11% by weight of oxygen (3). As this product was formed in the vicinity of the corroded titanium (1) it seemed reasonable to believe it might play an important role in the titanizing process. Therefore, experiments were performed to study this process in a fused salt bath, using titanium-oxygen alloys as a starting material, and to study the properties of the coatings obtained.

Experimental

Preparation of Titanium-Oxygen Alloys

The alloys were prepared by heating metallic titanium powder and titanium dioxide in a vacuum furnace (4) at about 1150°C. The purity of the titanium powder[2] used was better than 99%, and the titanium dioxide was of C. P grade. Charges were calculated on the basis of the desired oxygen content, which was supplied by the titanium dioxide in the charge. For instance a titanium-oxygen alloy of the composition 90 Ti–10 O (or $TiO_{0.11}$) was made up by taking about 51 parts by weight of titanium and 5 parts by weight of titanium dioxide. Each charge was ground in a mortar, thoroughly mixed, and heated in an alundum crucible in a vacuum furnace at less than 10 μ of gas pressure at 1150°C for 4 hr.

The alloys prepared, containing approximately 5, 7, 10, 20, and 30 at. % of oxygen, had a metallic, titanium-like luster and color, those with a higher oxygen content being darker. They were brittle, could be crushed, and showed a quite homogenous crystalline structure under the microscope.

Titanium fines screened out of crushed sponge were also used. They contained more oxygen than coarse sponge. Analysis of one sample showed 97.7 at. % titanium.

Experimental Procedure

Three series of plating experiments were carried out with the titanium-oxygen alloys.

The first was of an exploratory nature, and was simply performed in air with potassium chloride mixed with 20% of different titanium-oxygen alloys.

The second series was conducted in an inert atmosphere. The furnace was so arranged that its mullite tube could be

[1] Present address: Department of Metallurgy, Montana School of Mines, Butte, Mont.

[2] From the Belmont Smelting and Refining Works, Inc., Brooklyn, N. Y.

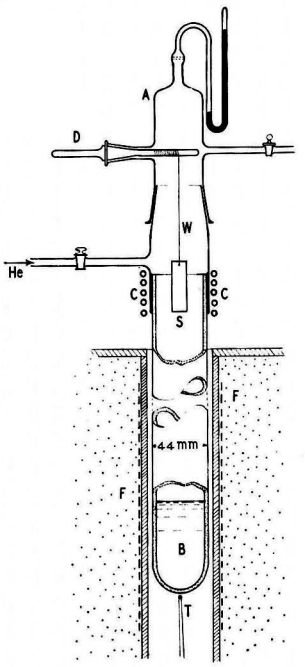

FIG. 1. Device for lowering the sample into the molten salt bath and raising the sample in an atmosphere of helium. S—sample to be titanized; B—molten salt bath containing TiO_x; W—Pt wire; D—cranking device; F—furnace; C—coil with cooling water; A—cap of Pyrex glass; T—end of the thermocouple.

connected either to the vacuum system or to a source of dry purified helium.

The ground and polished specimen, embedded in a mixture of titanium alloy and salt (KCl or NaCl in a porcelain or iron crucible) was dried in the furnace, which then was flushed with helium. During the coating experiments at 900°–1000°C the pressure in the furnace was held a few centimeters above atmospheric pressure to prevent ingress of air. Separation of the sample from salt occurred as already described (2).

This method was time consuming and somewhat wasteful because (*a*) some of the fine titanium powder was further oxidized during the leaching process, (*b*) some titanium, transformed into chloride, was hydrolyzed, and (*c*) the salt dissolved in the same process is lost if not recovered from the solution.

As a result, the third series of experiments was made to find a better way to separate the coated sample from the molten salt bath without exposing it and the sample to air. The experiments were performed on a small scale by inserting a winding device into the cap on the mullite tube which held the bath, as sketched in Fig. 1. On the spindle was wound a fine platinum wire to the end of which the sample could be hooked.

First the cap, A, was removed, the sample hooked to the end of the wire, W, the salt and titanium oxide mixture was charged into the bottom, B, of the tube, and the cap replaced so that the sample was somewhere in the middle of the tube. Then helium gas was fed into the tube and the current was turned on. At a temperature of 1000°C the sample was lowered into the bath, B, left there for 3 hr, and raised out into the water cooled zone, C, while the furnace was shut off. When the furnace was cooled below 400°C, the sample was removed, a new sample was hung in its place, and the experiment was repeated. In this way several samples could be titanized using the same bath with insignificant titanium losses.

In a modification of this series of experiments the disadvantage of heating and cooling the furnace for each separate sample was overcome as follows. When the titanized sample cooled off in zone C with the furnace still on, the helium pressure was increased and cap A was lifted; then the sample was replaced by a new one, the tube closed, and after a short time of flushing with helium the new sample was lowered into the bath, B, and so on. Thus, the penetration of air was prevented by the countercurrent of helium and by "getters" (such as pieces of titanium above the sample) in the inside of the tube. A series of runs were carried out continuously in this way without changing the temperature of the furnace. Each sample was weighed before and after the run (the thin adhering salt layer was washed off) to obtain the increase in weight due to the coating.

RESULTS

Tests in Air and Helium

Only experiments performed in air with titanium oxide alloys containing 10 at. % of oxygen or less were somewhat successful, although in all cases the inside walls of the crucibles were covered with a shining layer of titanium (2). To avoid further oxidation of titanium by air, the next coating experiments were made on copper in helium using titanium alloys containing 5, 7, and 10 at. % oxygen. Results are summarized in Table I.

The table shows that pure titanium did not produce coherent coatings, but that titanium-oxygen alloys were effective. The samples usually showed an increase in

TABLE I. *Deposition of* Ti *on* Cu *samples* (He *atmosphere*) *at 850°C*

O in TiO_x in at. %	Bath: TiO_x* in wt %	Time in hr	Cu sample	Quality of Ti coating
0	5 (x = 0)	5	Wire, spiral	Poor, only a few Ti spots.
5	15	4	Penny	Good, coated all over.
5	15	4	Wire, spiral	Good, coated all over.
5	15	2	Plate	Good, coated all over.
5	20	4	Plate	Fairly good, coated but rough.
7	15	2.5	Penny	Good, coated all over.
10	5	1.5	Plate	Coated all over, except a few spots.
10	10	1.5	Plate	Good, coated all over.
10	15	1.5	Wire	Embedded part well coated.
10	20	3	Plate	Good, coated all over.

* Balance being KCl.

weight of 10–13 mg, from the charge which usually contained 1 g of the titanium-oxygen alloy.

Thus, only about 1 or 2% of the alloy in the salt bath was used for the coating. X-ray diffraction patterns of the unused and recovered alloy showed that the latter differed from the original one only by a slight increase in oxygen content. If so, the recovered alloy should be able to produce coatings on new samples, and experiments on both copper and iron samples showed this to be true.

Deposition of Titanium on Iron and Steel in a Helium Atmosphere

Ingot iron, some iron pennies, and 1012 steel samples were used for the coating experiments. Since iron-titanium-oxygen alloys formed during the deposition process on the iron surface (5) have a higher melting point than the respective copper alloys, higher temperatures of 900°–1000°C were used. Temperatures below 900°C as well as mixtures with less than 10 wt. % of the titanium alloys were usually insufficient to produce good coatings (exception, *see* sample 9, Table II). The samples were well coated from all sides.

In Fig. 2 some of the mild steel objects of intricate shape containing about 0.15% carbon, coated all over with titanium, are shown.

This titanizing method has certain advantages as compared with the older method (2): (*a*) more uniform coatings covering all sides of the samples can be achieved, (*b*) a titanium metal of inferior grade can be used, thereby lowering the cost of raw materials, and (*c*) there is less waste of titanium through oxidation by air.

Four variables may influence the quality and the thickness of the coatings produced: temperature, time, oxygen content of the TiO_x alloys, and composition of the bath. The effects produced by each of these variables were studied, using ingot iron samples and changing the four variables in a systematic manner.

Most of the samples used were in the form of 58 x 19 x 16 mm strips of ingot iron. Ground, polished, and brushed samples were embedded vertically in the bath mixtures in crucibles made of iron pipe. The inside of the crucibles was precoated with titanium to avoid drawing titanium from the baths in the subsequent experiments. Smaller samples, (indicated with *a* in Table II) 13 x 13 x 3 mm, were embedded horizontally in porcelain crucibles filled with the bath mixture. All coatings were made under helium gas.

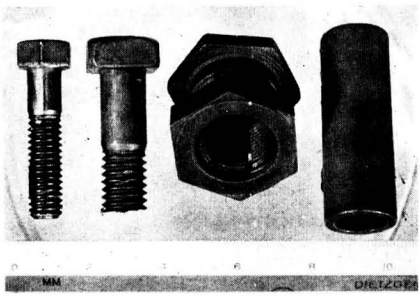

FIG. 2. Four mild steel objects coated with Ti in 3 hr, 950°C, using a TiO_x alloy with 5 at. % O, in a mixture with NaCl (10 wt % of the alloy and 90% NaCl). He atmosphere.

After coating, the samples were separated from the salt, examined, weighed, and corrosion tested. Measurements of the average increase in thickness for some samples were also made. This increase, measured with a micrometer, did not represent the thickness of the titanium coating because titanium diffused inward into the iron and iron also diffused outward into titanium. The actual thickness of the coatings was measured with a metallographic microscope on cross sections of the coated samples perpendicular to the surface. To reveal the coating microstructure the polished sections were treated by cumulative stain etching (6). The titanium coating, separated into several thin layers, appeared blue in color after etching, while the color of the diffusion layer was quite different, so that the coating and the diffusion layer could be differentiated clearly. Data are given in Table II. The following conclusions can be drawn from Table II with regard to the four variables studied:

Influence of temperature.—Samples 1, 4, and 7 clearly show the increase of weight with increasing temperature. The same trend is found when the thicknesses of the diffusion layers plus that of the coatings high in titanium content obtained at temperatures of 850°, 950°, and 1000°C are considered. The thickness of the coatings plus the diffusion layers agree well with those given previously (2), indicating that the coating process is the same regardless of whether solid titanium or titanium-oxygen alloys are used as a titanium source. The relationship between the increase in thickness of the titanium coating and the diffusion layer with temperature and time is further shown in Fig. 3. To demonstrate the difference between the coating and diffusion layer, a section through a sample is shown as Fig. 4.

Influence of time.—Time has an effect similar to that of temperature as clearly demonstrated by Fig. 3. However, growth rates of the titanium coating and of the diffusion layer are quite different: the thickness of the coating, which is of paramount importance for protection from corrosion, grows only slowly in the course of time, while the diffusion layer increases faster during the same period of time. So it may happen that with prolonged time of treatment the coating layer becomes thinner while a much thicker diffusion layer is being created. Evidence of this phenomenon can be seen in Table II, by comparing the thickness data for samples 15*a* and 16*a*.

Since temperature has a more marked effect than time on the thickness of the coating, a higher temperature and a shortened processing time should be applied for the production of thicker outer coatings. For instance, a sample prepared at 1000°C for 2 hr had a thicker coating layer than the one made at 950°C for 6 hr, although the latter had a slightly thicker diffusion layer due to longer diffusion time.

Influence of the composition of the TiO_x *alloy.*—Samples 7, 11, and 12 were coated at identical conditions except for the composition of the titanium-oxygen alloys. Thus, sample 7 (with 95 at. % Ti in the TiO_x alloy) gained 0.0065 g/cm², sample 11 (with 90 at. % Ti) gained 0.0059 g/cm², while sample 12 (with 80 at. % Ti) increased in weight by only

TABLE II. *Titanium coatings on ingot iron obtained in fused salt baths containing* TiO_x *alloys*
Helium atmosphere

Sample No.	Coating		Bath composition		Weight increase g/cm²	Avg increase in thickness,‡ mm	Thickness of	
	Temp, °C	Time, hr	Wt. % KCl†	At % Ti in TiO_x			Coating, mm	Diffusion layer, mm
1	850	4	90	95	0.0005	0.010	0.004	0.000
2	850	6	90	95	0.0008	0.013	0.006	0.000
3	950	2	90	95	0.0026	—	0.008	0.044
4	950	4	90	95	0.0045	—	0.012	0.068
5	950	6	90	95	0.0052	—	0.014	0.088
6	1000	2	90	95	0.0060	0.043	0.015	0.082
7	1000	4	90	95	0.0065	—	0.016	0.135
7*a*	1000	4	90	95	—	0.065	0.016	0.112
8	1000	4	80	95	0.0075	0.053	0.012	0.078
9	1000	4	95	95	0.0042	0.025	0.016	0.064
10	1000	4	90*	95	0.0066	0.050	0.015	0.115
11	1000	4	90	90	0.0059	0.038	0.012	0.100
12	1000	4	90	80	0.0032	0.013	0.012	0.084
13	1000	4	90	Ti fines	0.0061	0.048	0.014	0.067
14	1000	6	90	Ti fines	—	0.063	0.015	0.103
15	1000	6	90	95	0.0086	—	0.016	0.160
15*a*	1000	6	90	95	—	0.093	0.020	0.150
16*a*	1000	9	90	95	—	—	0.013	0.164
17*a*	1150	4	90*	Ti fines	—	—	0.021	0.245

* NaCl instead of KCl.
† Balance TiO_x.
‡ Measured with a micrometer.

0.0032 g/cm², all in 4 hr. Sample 13 showed results like those of sample 7. Analysis showed that the titanium fines contained 97.7% titanium as compared to 98.3% Ti for TiO_x with 95 at. % Ti. This is the optimum composition of the titanium bearing ingredient, since mixtures with less or no oxygen produce bad coatings. Titanium fines can be obtained at a lower price since it is not useful for ingot melting.

Influence of the composition of the bath.—Comparison of samples 9, 7, and 8 shows that a bath with a larger proportion of titanium gives a thicker coating. The increase in thickness measured by a micrometer followed the same trend. However, addition of the titanium compound is limited by the decreased fluidity of the resulting bath, which becomes too viscous if the TiO_x content is as high as 20 wt %.

As to the use of sodium or potassium chloride for the dispersion medium, samples 11 and 7 and also other experiments showed no appreciable difference in the quality of the coatings produced.

Influence of the metal to be titanized.—As already mentioned (2) many metals can be coated with a titanium. The quality of the coating on iron depends on its carbon content: electrolytic, ingot iron, and mild steel containing up to 0.2 wt % carbon can be titanized without difficulty by the method described. The higher the carbon content of iron, the higher the temperature required to produce good coatings. Evidently formation of titanium carbide on the surface of the steel samples hampers the diffusion inward and the accumulation of titanium on the surface of the samples.

Deposition of titanium in used baths in a continuous process.—In all of these experiments the coated sample was separated from the bath by leaching with water, and the unused titanium-oxygen alloy was recovered. However, this method wastes time and materials.

Obviously, a better way to separate the coated sample from the bath is to withdraw the sample from the molten bath into an inert atmosphere. This procedure was tested on a small scale using an arrangement sketched in Fig. 1. The bath, consisting of 70 g of 90 wt % sodium chloride and 10% titanium sponge mixture, was charged into the tube. Then the cap A was put on, the tube was evacuated, helium was admitted, and the sample was titanized at 1000°C in a manner already described. Four samples were coated successfully in this way until the platinum wire broke.

In a modification of this series of experiments, the cooling of the furnace was avoided and samples were removed in helium gas as described under the experimental procedure. This series was discontinued after the sixth run because of the breakage of the platinum wire. Nevertheless, all the samples had good titanium coatings, even those immersed in the bath for only 1.5 hr. Those immersed for 11.5 hr increased in weight about three times as much as those deposited at 2 hr. Increases in weight for the samples of the six runs were added and gave a sum of only 0.0346 g of titanium as compared with the total of 6.84 g originally present in the charge, showing that a large amount of titanium was still left unused. This titanium-oxygen alloy was recovered by filtering the leaching solution, and drying the residue in a vacuum oven at 105°C overnight. A gram of this residue was mixed with 9 g of sodium chloride to make a bath which was run at 1000°C for 4 hr. A piece of ingot iron embedded in this bath was found to be well coated with titanium. This experiment indicated that the residual titanium-oxygen alloy was still active, and that many other samples could be titanized in the same bath.

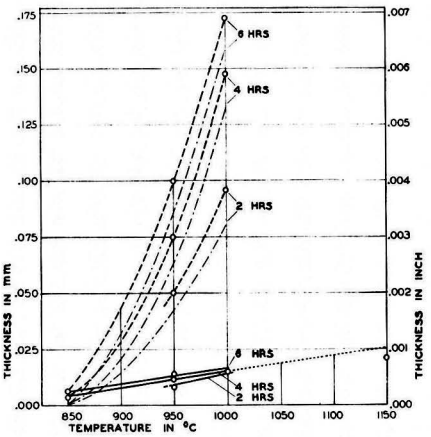

FIG. 3. Increase in thickness of titanium coatings (solid lines) and diffusion layers (dash-dot) with temperature and time. Dashed lines: total thickness of the deposit (coating plus diffusion layer). Conditions of coating, see Table II.

FIG. 4. Structure of a coating and diffusion layer produced on ingot iron (sample No. 14, Table II). A—Ti coating, B—diffusion layer, C—Fe core. Magnification 200×.

The success of the continuous run showed the practicability of the process and indicated the possibility of working on a larger industrial scale, provided the proper type of furnace and a suitable device for moving the specimens in and out of the bath and furnace under the protection of an inert gas were available.

Chemical and Physical Characteristics of the Coating

Samples titanized under different conditions were used for the tests. The objects were completely resistant to the action of dilute and concentrated nitric acid, and no copper was deposited on immersion in a copper sulfate solution. However, red specks or pinholes appeared if the objects were not well cleaned before titanizing. Not only the outside surface, but the deep threads of screws and the inside of the pieces of iron tubing were titanium plated. The surface of the objects was dark grey, but on polishing the typical color of titanium metal appeared (Fig. 2).

The high corrosion resistivity of the titanium coating was demonstrated with samples partially immersed in the titanizing bath and afterwards treated with nitric acid. The uncoated parts were severely attacked by the nitric acid (Fig. 5), while the coated parts were intact. Generally, the titanium coatings show the same corrosion properties (9) as solid titanium metal although corrosion rates of the coatings were not determined. Further tests included hardness measurements of the titanium coatings with a Knoop Diamond Indenter in a Tukon Hardness Tester machine, bending of the coated samples to examine the tendency of the coating to pull loose under stress, and tensile tests with a Dillon Tensile Tester to determine to what extent the base metal could be stressed before there was any separation of the coating.

The hardness tests, made chiefly on titanized Armco ingot iron samples, did not give very definite results, but several trends could be picked out: (*a*) almost without exception hardness increased with thicker coatings; (*b*) coatings were hardest when TiO_x with 95 at. % Ti, or titanium fines was used; (*c*) increasing the amount of the titanium-oxygen alloy in the bath did not have as great an influence on the hardness as did temperature or time variations; (*d*) sodium or potassium chloride baths gave practically the same results.

Samples that had a Knoop hardness traverse run across their cross sectioned surfaces (7, 8) gave results that were in agreement with the general trend, although the actual values were not the same as obtained by surface tests. In each instance the ingot iron base metal was much softer than the titanium coating which was especially hard at the line in contact with the diffusion layer (10). Qualitative abrasion tests also proved that the outermost surface of the titanium coatings is comparatively soft, and is then followed by much harder layers and finally by the soft iron core.

Bend tests showed that titanium coatings held fast to the side of the bent sample in tension, and only tore apart if the base metal, which was brittle, was ripped by the severity of the bend. On the compression side there was a tendency for some of the coatings to buckle in strips, which climbed on one another and flaked off. Nevertheless, the coatings obtained in a helium atmosphere withstood bend tests up to 30 degrees quite well.

In tensile tests the titanium coatings were all quite sound and adherent up to a load of half that required to break the sample, but after rupture it was found the coatings had cracked, checked, and flaked off.

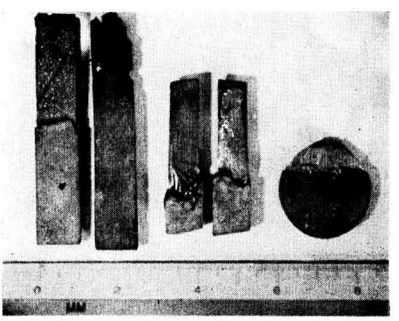

FIG. 5. The uncoated parts of iron, copper, and nickel samples are severely corroded by nitric acid.

Conclusions

Thick and corrosion resistant coatings of titanium on ingot iron, mild steels, and other metals can be obtained by treating them under an inert gas in fused salt baths containing a titanium-oxygen alloy high in titanium content, and as large an amount of such alloy as possible without sacrificing the fluidity of the bath. High temperatures and longer coating times are preferable. A typical run consists of a bath containing 90% sodium chloride, 10% TiO_x with 95 at. % Ti or titanium fines of similar oxygen content. An ingot iron sample is covered at 1000°C in 4 hr with a coating about 0.0006 in. (0.015 mm) thick. Including the diffusion layer the thickness of the whole layer is about 0.0051 in. (0.13 mm) in this case. An industrial application of the titanizing process described is possible since it can be arranged for continuous runs. There is some similarity of the coatings described with those obtained electrolytically by Sibert and Steinberg (10).

The titanium coating is harder than the core and is quite adherent under reasonable stress. Only when the base metal is deformed beyond its elastic limit is there a tendency for the coating to develop cracks, checks, and to flake off.

Acknowledgments

The authors are grateful to the Wright Air Development Center for support of this work and permission to publish the results obtained. The mechanical properties of the coatings were explored by Dr. C. B. Gill. The thickness measurements under microscope were made by Mr. P. J. Chao.

Manuscript received August 1, 1955. This paper was prepared for delivery before the San Francisco Meeting, April 29 to May 3, 1956. Based on a portion of work carried out at the Missouri School of Mines and Metallurgy for the Wright Air Development Center under Contract No. AF 33(616)-75.

Any discussion of this paper will appear in a Discussion Section to be published in the June 1957 Journal.

References

1. C. B. Gill, M. E. Straumanis, and A. W. Schlechten, *This Journal*, **102**, 42, Fig. 2 (1955).
2. A. W. Schlechten, M. E. Straumanis, and C. B. Gill, *ibid.*, **102**, 81 (1955).
3. M. E. Straumanis, K. C. Chiou, and A. W. Schlechten, in preparation for publication.
4. P. Ehrlich. *Z. anorg. Chem.*, **247**, 53 (1941).
5. R. L. Hadley and G. Derge, *J. Metals*, **7**, 55 (1955).
6. E. Ence and H. Margolin, *ibid.*, **6**, 346 (1954).
7. M. B. Bever and C. F. Floe, in "Surface Protection against Wear and Corrosion," p. 85, 87, 88, American Society of Metals, Cleveland (1954).
8. U. Zwicker, *Metalloberflache*, **6**, A81 (1952).
9. M. E. Straumanis and P. C. Chen, *Corrosion*, **7**, 229 (1951).
10. M. E. Sibert and M. A. Steinberg, *This Journal*, **102**, 641, *see* e.g. Fig. 6 (1955).

Two Arsenate Phosphors and the Significance of Their Emission

Gorton R. Fonda[1]

The General Electric Company, Schenectady, New York

ABSTRACT

Four phosphors of weak to moderate luminescence were prepared: two from zinc arsenate activated separately with lead and manganese, and two from calcium fluoroarsenate activated with antimony alone and with antimony and manganese together. Their manganese emission band was shifted to longer wave lengths than is characteristic of their phosphate homologues: from 6380Å to 6550Å in the case of the zinc compounds, and from 5680Å to 6200Å for the fluoroapatites. The effect was ascribed to depression of excitation levels of activator ions under increased field strength of oxygen ions in their environment.

Introduction

Two noteworthy phosphors of phosphate composition have been developed in recent years: zinc phosphate activated with manganese (1) and calcium halophosphate activated with antimony and manganese (2). Arsenates are closely related to phosphates; in fact, the law of isomorphism was discovered by the observation that phosphates and arsenates conform to it. Properties of their various salts are very similar, their analogous salts have the same structure, their solubility is of the same order, and they respond similarly to various reagents. Just as there is a mineral, apatite, which has the composition of calcium fluorophosphate, so there is likewise a mineral, svabite, a calcium fluoroarsenate which has a similar composition and structure.

It seemed of interest, therefore, to investigate arsenates and haloarsenates as possible bases for the emission of luminescence. As early as 1949, two pairs of phosphors were found which exhibited similar composition and activation to the phosphates mentioned above. They

[1] Present address: 1028 Parkwood Blvd., Schenectady, N. Y.

included zinc arsenate activated with manganese, which in addition could also be activated with lead, and calcium fluoroarsenate activated with antimony alone and with antimony and manganese together. Full publication of their characteristics has been delayed until the present. Some optical properties of the fluoroarsenates have already been recorded (3). Measurements of their spectral emission disclosed a greater shift to longer wave lengths than exhibited by the corresponding phosphates. Explanation for the change appears to lie in the field strength exercised on the activator ions by the oxygen ions of their environment. The same explanation can be applied to the variations in spectral emission that characterize other groups of oxygen-dominated phosphors whose composition and structure are related.

Zinc Arsenate Phosphor

At 25°C, essentially no fluorescence was obtained with the arsenates of calcium, magnesium, and cadmium under 2537Å, 3650Å, or cathode rays. Zinc arsenate responded to activation by both manganese and lead to emit fluorescence of moderate intensity, lying in the orange and whitish blue, respectively.

These phosphors were prepared by firing at 700°–1000°C, preferably in an atmosphere of nitrogen, a mixture of zinc oxide and arsenic pentoxide in a proportion to yield the orthoarsenate, $Zn_3(AsO_4)_2$. A compound of the activator was added before firing. There was only a small loss in weight, and this was due to the water content of the pentoxide; the loss remained constant whether the crucible was placed in the furnace at full temperature or brought up to temperature slowly. Maximum brightness resulted from firing at 800°C for 3 hr.

The concentration of manganese, introduced as carbonate, was about 0.5% by weight. Its fluorescence was reduced when lead was present as well. As shown by the curves of Fig. 1, its peak emission at room temperature was at 6550Å; at −193°C it was displaced to 6720Å. Under excitation by 2537Å, its quantum output at room temperature was about 10% of that of magnesium tungstate.

When a phosphor was prepared by addition of 2% lead oxide and firing at 800°C for 1 hr, the product emitted a broad band at room temperature with a peak at 4500Å but extending so strongly into the higher wave-length range, as shown in Fig. 1, that the color of its fluorescence was a bluish white. Reduction in temperature to −193°C served likewise to displace its peak luminescence to longer wave length, 4700Å. At room temperature its quantum output was somewhat higher than that of the manganese activated phosphor.

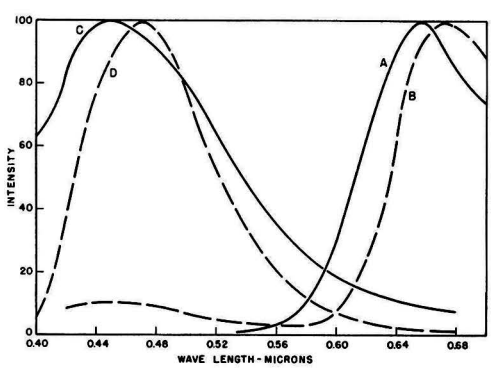

FIG. 1. Emission spectra of zinc arsenate phosphors excited by 2537Å. A—$Zn_3(AsO_4)_2$:Mn at 25°C; B—$Zn_3(AsO_4)_2$:Mn at −193°C; C—$Zn_3(AsO_4)_2$:Pb at 25°C; D—$Zn_3(AsO_4)_2$:Pb at −193°C.

Calcium Fluoroarsenate Phosphor

When the experiments were extended to the haloarsenates, calcium fluoroarsenate was the only compound which showed a notable response to excitation by 2537Å, 3650Å, or cathode rays at 25°C. It was prepared from a mixture of 9 moles calcium oxide, 3 moles arsenic pentoxide, and 1 mole calcium fluoride. Faint or weak luminescence was obtained with activation by bismuth, cerium, lead, tin, and thallium. The brightest phosphors resulted by adding antimony or manganese or both as activators and firing at 1150°C in a quartz tube closed at the end within the furnace and plugged with glass wool at the outer end. The preparation of this phosphor has been briefly described by Rothschild (4).

With antimony alone the fluorescence was a greenish yellow, with a peak at 5000Å as shown in Fig. 2. Its brightness was a maximum when 0.5–4.0% antimony as antimony oxide was added to the mixture before firing. Its quantum output under excitation by 2537Å was 15% of that of magnesium tungstate. As determined from reflection measurements (5) its absorption of 2537Å was 81%. Its quantum efficiency would therefore be 19% of magnesium tungstate (3).

With manganese alone, which had been added as the carbonate, there was a weak red emission. Its intensity was greatly increased on addition of antimony, denoting that the latter had a sensitizing action. The peak of the manganese emission was at 6200Å. With 1% manganese its brightness remained at a maximum over the range of 0.5–2.0% antimony. The spectral distribution of a product prepared with 1% manganese and 2.0% antimony is given in Fig. 2. Despite the appreciable antimony content, the

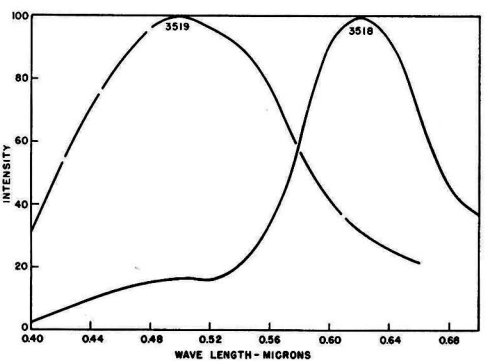

FIG. 2. Emission spectra of calcium fluoroarsenate phosphors excited by 2537Å. 3518—$3Ca_3(AsO_4)_2 \cdot CaF_2$:Sb:Mn at 25°C; 3519—$3Ca_3(AsO_4)_2 \cdot CaF_2$:Sb at 25°C.

TABLE I. *Spectral emission of arsenate and phosphate phosphors*

Phosphor	Peak Emission (Å)	
	Sb band	Mn band
$Zn_3(AsO_4)_2$:Mn	—	6550
$Zn_3(PO_4)_2$:Mn	—	6380
$3Ca_3(AsO_4)_2 \cdot CaF_2$:Sb:Mn	5000	6200
$3Ca_3(PO_4)_2 \cdot CaF_2$:Sb:Mn	4800	5680
$3Ca_3(PO_4)_2 \cdot CaCl_2$:Sb:Mn	4800	6000

antimony band is almost completely suppressed by the manganese. Under excitation by 2537Å its quantum output was 27% of that of magnesium tungstate. With an absorption of 84% for 2537Å, its quantum efficiency became about 30% of magnesium tungstate.

X-ray diffraction patterns showed these fluoroarsenates to be of apatite structure with a somewhat larger unit cell than characterizes the fluorophosphate. This result is in agreement with measurements by Rothschild on calcium apatite phosphors which he prepared (4).

Comparison of Arsenate and Phosphate Phosphors

The two arsenate phosphors just described are similar in composition and isomorphous in structure with the corresponding phosphates. Both pairs have the same activators. It is therefore reasonable to expect a relationship in spectral emission between the arsenates and phosphates of the same type. A comparison is given in Table I.

Discussion

An explanation for the differences observed can be found in the differences in field strength to which activator ions are subjected by their environment. This explanation should be applicable to any group of phosphors which have related composition and structure. It has been applied by Klasens, Zalm, and Huysman to double fluorides of perovskite structure which have the composition ABF_3, where A is a monovalent alkaline metal and B a divalent metal of the second periodic column (6). The spacing between a fluorine ion and the activator ion, manganese, depends upon the ionic size of the metals A and B. An increase in this spacing was accompanied by a corresponding shift of the peak emission to shorter wave lengths. As the authors phrase it, "the greater the space available for the manganese ion, the more the state of the free ion will be approached, hence the shift to shorter wave length."

When a manganese ion is in the field of the crystal lattice, the distances between its energy levels become smaller. The outer orbits of the ion, those occupied by excited electrons, are under the repulsive force exerted by the field of the adjacent anions and their energy levels are correspondingly depressed. The extent of the depression depends on the field exercised by the anions and this, in turn, on their proximity, the smaller the spacing, the greater is the field and the greater likewise is the depression in the energy levels of the excited electrons; consequently, the greater is the shift in emission to longer wave lengths.

The view of Klasens, Zalm, and Huysman (6) is applicable to other phosphors. Although similar quantitative data on spacings between manganese ions and anions are not generally available, the direction in which the change in spacing occurs can frequently be perceived from related characteristics, such as the relative ionic sizes of the cations in a series of related compounds, or the relative spacings of cations and anions in their oxides. Inasmuch as manganese substitutes for the cation of such compounds, the change to a larger cation carries with it an increase in the spacing between manganese and its surrounding oxygen ions. A possible illustration that is at least suggestive, is offered by the silicates of Table II activated with manganese to give a double band emission. The emission peaks cited are the currently accepted values.

Both bands are shifted to longer wave length as the spacing is reduced in the metallic oxide from which the phosphor was prepared.

The silicates are, it is true, all of different structure, and this tends to weaken the validity of the illustration because structural features may be playing a more fundamental role than the spacings in the oxides. It seems probable, however, that the coordination of a cation remains the same in a silicate as in its oxide. In the case of magnesium silicates, at least, the change from metasilicate to the orthosilicate produces only a moderate alteration in spectral emission, insufficient to affect the argument.

In a less debatable case, the same relation was found by Kreidl on partial substitution in sodium silicate glasses activated by manganese (7). Substitution of potassium, of larger ionic size, for one half of the sodium shifted the fluorescence from greenish yellow to green, a result of the enlarged spacing. Substitution of one half of the sodium by lithium, of smaller ionic size, produced the reverse effect by shifting the fluorescence to yellow.

With these examples in mind, the same viewpoint can be applied to the arsenates and phosphates of Table I. The situation is somewhat different. In the previous examples, the emission band was shifted to longer wave lengths when the cation of the compound was changed to one of smaller ionic size, thus bringing the manganese ion substituting for it closer to the oxygen ions which surrounded it. In the present example, the emission is shifted to longer wave lengths by changing the metal of the acid radical to arsenic, an element of larger ionic size than phosphorus. A brief consideration shows that the effect on the manganese ion is the same as in the previous examples.

The lower field strength of the larger arsenic ion allows an enlargement of the acid forming tetrahedron, in this case the AsO_4 group; a redistribution occurs in the field strength of the oxygen ions composing it, less is directed

TABLE II. *Effect of cation constituent on fluorescence of silicates*

Composition	Emission peaks (Å)	Cation to anion spacing in oxide (Å)
Zn_2SiO_4:Mn	5250, 6000	2.00, 3.22
$CaSiO_3$:Mn	5600, 6200	2.40
$CdSiO_3$:Mn	6000, 6240	2.35
$MgSiO_3$:Mn	6600, 7400	2.10
Mg_2SiO_4:Mn	6400, 7400	2.10

inward to the arsenic core than would be to the phosphorus core, and more becomes available for direction on the zinc or calcium ions which are dispersed around the acid tetrahedral groups. This decreases the spacing between zinc or calcium ions and oxygen ions. Whenever a manganese ion is substituted for zinc or calcium, the energy levels of its excited states are accordingly lowered as before, and the emission is shifted as before to longer wave lengths.

The antimony emission of the fluoroarsenate is also shifted to longer wave lengths, indicating that antimony ions are subjected to similar forces as manganese. This in turn denotes that antimony ions, as activators, substitute also for calcium in the lattice rather than for arsenic or phosphorus.

A similar situation arises in another pair of compounds which are related to one another, zinc germanate and silicate, both activated by manganese. The substitution of germanium, of larger ionic size than silicon, acts to shift the peak of the emission band from 5250Å to 5370Å.

In the halophosphates the substitution of chlorine for fluorine produces a similar shift. A chlorine ion is of larger ionic size than fluorine; its field strength, the quotient of its charge by its ionic radius, is therefore less. This results in a lower electrostatic attraction between it and its neighboring calcium ion so that the spacing between them is increased. The spacing between this calcium ion and its other neighboring anions, three oxygen ions, is correspondingly reduced under the stronger residual field of the calcium ion. When a manganese ion substitutes for this calcium, its energy levels are depressed as in the previous case where arsenic was substituted for phosphorus, and its emission is again shifted to the longer wave lengths cited in Table I for the chloroapatite.

ACKNOWLEDGMENT

The author is greatly indebted and very grateful to Dr. Frank J. Studer and Miss Gwen Lloyd of the Research Laboratory of the General Electric Co. for the absorption and spectral distribution measurements.

Manuscript received June 27, 1955. This paper was prepared for delivery before the Cincinnati Meeting, May 1 to 5, 1955.

Any discussion of this paper will appear in a Discussion Section to appear in the June 1957 JOURNAL.

REFERENCES

1. A. L. SMITH, *This Journal*, **98**, 363 (1951).
2. H. G. JENKINS, A. H. MCKEAG, AND P. W. RANBY, *ibid.*, **96**, 1 (1949).
3. S. JONES AND G. R. FONDA, Abstract No. 41 "Enlarged Abstracts of Papers Presented by the Electronic Division of the Electrochemical Society" (1952), page 39.
4. S. ROTHSCHILD, *Brit. J. Appl. Phys.*, Supplement No. 4, 32 (1955).
5. F. J. STUDER AND G. R. FONDA, *J. Opt. Soc. Amer.*, **39**, 658 (1949).
6. H. A. KLASENS, P. ZALM, AND F. O. HUYSMAN, *Philips Research Repts.*, **8**, 441 (1953).
7. N. J. KREIDL, *J. Opt. Soc. Amer.*, **35**, 249 (1945).

Reaction of Hydrogen with Uranium

W. M. Albrecht and M. W. Mallett

Battelle Memorial Institute, Columbus, Ohio

ABSTRACT

The reaction of hydrogen with uranium to produce uranium hydride was studied in the temperature range 96°–400°C at pressure levels of $p - p_0$ equal to 430, 150, and 70 mm of mercury (where p is system pressure and p_0 is the plateau dissociation pressure of the uranium hydride product). Reaction rates followed the linear law. At a given $p - p_0$, the linear rate increased with increasing temperature in the range 96° to about 250°C and decreased with increasing temperature from about 250° to 400°C. Variation of the linear rate with temperature and pressure in the range 96° to about 250°C is given by the equation:

$$r = 4.11 \times 10^{-3} p^{3/4} \exp(-1820/RT)$$

where r is in units of ml/cm²/sec and p is in units of mm Hg. In the range from about 250° to 400°C an empirical relationship between the reaction rate and pressure is proposed where the rate is a function of $p - p_0/p_0$. However, since none of the reaction mechanisms was determined, the significance of the pressure dependencies is not known. Two different initial reactions were obtained. One in the range 96° to about 250°C at $p - p_0$ of 70 and 150 mm Hg and 96°–400°C at $p - p_0$ of 430 mm Hg showed a gradual increase in the rate of hydrogen consumption until the rate became linear. The other initial reaction followed the parabolic rate law in the range of about 250°–400°C at $p - p_0$ of 70 and 150 mm Hg.

Introduction

Katz and Rabinowitch (1) have reviewed most of the investigations of the kinetics of the reaction of uranium with hydrogen carried out before 1944. Another study was made by Straetz and Draley.[1] Most of this work was performed in systems containing hydrogen at 1 atm pressure. It was found generally that the reaction followed a linear rate law, with a maximum reaction rate occurring at about 225°–250°C. This could be explained since the plateau dissociation pressure, p_0, that is the equilibrium hydrogen pressure of a uranium-uranium hydride-hydrogen system, increases very rapidly with temperature at about 250°C. The isothermic plateau dissociation pressure is about 4 mm Hg at 250°C and 760 mm at 433°C. Therefore, at a fixed system pressure, p, the excess pressure, $p - p_0$, over the dissociation pressure decreases with increasing temperature, and it would be expected that the reaction rate would decrease. With the system maintained at 1 atm pressure of hydrogen, there would be no reaction to produce hydride at 433°C and above.

There have been other investigations (1)[2] in which the effect of pressure on the kinetics of the reaction was studied. These investigations were carried out in a constant-volume apparatus in which the rate of decrease of pressure with time at constant temperature was determined. Data are reported which follow the equation $-(dp/dt) = K(p_t - p_0)^{5/2}$, where p_t is the residual hydrogen pressure after the reaction has proceeded for time, t. However, there is no ready explanation of the 5/2 power in the equation.

For the present study, the kinetics of the reaction of hydrogen with uranium was studied under the condition that $p - p_0$ is a constant, that is, the hydrogen pressure in excess of the plateau dissociation pressure of the uranium hydride product was constant. The temperature range of 100°–400°C was chosen.

Values of p_0 used in this study were obtained previously.[3] The variation of p_0 with temperature is given by the equation $\log p_{mm} = -4590/T + 9.39$, which is in good agreement with data presented by other investigators (1).

Experimental Procedure

Materials

The uranium used in this study was fabricated (2) into a ⅜-in. diameter rod. Test specimens were machined from these rods. Analysis of the uranium was obtained by spectrographic, chemical, and vacuum-fusion techniques. The total of all the measured impurities was less than 400 ppm, and each impurity was present in a concentration of less than 100 ppm. The following elements were detected as impurities: aluminum, carbon, chromium, cobalt, copper, iron, magnesium, manganese, nickel, nitrogen oxygen, silicon, and a few others in very low concentrations.

Pure hydrogen was obtained from the thermal decomposition of uranium hydride. The hydride was prepared by reacting dried tank hydrogen with degreased high purity uranium chips.

Method

The general method for measuring the rate of reaction between uranium and hydrogen has been described previously for other metal-gas reactions (3, 4). The apparatus is basically the same as that described in a previous paper (3), but a pressure regulator has been incorporated in the

[1] Classified information.

[2] Classified information.

[3] Classified information.

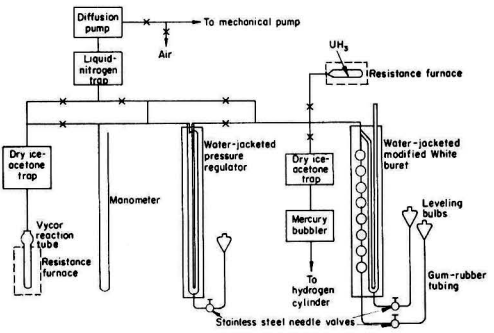

FIG. 1. Schematic diagram of modified Sieverts apparatus

design. A schematic diagram of the apparatus used is shown in Fig. 1. The system was evacuated by a two-stage mercury-diffusion pump backed by a mechanical pump.

The modified White gas buret (5) used to store the hydrogen and to measure the consumption rate consisted of eight bulbs, each of approximately 50 ml, and an open-end mercury manometer, one arm of which was a graduated 50-ml buret. The pressure regulator (see Fig. 1) consisted of an outer Pyrex tube, 40 mm in diameter and 90 cm long, which was connected to the reaction tube. An inner 2-mm Pyrex capillary tube which extended from the top to about 3 cm above the bottom of the outer tube was connected to the gas buret. The pressure, p, to be maintained in the reaction tube was set by lowering the mercury level in the pressure regulator a distance, p mm, below the mercury level when at barometric height. In operation, hydrogen was consumed by a specimen and replacement gas bubbled through the mercury from the capillary tip to maintain the desired pressure (± 1 mm of mercury) in the reaction tube. Both the buret assembly and pressure regulator were water jacketed and maintained at constant temperature (± 0.5°C during the course of a reaction rate run).

The Vycor reaction tube was sealed to the system with Apiezon W wax, and its dead volume was decreased with a solid Pyrex rod. This dead space also was used to hold a platinum platinum-10% rhodium thermocouple in contact with the top of a specimen. The thermocouple was used to measure the specimen temperature during the course of a rate experiment.

The reaction tube was heated with a resistance-wound furnace which was controlled by a Foxboro controller, using a Chromel-Alumel thermocouple placed at the resistance windings of the furnace. Temperature of a specimen was maintained to ± 3°C.

Prior to specimen preparation, machined uranium cylinders about 0.8 cm in diameter and ranging from 1 to 4 cm long were abraded with 240-grit silicon carbide paper and vacuum annealed at 600°C for 3 hr. Specimens then were abraded with 240, 400, and 600-grit silicon carbide papers. After the dimensions and weight of the specimens were determined, they were given a final polish with dry 600-grit silicon carbide paper, immediately placed in the reaction tube, and sealed into the system. The system was evacuated for 1 hr at a pressure better than 10^{-5} mm Hg. During this evacuation, the portion of the reaction tube above the specimen was flamed periodically to remove adsorbed gases from the walls of the tube. The specimen was then slowly heated to the temperature of the reaction-rate run and held at temperature for a period of about 1½ hr. It was found necessary to take these precautions to keep the induction period of the reaction to a minimum.

While the specimen was being heated at temperature, hydrogen was generated and stored, and the pressure regulator adjusted to the pressure conditions of the run.

With the specimen at the desired temperature, hydrogen was admitted from the gas buret through the pressure regulator which maintained the desired pressure in the reaction tube. By manipulations of the buret leveling bulb and stainless steel needle valve, the buret was continuously balanced to atmospheric pressure. Readings of the buret manometer arms were made at ½- to 2-min intervals, depending on the reaction rate. The quantity of gas consumed by the specimen was the difference between the volume added from the buret and volume remaining in the gas phase in the calibrated dead space. Original geometric dimensions of specimens were used in calculating the quantity of hydrogen reacted per unit area, in units of ml STP hydrogen per cm².

RESULTS AND DISCUSSIONS

Films

Visual observation of the surface of a uranium specimen during the course of a run showed that at the start of a reaction a very thin blue-black hydride film formed which was considered to be adherent to the metal since it showed no evident cracking or flaking. The same type of protective film existed throughout the reaction where the parabolic rate law was followed. No extensive investigation of the adherent films could be made since they could not be preserved upon cooling of the specimen from the temperature of the rate experiment. As soon as the furnace was removed from the reaction tube, the reaction product began dusting off the specimen. At the longer times wherever the linear rate law was followed there was a continual dusting of the hydride.

Inspection of the metal surfaces at the end of a reaction experiment showed them to be relatively smooth. The decrease in the surface areas during the experiments averaged about 3% or less, based on the decrease in the dimensions of the metal specimens. Since the change in surface area was so small, no corrections were made on the original geometric dimensions in calculating the quantity of hydrogen consumed per unit area.

Rate Data

Rates of reaction of pure hydrogen with massive uranium were determined in the range 96°–394°C at three hydrogen pressure levels of $p - p_0$: 430, 150, and 70 mm of mercury. At all pressure levels, after initial deviations, the rates followed the linear law, $w = rt$, where w is the ml STP hydrogen consumed per cm² of surface, t is time, and r is the linear reaction rate in units of ml/cm²/sec. In each case, the linear rate increased with increasing temperature at lower temperatures, but decreased with increasing temperatures above a certain temperature which depended upon the pressure.

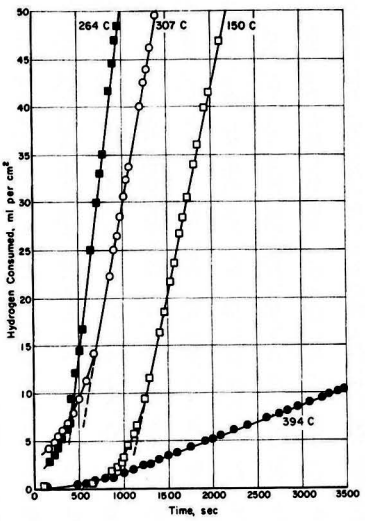

FIG. 2. Reaction of uranium with hydrogen for $p - p_0 =$ 430 mm Hg.

For $p - p_0 = 430$ mm of mercury, Fig. 2 shows typical plots of w vs. t. It is seen that after initial deviations (a gradual increase in rate) the data follow the linear law. Values of the linear rate, calculated from the various plots, are given in Table I. The rates range from 3.5×10^{-2} ml/cm²/sec at 102°C to a maximum of 7.6×10^{-2} ml/cm²/sec at 264°C, and then decrease to 3.6×10^{-3} ml/cm²/sec at 394°C.

In Fig. 3 are typical plots of w vs. t for $p - p_0 = 150$ mm of mercury pressure. In Table II are given the values of the linear rates which range from 1.2×10^{-2} ml/cm²/sec at 96°C to 2.8×10^{-2} ml/cm²/sec at 200°C, and then decrease to 1.9×10^{-3} ml/cm²/sec at 356°C. However, at this pressure level two different types of initial deviations were obtained. In the range 96°–200°C and at 356°C the reaction rate gradually increased until the rate became linear. However, in the range 254°–326°C the initial reactions followed the parabolic rate law, $w^2 = rt$, where r is the parabolic rate (ml/cm²)²/sec. The parabolic behavior can be seen in Fig. 4, where the square of w is plotted as a function of t for a number of runs, and it is seen that the data fall on straight lines. The parabolic rates which were obtained from these plots and the initial time that the

TABLE I. *Rates for the reaction of uranium with hydrogen at $p - p_0 = 430$ mm Hg*

Temp, °C	p_0, mm Hg	Linear rate, ml/cm²/sec
102	0.002	3.5×10^{-2}
150	0.035	4.3×10^{-2}
155	0.050	4.4×10^{-2}
171	0.12	4.9×10^{-2}
206	0.63	5.5×10^{-2}
264	5.5	7.6×10^{-2}
307	30	5.0×10^{-2}
308	30	2.9×10^{-2}
346	93	1.5×10^{-2}
394	316	3.6×10^{-3}

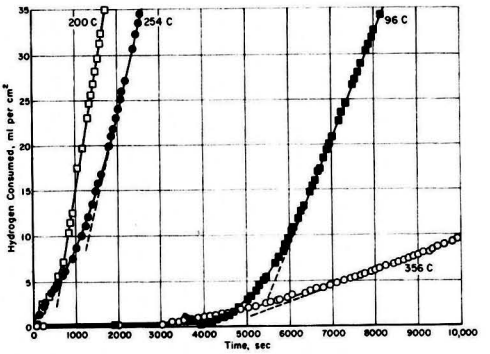

FIG. 3. Reaction of uranium with hydrogen at $p - p_0 =$ 150 mm Hg at 96°–356°C.

parabolic rate was followed are also given in Table II. The rates ranged from 3.8×10^{-2} (ml/cm²)²/sec at 254°C to 2.2×10^{-2} (ml/cm²)²/sec at 326°C.

For $p - p_0 = 70$ mm Hg, Fig. 5 shows typical plots of w vs. t. The linear rates obtained from such plots are given in Table III. Values range from 7.7×10^{-3} ml/cm²/sec at 96°C to 1.3×10^{-2} ml/cm²/sec at 206°C, and then decrease to 3.0×10^{-3} ml/cm²/sec at 253°C. In the range 96°–206°C initial deviations showed a gradually increasing rate, and in the range 206°–303°C they showed a parabolic rate. Parabolic plots are included in Fig. 4. The parabolic rates and the time that the parabolic rate was followed are given in Table III. Rates range from 2.1×10^{-2} (ml/cm²)²/sec at 206°C to 1.1×10^{-2} (ml/cm²)²/sec at 303°C.

It has been found generally that the temperature dependence of rate measurements follows the Arrhenius-type equation, $k = A \exp(-Q/RT)$, where k is the rate constant, A is the frequency factor, and Q is the energy of activation. Therefore, a plot of logarithms of the rate constants vs. the reciprocals of the absolute temperatures should yield a straight line. Such plots are given in Fig. 6 for the linear rates which are constant at a given pressure for the reaction of massive uranium with hydrogen at the three levels of $p - p_0$ equal to 430, 150, and 70 mm of Hg pressure. Equations for the best straight lines through the various sets of points were determined by the method of least squares. It can be seen that the rate constants go

TABLE II. *Rates for the reaction of uranium with hydrogen at $p - p_0 = 150$ mm Hg*

Temp, °C	p_0, mm Hg	Time of initial parabolic reaction, sec	Parabolic rate, (ml/cm²)²/sec	Linear rate, ml/cm²/sec
96	0.001	None	—	1.2×10^{-2}
110	0.003	None	—	1.6×10^{-2}
121	0.006	None	—	1.5×10^{-2}
146	0.028	None	—	1.7×10^{-2}
163	0.070	None	—	2.1×10^{-2}
200	0.60	None	—	2.8×10^{-2}
254	4.7	500	3.8×10^{-2}	2.0×10^{-2}
300	25	1200	3.2×10^{-2}	9.1×10^{-3}
326	53	600	2.2×10^{-2}	5.6×10^{-3}
356	123	None	—	1.9×10^{-3}

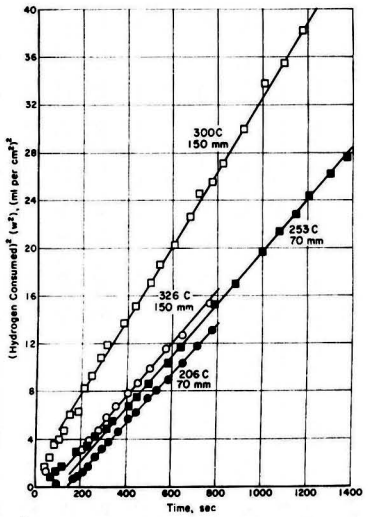

FIG. 4. Parabolic plot of initial reaction of uranium with hydrogen at $p - p_0 = 150$ and 70 mm Hg.

through a maximum at each level. The expressions for the linear rate constants are given in Table IV. At the higher temperature where the linear rate decreases with increasing temperature, an apparent negative "energy of activation" is obtained. Theoretically this is meaningless. Therefore, some other pressure dependency in addition to $p - p_0$ is necessary to define the reaction in the higher temperature range (250°–400°C).

The effect of pressure on the linear reaction rates can be seen in Fig. 6. From the equations given in Table IV, linear rates were calculated at all three $p - p_0$ levels at temperatures in the range 100°–250°C. Also in this range, p_0 is small, 1 mm of mercury or less, and the quantity $p - p_0$ is not significantly different from the system pressure, p. Therefore, pressure dependency of the reaction up to 250°C may be considered as a function of p alone. A plot of log r vs. log p gave straight lines with slopes of about 0.75, which indicates the following relationship between rate and pressure:

$$r = \frac{dw}{dt} = kp^{3/4}$$

A plot of the logarithms of the values of $r/p^{3/4}$ vs. $1/T$ is given in Fig. 7. Using these data, and applying the method of least squares the following equation for the linear rate, r, in ml/cm²/sec, was obtained,

$$r = 4.11 \times 10^{-3}\, p^{3/4} \exp - 1820/RT$$

where p is in mm of mercury for the range 96°–250°C.

Various reaction mechanisms were considered to explain the reaction in the higher temperature range (250°–400°C). Such theoretical treatments as that presented by Peterson, Fassell, and Wadsworth (6) were tried. In this, a pressure dependency based on Langmuir's adsorption isotherm Type-I was found for the linear oxidation of tantalum. However, no such dependency could be shown for the present work.

Since the hydrogen-uranium reaction is at nearly equilibrium conditions, it would appear that some function including $p - p_0$ (7) is necessary to explain the pressure dependency. Qualitatively, the reaction in the forward

TABLE III. *Rates for the reaction of uranium with hydrogen at $p - p_0 = 70$ mm Hg*

Temp, °C	p_0, mm Hg	Time of initial parabolic reaction, sec	Parabolic rate, (ml/cm²)²/sec	Linear rate, ml/cm²/sec
96	0.001	None	—	7.7×10^{-3}
145	0.026	None	—	1.1×10^{-2}
168	0.15	None	—	1.2×10^{-2}
206	0.70	800	2.1×10^{-2}	1.3×10^{-2}
220	1.2	1000	2.2×10^{-2}	8.2×10^{-3}
253	4.6	4000	2.1×10^{-2}	3.0×10^{-3}
303	26	9000	1.1×10^{-2}	None

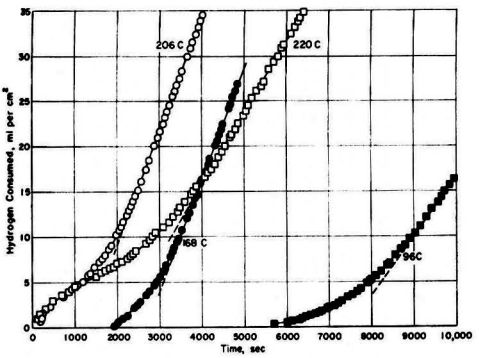

FIG. 5. Reaction of uranium with hydrogen at $p - p_0 = 70$ mm Hg at 96°–220°C.

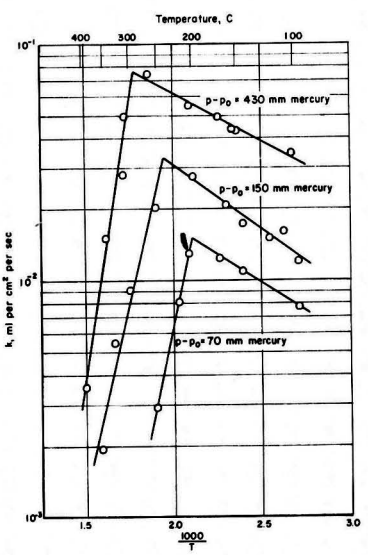

FIG. 6. Temperature dependence of linear rate constant for uranium-hydrogen reaction.

TABLE IV. *Expressions for linear rate constants for the reaction of uranium with hydrogen*

Pressure, $p - p_0$, mm Hg	Temp range, °C	Expression for linear rate constant k	Approximate error, in a calculated k, relative %
430	102–264	$0.421 \exp(-1890/RT)$*	3.5
	307–394	$6.30 \times 10^{-10} \exp(20{,}700/RT)$	20
150	96–200	$0.399 \exp(-2540/RT)$†	5.0
	254–356	$2.35 \times 10^{-8} \exp(14{,}500/RT)$	19
70	96–168	$0.118 \exp(-2160/RT)$‡	1.2
	206–253	$8.41 \times 10^{-10} \exp(15{,}700/RT)$	1.1

*, †, ‡ = Activation energies for these reactions are 1890 ± 110, 2540 ± 200, and 2160 ± 80 cal/mole, respectively.

direction (hydride produced) is dependent on the system pressure while the reaction in the reverse direction (hydride dissociated) is dependent on the dissociation pressure of the hydride. Thus, the net forward reaction to produce hydride is dependent on the quantity $p - p_0$. However, as noted in Fig. 6, the application of this dependency alone gave an apparent negative activation energy in the range 250°–400°C. After many considerations, an empirical equation was found which could be applied to the data. The equation is:

$$r = k \frac{(p - p_0)}{p_0}$$

Fig. 8 shows a plot of $\log r/(p - p_0/p_0)$ vs. reciprocal temperature for the data in the range of about 250°–400°C. The best straight line was drawn through the points using the method of least squares. The apparent activation energy was calculated to be 11,900 ± 1300 cal/mole. The scatter of data arises from the difficulty of keeping $p - p_0$ constant. Since p_0 increases rapidly with temperature in the range 250°–400°C, small variations in temperature produce large errors in the selected p_0 for an experiment.

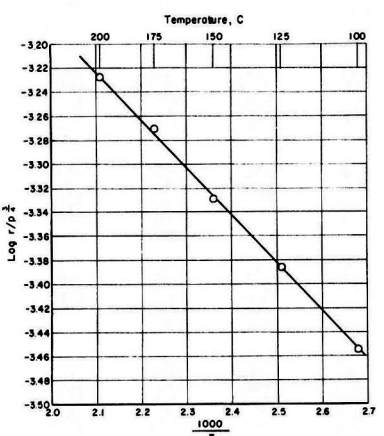

FIG. 7. Variation of rate constant with temperature for pressure dependency of $p^{3/4}$.

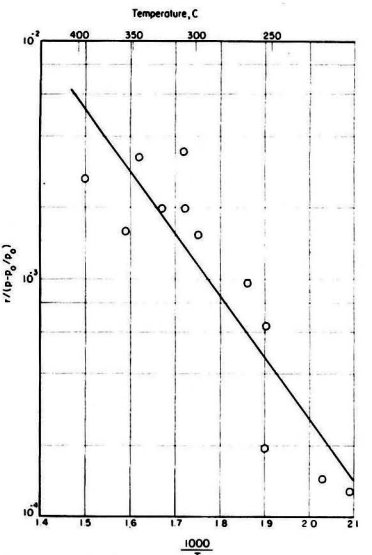

FIG. 8. Variation of rate constant with temperature for pressure dependency of $p - p_0/p_0$.

Duplicate rates obtained at $p - p_0 = 430$ mm Hg and 307°C varied from 2.0×10^{-3} to 3.5×10^{-3} ml/cm²/sec.

Upon consideration of the meager parabolic data obtained in the study, there appeared to be very little change of the parabolic rate with temperature and pressure. Therefore, no attempts were made to derive any relationships between these variables for the parabolic data.

CONCLUSIONS

The reaction of uranium with hydrogen was found to follow a linear rate law after initial deviations. Inspection of the data indicates that there are at least two different rate-controlling processes in the temperature and pressure ranges investigated. In the range 96°–250°C a pressure dependency of $p^{3/4}$ was obtained. At higher temperatures, 250°–394°C, reasonable fit of the data was obtained with a pressure dependency of $p - p_0/p_0$. However, since none of the reaction mechanisms was determined, the significance of these pressure dependencies is not known.

ACKNOWLEDGMENTS

The authors gratefully acknowledge the assistance of Mr. W. R. Hansen and Mr. B. G. Koehl in making the experimental reaction rate runs.

Manuscript received March 24, 1955. This paper was prepared for delivery before the Cincinnati Meeting, May 1 to 5, 1955. The work was performed under AEC Contract W-7405-eng-92.

Any discussion of this paper will appear in a Discussion Section to be published in the June 1957 JOURNAL.

REFERENCES

1. J. J. KATZ AND E. RABINOWITCH, "The Chemistry of Uranium," Part I, p. 193 ff, National Nuclear Energy Series, McGraw-Hill Book Co., Inc., New York (1951).

2. M. W. Mallett and A. F. Gerds, *This Journal*, **102**, 292 (1955).
3. J. Belle, B. B. Cleland, and M W. Mallett, *ibid.*, **101**, 211 (1954).
4. M. W. Mallett and W. M. Albrecht, *ibid.*, **102**, 407 (1955).
5. A. H. White, *J. Am. Chem. Soc.*, **22**, 343 (1900).
6. R. C. Peterson, W. M. Fassell, and M. E. Wadsworth, *J. Metals*, **6**, 1038 (1954).
7. L. S. Darken and R. W. Gurry, "Physical Chemistry of Metals," p. 465 ff. Metallurgy and Metallurgical Engineering Series, McGraw-Hill Book Co., Inc., New York (1953).

Allotropic Modifications of Calcium

J. F. Smith, O. N. Carlson, and R. W. Vest

Institute for Atomic Research, Iowa State College of Agriculture and Mechanic Arts, Ames, Iowa

ABSTRACT

X-ray diffraction patterns of calcium samples of different purities have shown that 99.9+% Ca exists in only two allotropic forms: face-centered cubic to 464°C and body-centered cubic from 464°C to the melting point. These results for the high temperature allotrope differ from the widely accepted structure; handbooks and tables currently list the high temperature allotrope as hexagonal closest-packed. It has been further shown that a previously reported intermediate allotrope of complex structure is due to contamination. The temperature dependence of the electrical resistivity of the 99.9+% Ca was found to be linear for both the face-centered cubic allotrope and for the body-centered cubic allotrope. Calcium was observed to be self-annealing at room temperature.

Introduction

An x-ray diffraction investigation of calcium was undertaken because calcium was reported to exist in three allotropic forms (1) and because there was some question about the lattice type of the intermediate allotrope existing between 300° and 450°C. Evidence for the existence of an intermediate allotrope in this temperature range has been reported (2–4). Further, there existed a discrepancy in the reported structure of the high temperature allotrope; Graf (5) originally reported the high temperature allotrope to be b.c.c. while Ebert, Hartman, and Peisker (6) reported h.c.p. Graf (4) extended his investigation using five different grades of calcium, one of which was obtained from Ebert. Graf found both high temperature forms; from the sample obtained from Ebert both forms were obtained on the same diffraction pattern. The intermediate allotrope was found in all five calcium samples. Graf concluded from his studies that there were three allotropes of calcium and that the structure of the high temperature form of pure calcium was h.c.p. However, Graf's estimate of purity was apparently based on method of preparation since no analytical data were given for the higher purity calcium samples. His conclusion about the high temperature phase is in disagreement with results obtained in this investigation.

Experimental and Results

Calcium Preparation

Purification studies preceded preparation of the metal used in the experimental investigation. Crude calcium metal which had been prepared by the alumino-thermic reduction of calcium oxide (7) was obtained from the New England Lime Co., Canaan, Conn. Past research by the authors has shown that this material can be separated readily from most of its impurities by a vacuum distillation. Typical results of a single vacuum distillation at 900°C are shown in Table I. Distillations on a 200-lb scale were carried out in a 310 Nb stabilized stainless steel retort at pressures of the order of 10^{-3} mm Hg, and the condensate was collected on an air-cooled condenser maintained at 300°–400°C. Analyses were run on calcium granules obtained by grinding the calcium in a Wiley Mill; fine particles were removed by screening. Data in Table I illustrate that magnesium is not readily removed by this distillation process.

For this investigation, calcium of the highest possible purity was desired and methods for the removal of the magnesium were considered. Fujita, Yokomizo, and Kurozaki (8) effected a magnesium separation by collecting the metallic vapors on a hot surface (600°–800°C), while work done by Betcherman and Pidgeon (9) on the vapor pressures and rates of sublimation of calcium and magnesium suggested that magnesium might be preferentially sublimed from calcium at a temperature below the melting point of calcium metal. Considerable experimental work was done on the latter approach to determine conditions for removal of magnesium.

Calcium of three different grades, hereafter referred to as calcium A, calcium B, and calcium C, was prepared for use in this investigation. Calcium A was prepared by four successive distillations at 900°C. The magnesium content was not noticeably reduced.

The other two specimens were prepared in the following manner. Calcium metal which had been purified by vacuum distillation and thus contained magnesium as the

TABLE I. *Analysis of major impurities in N.E.L. calcium before and after distillation at 900°C*

Impurity	Analysis before distillation in wt %	Analysis after distillation in wt %
Al	0.1–0.2	0.002
Fe	0.01	0.005
N	0.06–0.1	0.003
Mg	0.3	0.3
Mn	0.02	0.003

TABLE II. *Analysis of calcium samples used in this study*

Impurity	Calcium A analysis in wt %	Calcium B analysis in wt %	Calcium C analysis in wt %
Mg	0.300	0.110	0.010
N	0.025	0.022	0.011
Fe	0.006	0.010	0.010
Al	0.001	0.001	0.001
Mn	0.004	0.005	0.005
Net Ca.....	99.66	99.85	99.96

major impurity (0.3 wt%) was ground to a fine particle size (−20 mesh). About 500 g of this material was heated in an evacuated chamber at 600°C for 8 hr at a pressure of less than 10^{-4} mm Hg. The sublimate containing most of the magnesium was collected on a water-cooled condenser. The calcium remaining in the charge was then distilled off under vacuum by heating to 900°C. The resulting condensate appeared to divide naturally into two nearly equal portions. Calcium B was that portion which appeared to have distilled off last and still contained appreciable amounts of magnesium. Calcium C, that portion which distilled off first, contained very little magnesium. This was then redistilled for final purification. The reason for this unusual separation is not fully understood at this time. Possibly during sublimation the magnesium was depleted from the outer region of each calcium granule and on subsequent distillation the magnesium-depleted regions were the first to distill.

Aluminum, iron, magnesium, and manganese contents were determined spectrographically, and the nitrogen content was determined by the micro-Kjeldahl method. Analyses are shown in Table II. No values are reported for oxygen or carbon because of the difficulty in analyzing for these elements in calcium. However, there is no reason to expect appreciable contamination from either of these elements. The most likely source of carbon would be the diffusion pump oil, and a liquid nitrogen cold trap was used in the vacuum line to prevent oil vapors from reaching the calcium. An estimate of <0.01 wt % oxygen would seem to be a reasonable value since oxygen and nitrogen contamination both results from reaction of calcium with residual air in the vacuum system. Spectrographic analyses of the initial calcium showed trace amounts of boron, cadmium, silicon, sodium, lithium, and potassium. These may have carried through to the final product.

Contamination during Fabrication and Experimentation

Because of the high reactivity of calcium, particularly at elevated temperatures, it was found necessary to take precautions against contamination during fabrication and during the thermal changes in the experiments. Fabrication was accomplished in the following manner. Calcium was fused in a sealed iron tube at a temperature above 900°C. Subsequently, the iron was turned off in a lathe, leaving a solid calcium rod. For x-ray diffraction studies, a calcium rod $\frac{3}{8}$ in. in diameter by 1 in. long was milled into a bar with a thickness of $\frac{3}{16}$ in. An additional $\frac{1}{16}$ in. was removed by filing under a dry helium atmosphere. The resulting specimen was $\frac{1}{8}$ in. x $\frac{3}{8}$ in. x 1 in. For resistivity studies, calcium was turned in a lathe to form a rod 0.2 in. in diameter by 5 in. long.

Spectroscopic analysis showed that the pick-up of iron from the crucible was less than 50 ppm. Calculations using ambient temperature and pressure indicated that charging and sealing the crucibles in air could result in a maximum increase in nitrogen and oxygen content of 350 ppm. This contamination would be considerably less if there were any tendency toward segregation at the surface.

X-ray and resistivity studies were carried out under an inert atmosphere of helium. The high vapor pressure (10, 11) of calcium precluded a vacuum, and the high rate of reactivity at elevated temperatures made an inert atmosphere necessary. Initial experiments showed that commercial "Grade A" helium contained sufficient oxygen and water vapor to react with calcium to form a surface film which masked the x-ray reflections from the metal lattice. Thus helium was purified via a train which consisted of a series of two liquid nitrogen cold traps preceded by a getter-furnace filled with calcium turnings heated to 600°C. The specimen chamber and purification train were filled by first evacuating to a pressure of 5×10^{-6} mm Hg and then slowly introducing the helium. Evacuation and refilling were repeated several times before the sample was heated. With this helium purification a calcium sample could be kept in the x-ray camera for a week or more with daily heating and cooling without picking up a detectable oxide film. Helium purification was also used for the resistivity measurements.

X-Ray Diffraction Results

All x-ray patterns were taken with a Geiger-counter diffractometer adapted for high temperature studies as described by Chiotti (12). All diffraction peaks were confirmed with two independently prepared bar specimens. Data for calcium A were also checked with powder patterns. Interfering oxide and hydroxide peaks appeared rapidly in the powder pattern even under purified helium. Temperatures were measured with a chromel-alumel thermocouple in contact with the base of the test specimens.

Results indicate that calcium is self-annealing at room temperature. Diffraction peaks were observed to have normal shape and intensity as soon as measurement could be made after cold working by milling and filing. Minimum time between working the sample and observing the first diffraction peaks was approximately 10 min. Corroborative evidence for this self-annealing is available from past experience in the lack of hardening after extensive cold working.

Face-centered cubic phase.— There is no doubt that the room temperature phase of calcium is f.c.c. This phase was first

TABLE III. *Reflections from complex phase at 319°C*
Copper Kα radiation*
Calcium A

2θ	d	sin²θ
26.52	3.358	0.05244
27.50	3.241	0.05641
28.20	3.162	0.05934
30.80	2.901	0.07054
34.15	2.624	0.08644
45.60	1.988	0.1502
47.20	1.924	0.1603
52.30	1.748	0.1945
56.05	1.667	0.2209
67.00	1.396	0.3046
73.50	1.287	0.3576
75.40	1.260	0.3739
90.70	1.083	0.5062
110.15	0.9395	0.6724
118.00	0.8986	0.7348

* The 2θ values were converted to *d*-spacings with National Bureau of Standards tables based on the $K\alpha_1$ wave length of 1.54050Å.

pattern could not be indexed on the basis of a cubic, hexagonal, or tetragonal lattice. An attempt to index the pattern in the orthorhombic system by numerical methods (14–16) was unsuccessful. The possibility that the diffraction pattern represents a multiple phase region still exists.

This complex phase was not found initially in calcium C. After a specimen of calcium C had been in the camera for four days, with a considerable fraction of the time at high temperatures, some peaks characteristic of the complex phase appeared in addition to those of the f.c.c. phase in patterns run at 414° and 450°C. When the specimen was taken from the camera, the surface removed by filing, and the specimen remounted, the peaks from the complex phase no longer appeared. The appearance of the complex phase after prolonged heating at elevated temperatures and the elimination of this phase by removal of the surface layer were reproducible. It was concluded from this behavior that the appearance of the complex phase was due to a change in the surface layer of the calcium. In addition it was reasoned that, since the complex phase was characteristic of the lower purity calcium A and

TABLE IV. *Comparison of observed transitions in calcium*

Temp, °C	Graf*	Calcium A 99.66%	Calcium B 99.85%	Calcium C 99.96%
100	f.c.c. $a = 5.57$Å	f.c.c. $a = 5.612 \pm 0.012$Å	f.c.c.	f.c.c. $a = 5.582 \pm 0.004$Å
200				
300	300°C	300°C	300°C	
400	complex 450°C	complex 375°C	complex 450°C	464°C
500	h.c.p. $c/a = 1.64$	h.c.p. $c/a = 1.63$ 500°C		
600		b.c.c. $a = 4.474 \pm 0.004$Å	b.c.c.	b.c.c. $a = 4.477 \pm 0.007$Å
700				
800				

* Data represent Graf's best calcium.

reported by Hull (13) who gave the lattice parameter as $a = 5.57$Å. All subsequent investigators have corroborated this structure. In this investigation all of the calcium samples were f.c.c. at room temperature, and the lattice parameter at 18°C was $a = 5.612 \pm 0.012$Å for calcium A and $a = 5.582 \pm 0.004$Å for calcium C. No attempt was made to obtain high precision parameters; parameters were calculated primarily for phase identification. The f.c.c. phase was found to persist up to about 300°C in calcium A and calcium B and up to about 460°C in calcium C.

Complex phase.—A phase of complex nature was found in calcium A between 300° and 375°C and in calcium B between 300° and 450°C. Diffraction peaks for calcium A at 319°C are listed in Table III. The correspondence of the diffraction peaks indicates that this is the intermediate phase reported by Graf (4). In agreement with Graf this

calcium B, this behavior must result from an increase in impurity content at the surface. Such an increase might occur in at least three possible ways. First, there might be enough residual contaminant in the helium atmosphere to react with the calcium surface at elevated temperatures. Calcium is known to react rapidly with many gases at elevated temperatures. Second, preferential sublimation of calcium at elevated temperatures could enrich the surface in nonvolatile impurities. Evidence for calcium sublimation was inferred from the embrittlement of the tantalum heating element which necessitated frequent replacement during the course of the experiments. Third, differential solubility as a function of temperature could have created a concentration gradient (17) between the surface and the bulk of the sample. A temperature gradient between the surface and the base of the calcium undoubtedly existed because of the geometry of the furnace

and sample mount. Any one of these factors, or combination of them, could account for the observed behavior of calcium C.

Hexagonal closest-packed phase.—The high temperature allotrope of calcium is widely quoted in handbooks and tables as being h.c.p. In this investigation an h.c.p. phase was found in the lowest purity calcium A between 375° and 500°C, but was not found as a stable phase in calcium B or calcium C. This phase was indexed on the basis of Graf's parameters, and a check of the measured d values with a Bunn chart (18) gave $c/a = 1.63$ with $c = 6.49$Å and $a = 3.97$Å. Graf reported $c/a = 1.64$. However, even in calcium A the hexagonal phase gave way to a b.c.c. phase over 500°C. None of Graf's published patterns was taken above 500°C.

Body-centered cubic phase.—All of the samples exhibited a b.c.c. phase at high temperature. The stable range for this phase in calcium A was between 500°C and the melting point, while the range for calcium B and calcium C was between 460°C and the melting point. The measured lattice parameter for calcium C at 500°C was 4.477 ± 0.007Å. The results of this investigation are tabulated with the results of Graf in Table IV.

Electrical Resistance Measurements

Electrical resistance measurements were made to check the transition points. These were made by an alternating current potentiometric method using the apparatus described by Chiotti (19). Automatic recording and control of the temperature were employed with a slow heating and cooling speed (1°C/min). Temperature was measured with a chromel-alumel thermocouple in direct contact with the test piece between the resistivity probes. Probes were electrolytic iron wire spot-welded to the test piece.

Fig. 1 shows discontinuities in resistance vs. temperature near 300°, 375°, and 500°C for calcium A. Transitions are not sharp, but correspondence to x-ray values is satisfactory. No cooling cycle was run because of the melting of the test piece at 849°C; this value for the melting point is in excellent agreement with the value of 851 ± 1°C reported by Antropoff and Falk (20).

A graph for the corresponding heating cycle using calcium C is also shown in Fig. 1. Only a single break appears at 464°C. Repeated thermal cycling produced no additional effect except a slight smearing of the transition point. A slight surface film was noted on the specimen after the third heating and cooling cycle. The temperature dependence of the electrical resistivity for both phases of calcium C is seen to be linear.

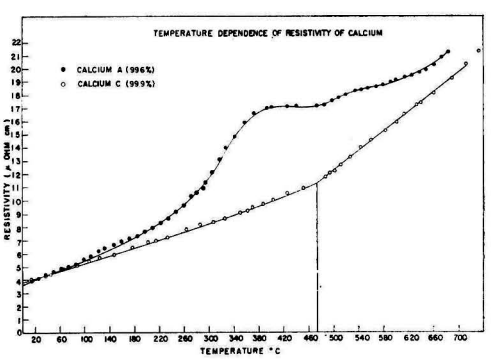

FIG. 1. Temperature dependence of resistivity of calcium. ●, Sample A, heating cycle; ○, sample C, heating cycle.

DISCUSSION

The results show that calcium is quite sensitive in its behavior to small amounts of impurities. The complex phase has been shown to be the result of contamination and must be representative of a calcium alloy system. The broad and ill-defined transition for the appearance of this phase found in this and in previous investigations fits with this interpretation. The metastability of the phases in the low purity calcium A also supports this view. In calcium A lines from all four phases could be found in the diffraction pattern immediately after rapid cooling from high temperature. The patterns stabilized to f.c.c. after approximately one hour at room temperature. Even in calcium B some metastability was noted. In contrast no metastability was observed in calcium C, patterns were of the equilibrium phase as soon as peaks could be observed from calcium C after crossing the transition temperature in either direction. Similarly, in the resistance-temperature curves, calcium A transitions were broad and sluggish, while the calcium C transition was relatively sharp.

Transformation from f.c.c. to b.c.c. with increasing temperature is consistent with Zener's theory (21) of the stability of b.c.c. phases. This theory predicts a large amplitude for the (110) [110] shear strain which gives rise to a large entropy term. Thus the free energy is lowered with increasing temperature, and the b.c.c. structure tends to be stabilized.

Supporting evidence for the importance of the entropy term in phase stabilization is Brooks' recent calculation (22) of the cohesive energy of calcium. Brooks calculated a cohesive energy of 46 kcal/mole which compares with an observed value of 48 kcal/mole. This calculation was a modification of the Wigner-Seitz (23) calculation in which structural considerations are neglected by using an approximation of spherical symmetry about an atom. The important factor in the energy evaluation is the volume per atom. The agreement between observed and calculated cohesive energy indicates the possibility that in two phases having the same volume per atom the factor controlling the relative stability may be the entropy term. In calcium Graf (4) has observed that the volume per atom in the h.c.p. and the b.c.c. phases is almost identical. Calculations based upon the observed impurity content necessary to stabilize the h.c.p. phase in this investigation show that the entropy of mixing causes a difference in entropy between the b.c.c. and h.c.p. phases of <0.1 e.u. This seems hardly sufficient to stabilize the h.c.p. phase. A second, and possibly more important, entropy term could arise from changes in the vibrational spectrum due to nonperiodic impurity atom sites. Thermodyamic studies on various purities of calcium might provide some valuable information on the problem of phase stability and transformation.

Two conclusions can be made on the basis of this in-

vestigation. First, under ambient pressure pure calcium exists in only two allotropic modifications. Second, the high temperature allotrope in pure calcium (99.9%) is b.c.c. and not h.c.p. as currently tabulated in structure compilations.

ACKNOWLEDGMENTS

The authors are indebted to Dr. V. A. Fassel and his group for the spectrographic analyses and to Dr. C. V. Banks and his group for the chemical analyses. Thanks are also extended to Dr. P. Chiotti for the use of his resistivity apparatus.

Manuscript received August 1, 1955.
Any discussion of this paper will appear in a Discussion Section to be published in the June 1957 JOURNAL.

REFERENCES

1. C. L. MANTELL AND C. HARDY, "Calcium Metallurgy and Technology," pp. 12 and 16, Reinhold Publishing Co., New York (1945).
2. P. BASTEIN, *Compt. rend.*, **198**, 831 (1934); *Rev. Met.*, **32**, 120 (1935).
3. A. SCHULZE AND H. SCHULTE-OVERBERG, "A Polymorphous Transformation in Calcium," *Metallwirtschaft*, **12**, 633 (1933).
4. L. GRAF, *Physik. Z. vereinigt mit dem Jarbuch der Radioaktivität und Elektronik*, **35**, 551 (1934).
5. L. GRAF, *Metallwirtschaft*, **12**, 649 (1933).
6. F. EBERT, H. HARTMAN, AND H. PEISKER, *Z. anorg. u. allgem. Chem.*, **213**, 126 (1933).
7. C. C. LOOMIS, *Trans. Electrochem. Soc.*, **89**, 119 (1946).
8. E. FUJITA, H. YOKOMIZO, AND Y. KUROZAKI, *J. Electrochem. Soc. Japan*, **19**, 196 (1951).
9. I. I. BETCHERMAN AND L. M. PIDGEON, *Can. Mining Met. Bull.*, **44**, 253 (1951).
10. P. E. DOUGLAS, *Proc. Phys. Soc. (London)*, **67**, No. 418B, 783, 787 (1954).
11. N. B. PILLING, *Phys. Rev.*, **18**, 362 (1921).
12. P. CHIOTTI, *Rev. Sci. Instr.*, **25**, 683 (1954).
13. A. W. HULL, *Phys. Rev.*, **17**, 42 (1921).
14. R. HESSE, *Acta Cryst.*, **1**, 200 (1948).
15. A. J. STOSICK, *ibid.*, **2**, 271 (1949).
16. H. LIPSON, *ibid.*, **2**, 43 (1949).
17. L. S. DARKEN AND R. A. ORIANI, *Acta Metallurgica*, **2**, 841 (1954).
18. C. W. BUNN, "Chemical Crystallography," p. 380, Oxford University Press, New York (1945).
19. P. CHIOTTI, *Rev. Sci. Instr.*, **25**, 876 (1954).
20. A. ANTROPOFF AND E. FALK, *Z. anorg. u. allgem. Chem.*, **187**, 405 (1930).
21. C. ZENER, "Elasticity and Anelasticity of Metals," pp. 32–37, University of Chicago Press, Chicago (1948).
22. H. BROOKS, Harvard University, Unpublished data.
23. E. WIGNER AND F. SEITZ, *Phys. Rev.*, **43**, 804 (1933); *ibid.*, **46**, 509 (1934).

Selected Physical Properties of Ternary Electrolytes Employed in Ionic Mass Transfer Studies

M. EISENBERG,[1] C. W. TOBIAS, AND C. R. WILKE

Division of Chemical Engineering, University of California, Berkeley, California

ABSTRACT

Densities and viscosities of $CuSO_4$-H_2SO_4, $AgClO_4$-$HClO_4$, and $K_3[Fe(CN)_6]$-$K_4[Fe(CN)_6]$-NaOH solutions in water have been measured over a range of compositions. Experimental values of the integral diffusion coefficients are also given for silver perchlorate in aqueous perchloric acid, and for $K_3[Fe(CN)_6]$ and $K_4[Fe(CN)_6]$ in aqueous NaOH.

INTRODUCTION

Intensive efforts have been directed toward interpretation of concentration polarization and limiting current phenomena, taking into account pertinent physical properties of the electrolytes, cell geometries, and prevailing hydrodynamic conditions (1–4). Quantitative interpretation of polarization and limiting current data requires a knowledge of densities and viscosities of the electrolyte as well as the diffusion coefficients of the reacting ionic species. The most conveniently applicable electrode reactions for purposes of mass transfer studies include the reduction of cupric ion to metal, silver ion to metal, and of ferricyanide to ferrocyanide, or vice versa. In addition to the reacting ionic species, excess "neutral" electrolyte (some strong acid or base) is frequently added to the solutions in order to render negligible the contribution of migration to the ionic mass transport. A literature survey revealed little information on the physical properties of such ternary electrolytes.

In the course of ionic mass transfer studies in this laboratory (1, 3), densities and viscosities of the electrolytes employed were determined. Diffusion coefficients were also measured, except for copper sulfate solutions, for which reliable data have already been published (1).

$CuSO_4$-H_2SO_4-H_2O System

Materials.—All solutions were prepared with C.P. materials: copper sulfate ("Baker Analyzed") and sulfuric acid (General Chemical Co.). The compositions (molari-

[1] Present address: Stanford Research Institute, Stanford, California.

TABLE I. *Densities of aqueous* $CuSO_4$-H_2SO_4 *solutions**

Molarity of $CuSO_4$	Density, g/cc			
	15°C	20°C	25°C	30°C
0	1.0932	1.0908	1.0885	1.0856
0.05	1.0999	1.0975	1.0949	1.0922
0.10	1.1069	1.1045	1.1018	1.0988
0.20	1.1204	1.1180	1.1150	1.1120
0.30	1.1338	1.1315	1.1282	1.1252
0.40	1.1477	1.1451	1.1416	1.1386
0.50	1.1622	1.1592	1.1556	1.1522
0.60	1.1768	1.1736	1.1703	1.1671
0.70	1.1929	1.1892	1.1861	1.1830
0.80	1.2088	1.2052	1.2024	1.1994

* All solutions 1.5M in H_2SO_4.

TABLE II. *Densities and viscosities of aqueous* $CuSO_4$ + H_2SO_4 + *glycerol solutions*

Composition	20°C		25°C		30°C	
	Density	Viscosity	Density	Viscosity	Density	Viscosity
g-moles/l	*g/cc*	*cps*	*g/cc*	*cps*	*g/cc*	*cps*
0.368 $CuSO_4$ 0.751 H_2SO_4 6.38 Glycerol	1.2245	11.9	1.2210	9.14	1.2184	6.95
0.570 $CuSO_4$ 1.720 H_2SO_4 3.28 Glycerol	1.2135	4.90	1.2097	4.06	1.2068	3.40

ties) were determined analytically: Cu^{++} by the iodine-thiosulfate method and $SO_4^{=}$ gravimetrically as barium sulfate.

Densities.—Data reported in Tables I and II were obtained by means of a 50 cc pycnometer equipped with a capillary and calibrated with doubly distilled water. Solutions in the pycnometer were equilibrated in a thermostat controlled to ±0.01°C in the range 13°–35°C. The density of a given solution was determined at five or six different temperatures covering the above range. This procedure yielded for each solution a density-temperature curve that could be smoothed with an average density deviation of ±0.001 g/cc for the individual points from the line.

Viscosity.—Measurements were made by using an Ostwald viscometer with an efflux volume of approximately 1.5 cc. A working volume of 10 cc was always pipetted into the viscometer in order to maintain a constant head of solution. Efflux time was followed by visual observation and measured to 0.1 sec with an electric timer. The viscometer was calibrated with doubly distilled water at various temperatures in the range 13°–32°C. This yielded an "efflux time" vs. temperature curve that was subsequently used for calculation of viscosities of the solutions at any temperature within this range. For each of the solutions the efflux time was determined at five or six temperatures within this range. From the efflux time curves and densities of water and solution (x), the viscosity of the latter at several temperatures was determined by the familiar relation:

$$\mu_x = \mu_{H_2O} \frac{\rho_x t_x}{\rho_{H_2O} t_{H_2O}} \qquad (I)$$

where t_x and t_{H_2O} denote the efflux time at a given temperature of solution and water, respectively, and ρ_x and ρ_{H_2O} denote the respective densities.

Throughout these experiments, efflux times for water varied from 91.2 to 148.3 sec, and for the solutions from 93.0 to 235.7 sec. The experimental deviation was ±0.002 centipoise.

Data.—From a density-temperature graph containing curves for twelve solutions, all 1.5M in sulfuric acid and varying in copper sulfate molarity 0–0.760, a crossplot was prepared for 15°, 20°, 25°, and 30°C. This resulted in a four isotherm plot of density vs. copper sulfate molarity. The smoothed curves of this plot are given by the data of Table I. Average density deviation from the curves was ±0.0003 g/cc. Inasmuch as there were slight variations in sulfuric acid molarity of the solutions (1.493–1.508M H_2SO_4), the above deviation is not unexpected, and is not considered to be significant.

Similarly the viscosity temperature graph for the above mentioned solutions was crossplotted, and a smoothed plot of viscosity vs. copper sulfate composition prepared for 15°, 20°, 25°, 30°C. Although viscosity measurements could be reproduced to 0.002 centipoise, the average deviation from the smoothed curves represented by the data of Table III was ±0.02 centipoise. The magnitude of these deviations should be ascribed to the above-mentioned slight variations in the molarity of sulfuric acid.

Viscosity and density determinations were also made for two aqueous $CuSO_4$-H_2SO_4-glycerol solutions by the above methods. The results for temperatures 20°, 25°, and 30°C are reported in Table II.

Although some data on solutions of these substances are available in the literature (5, 6), they are not of a type or composition range which permit comparison with the present results. A comparison of the data of the Landolt-Börnstein Tables (7) for pure sulfuric acid solutions with the corresponding data in Table I can be made. After appropriate temperature interpolations, the two sets of data are in agreement within unity in the fourth place.

Viscosity data for aqueous $CuSO_4$-H_2SO_4 solutions could not be located in the literature.

$AgClO_4$-$HClO_4$-H_2O System

Materials.—Perchloric acid: 60% (Baker Analyzed); silver perchlorate: Reagent, (G. Frederick Smith Chemical Co.) Silver was determined as the chloride, and perchloric

TABLE III. *Viscosities of aqueous* $CuSO_4$-H_2SO_4 *solutions**

Molarity of $CuSO_4$	Viscosity, cps			
	15°C	20°C	25°C	30°C
0	1.50	1.33	1.21	1.12
0.05	1.55	1.37	1.24	1.14
0.10	1.60	1.49	1.27	1.16
0.20	1.69	1.48	1.33	1.20
0.30	1.80	1.56	1.39	1.25
0.40	1.92	1.65	1.46	1.31
0.50	2.03	1.75	1.54	1.37
0.60	2.16	1.87	1.64	1.45
0.70	2.30	2.01	1.76	1.53
0.80	2.47	2.17	1.90	1.64

* All solutions 1.5M in H_2SO_4.

TABLE IV. *Selected properties of perchloric acid*

Concentration	Temp	Density	Viscosity	Diffusion coefficient
g-moles/l	°C	*g/cc*	*cps*	*cm²/cc*
1.50	23	1.0823	0.955	
	25	1.0815	0.909	
	27	1.0806	0.873	
1.55	23	1.0855	0.956	At 30°C
	25	1.0843	0.910	$D = 3.88 \times 10^{-5}$
	27	1.0834	0.874	
1.60	23	1.0877	0.955	
	25	1.0867	0.909	
	27	1.0858	0.874	

TABLE V. *Densities of* $AgClO_4$ *in 1.5*M $HClO_4$

$AgClO_4$	$HClO_4$	Temp	Density
g-moles/l	*g-moles/l*	°C	*g/cc*
0.088	1.5	25.0	1.0976
0.195	1.5	25.0	1.1126
0.339	1.5	25.0	1.1382
0.482	1.5	25.0	1.1632
0.671	1.5	25.0	1.1913
0.931	1.5	25.0	1.2308
1.156	1.5	25.0	1.2710

acid titrated with sodium hydroxide to bromthymol blue endpoint.

Densities.—Densities were obtained by a standard method described above. The values measured between 0.088M–1.156M silver perchlorate in 1.5 perchloric acid fell on a straight line on a density vs. concentration plot, with a maximum deviation of 0.003 g/cc. Between the concentration limits 0.1–1.1M silver perchlorate in 1.5M perchloric acid this line can be represented by $\rho = 1.1005 + (M-0.1)\ 0.1565$. The values measured are given in Tables IV and V.

Viscosities.—Viscosities were measured by an Ubbelohde type viscometer, with an estimated error less than ±0.5% (Tables IV and VI).

Diffusion coefficients.—These were measured in McBain-Northrup type (8, 9) diaphragm cells. Cell constants were based on the integral diffusion coefficient for 0.1*N* potassium chloride diffusing into initially pure water until concentrations in the two compartments were 0.075*N* and 0.025*N*, respectively, using the value of 1.870×10^{-5} cm²/sec for D_{KCl} at 25°C as determined by Harned and Nuttal (10). D_{HClO_4} was obtained by contacting approximately 1.6M perchloric acid through the diaphragm with 1.2M acid, diffusion taking place until the concentration of perchloric acid changed by about 0.1–0.15M. In the measurement of D_{AgClO_4}, silver perchlorate dissolved in 1.5M perchloric acid, was allowed to diffuse into 1.5M perchloric acid initially free of silver perchlorate. In Table VII the values of the "integral diffusion coefficients" are given for four different average concentrations. The average represents the arithmetic mean of four concentrations, i.e., the initial and final concentrations in both compartments of the cell. Concentrations of perchloric acid and Ag^+ in both compartments were established by careful analytic procedures prior to and following the mass exchange. Reproducibility of values of the diffusion coefficients was better than ±1.5%.

TABLE VI. *Viscosities of* $AgClO_4$ *in Approximately 1.5*M $HClO_4$

$HClO_4$	$AgClO_4$	Temp	μ
g-moles/l	*g-moles/l*	°C	*cps*
1.532		23.0	0.954
		25.0	0.910
		27.0	0.874
1.540	0.0965	22.0	0.980
		25.0	0.921
		28.0	0.859
1.516	0.4945	22.0	1.012
		25.0	0.954
		28.0	0.876
1.523	1.153	22.0	1.088
		25.0	1.027
		28.0	0.944

TABLE VII. *Diffusion coefficients of* $AgClO_4$ *in 1.5*M $HClO_4$ *at 30°C*

Avg concentration of $AgClO_4$, g-moles/l	0.05	0.1	0.3	0.8
$D \times 10^{-5}$, cm²/sec	2.30	2.26	2.1	2.07

$K_3[Fe(CN)_6]$-$K_4[Fe(CN)_6]$-NaOH-H_2O System

Materials.—All materials used were Merck's reagent grade. Ferricyanide was determined by the iodometric procedure (11) and ferrocyanide by permanganate titration (12).

Densities and viscosities.—Values for these properties were determined by methods already described for the copper sulfate and silver chlorate solutions.

Electrical conductivities.—Electrical conductivities were determined in a conventional conductivity cell, calibrated with a potassium chloride solution, using an audio oscillator as a source for 1000 cycle alternating current, a Wheatstone bridge, and an oscilloscope as a zero instrument. Estimated accuracy was ±0.5%.

Results for a number of solutions for temperatures 25° and 30° are summarized in Table VIII.

Diffusion coefficients.—A capillary technique similar to the one first described by Anderson and Saddington (13)

TABLE VIII. *Densities, viscosities, and conductivities of solutions of* $K_3[Fe(CN)_6]$ *and* $K_4[Fe(CN)_6]$ *in approximately 2N* NaOH

Composition, g-moles/l			Temp	Conductivity	Density	Viscosity
$K_3Fe(CN)_6$	$K_4Fe(CN)_6$	NaOH				
			°C	*ohm⁻¹cm⁻¹*	*g/cc*	*cps*
0.00998	0.01011	1.958	25	0.2848	1.0807	1.368
0.01224	0.01228	2.011	25	0.2863	1.0833	1.382
0.04996	0.05052	1.923	25	0.2860	1.0949	1.394
			30	0.3050	1.0929	1.257
0.0919	0.01198	1.977	25	0.2907	1.0955	1.392
0.0994	0.1008	2.007	25	0.3038	1.1174	1.494
0.3058	0.1022	2.006	25	0.3139	1.1491	1.608
0.1994	0.2030	2.004	25	0.3017	1.1535	1.642
			30	0.3264	1.1515	1.468

was chosen for this work because of its apparent simplicity and reliability. (The McBain-Northrup diaphragm cell method was not used because of the anticipated attack of the strong alkali solution on the sintered glass diaphragm.)

In the method employed here diffusion takes place from a capillary tube into an effectively infinite reservoir in which the capillary is immersed. This feature has the advantage that the width of the diffusion zone is small compared to its length, thus minimizing the effects of convection currents.

Four capillaries were simultaneously filled by means of a syringe with solutions A-2 and B-2 (see below) containing potassium ferricyanide, potassium ferrocyanide, and sodium hydroxide. The large reservoir in which they were immersed at time $t = 0$ contained solution A-1, with no ferrocyanide, or solution B-1, which contained no ferricyanide.

If the axis of the capillary is taken as x-axis then the boundary conditions for the concentration C of the diffusing species are:

$$C = C_0 \quad \text{for} \quad 0 \leq x \leq L \quad \text{at } t = 0 \tag{II}$$

$$C = 0 \quad \text{for} \quad x > L \quad \text{for all } t \tag{III}$$

where t is the time and L the length of the capillary. The solution of the diffusion equation

$$\frac{\partial C}{\partial t} = D\frac{\partial^2 C}{\partial x^2} \tag{IV}$$

under these conditions is given by:

$$\frac{C_{avg}}{C_0} = \frac{8}{\pi^2}\sum_{n=0}^{\infty}\frac{1}{(2n+1)^2}\exp\left[-\frac{(2n+1)^2\pi^2 Dt}{4L^2}\right] \tag{V}$$

where C_{avg} is the average concentration of the diffusing species in the capillary after time t. Since L and t were known, an analytic determination of C_0 and C_{avg} sufficed for the calculation of the diffusion coefficient D.

In general the times were chosen so that C_{avg}/C_0 was about 0.6–0.7. To reduce experimental error several capillaries of different lengths and volumes were used.

For the diffusion of ferricyanide ion the reproducibility was ±1.5%. In the case of the ferrocyanide, however, it was at best ±4% due to the difficult endpoint determination in permanganate titration of the small volume of solution from the capillaries.

For diffusion of ferricyanide from solution B-2 in the capillaries into solution B-1, the following average results were obtained at 25°C:

Initial concentration, g-moles/l	*B-2*	*B-1*
Sodium hydroxide	2.027	2.027
Potassium ferrocyanide	0.1919	0.1919
Potassium ferricyanide	0.1963	—

$D_{avg} = 0.527 \times 10^{-5}$ cm²/sec at average viscosity $\mu = 1.419 \times 10^{-2}$ poise, hence

$$\frac{D\mu}{T} = 2.50 \times 10^{-10}\,\frac{\text{cm}^2\,\text{poise}}{\text{sec}\ ^\circ\text{K}} \tag{VI}$$

This value was used to calculate diffusion coefficients of the ferricyanide ion.

For diffusion of ferrocyanide ion from solution A-2 (in the capillaries) into solution A-1 the following average results were obtained at 25°C:

Initial concentration, g-moles/l	*A-2*	*A-1*
Sodium hydroxide	2.027	2.027
Potassium ferricyanide	0.1879	0.1879
Potassium ferrocyanide	0.2032	—

$D_{avg} = 0.418 \times 10^{-5}$ cm²/sec at average viscosity $\mu = 1.53 \times 10^{-2}$ poise, hence

$$\frac{D\mu}{T} = 2.15 \times 10^{-10}\,\frac{\text{cm}^2\,\text{poise}}{\text{sec}\ ^\circ\text{K}} \tag{VII}$$

This value was used in computing the diffusion coefficient of ferrocyanide ion.

Estimates from equivalent conductance data, corrected for viscosity, gave $D\mu/T$ values of 2.62 and 2.22 $\times 10^{-10}$ for ferri- and ferrocyanide, respectively. Since such estimates, usually satisfactory at low concentrations, were expected to be somewhat high, the results obtained in these measurements are considered reliable.

Manuscript received August 2, 1955.
Any discussion of this paper will appear in a Discussion Section to be published in the June 1957 JOURNAL.

REFERENCES

1. C. R. WILKE, M. EISENBERG, AND C. W. TOBIAS, *This Journal*, **100,** 513 (1953).
2. C. R. WILKE, M. EISENBERG, AND C. W. TOBIAS, *Chem. Eng. Progr.*, **49,** 663 (1953).
3. M. EISENBERG, C. W. TOBIAS, AND C. R. WILKE, *This Journal*, **101,** 306 (1954).
4. N. IBL, *Chimia (Switz.)*, **9,** 135 (1955).
5. H. M. GOODWIN AND W. G. HORSCH, *Chem. & Met. Eng.*, **21,** 181 (1919).
6. H. D. HOLLER AND E. PEPPER, *J. Am. Chem. Soc.*, **38,** 1021 (1916).
7. LANDOLT-BÖRNSTEIN, "Physikalisch-Chemische Tabellen", Vol. I, p. 397, Julius Springer, Berlin (1936).
8. A. R. GORDON, *Ann. N. Y. Acad. Sci.*, **46,** 285 (1945).
9. P. CHANG, "Measurement and General Correlation of Diffusion of Nonelectrolytes," Ph.D. Thesis, University of California, Berkeley (1954).
10. H. S. HARNED AND R. L. NUTTALL, *Ann. N. Y. Acad. Sci.*, **51,** 781 (1949).
11. I. M. KOLTHOFF AND N. H. FURMAN, "Volumetric Analysis," Vol. II, p. 427, John Wiley & Sons, Inc., New York (1929).
12. F. SUTTON, "Volumetric Analysis," 12th ed., p. 235, Blakiston and Co., Philadelphia (1935).
13. J. S. ANDERSON AND K. I. SADDINGTON, *J. Chem. Soc.*, **1949,** 381.

FUTURE MEETINGS OF

The Electrochemical Society

Cleveland, September 30, October 1, 2, 3, and 4, 1956

Headquarters at the Statler Hotel

Sessions will be scheduled on

Batteries, Corrosion, Electrodeposition,
Electronics—Semiconductors,
Electrothermics and Metallurgy, Theoretical
Electrochemistry (joint with Electrodeposition),
and Theoretical Electrochemistry

★ ★ ★

Washington, D. C., May 12, 13, 14, 15, and 16, 1957

Headquarters at the Statler Hotel

★ ★ ★

Buffalo, October 6, 7, 8, 9, and 10, 1957

Headquarters at the Statler Hotel

★ ★ ★

New York, April 27, 28, 29, 30, and May 1, 1958

Headquarters at the Statler Hotel

★ ★ ★

Ottawa, September 28, 29, 30, October 1, and 2, 1958

Headquarters at the Chateau Laurier

★ ★ ★

Electro Metallurgical Co.—ECS Sustaining Member

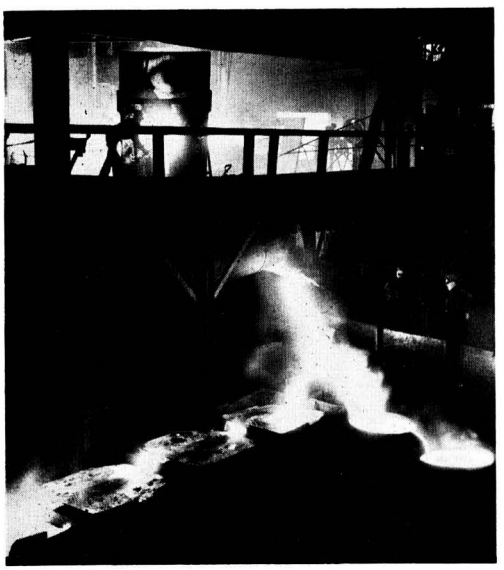

A huge electric smelting furnace is tapped at one of Electromet's seven ferroalloy plants. The alloy is cooled in slabs, shown at lower left of picture, and then crushed to its proper size.

Two men working in the small town of Spray, N. C., in 1892 stumbled on a revolutionary discovery which ultimately led to the formation of Electro Metallurgical Co., now a Division of Union Carbide and Carbon Corp. They had built a small electric furnace, which in those days was a novelty in itself, and were attempting to develop a new method for making aluminum. As one of the steps in the process, they wished to produce metallic calcium; so one day they placed in the furnace a mixture of slaked lime (calcium hydroxide) and carbon. After a run of several hours, a small quantity of the product was withdrawn and quenched in a pail of water. It at once gave off a pungent smelling gas that, when lighted, burned with a luminous flame. On later analysis, it was found that the lime and coke had joined under the great heat to form calcium carbide. When mixed with water, this gray-brown, stone-like product produced a gas known as acetylene.

This discovery marked the birth of the acetylene industry and heralded the beginning of calcium carbide production on a commercial scale. With this discovery also came a forerunner of Electro Metallurgical Co., which for 50 years has been a leading producer of calcium carbide and ferroalloys and metals. The forerunner was Union Carbide Co., which was formed in 1898 at Niagara Falls, N. Y.

Several years later another historic event took place. It was realized that with only minor changes a carbide furnace would be suitable for smelting many other materials. Among those were ferroalloys and metals. So, in 1906, an associate, Electro Metallurgical Co., was formed. Its first products were ferrochromium and ferrosilicon, two alloying metals that are used in making high-quality steel. Through its technical staff and research laboratories, this new company soon produced alloys of some eight other metals.

During the years preceding the First World War, both Electro Metallurgical Co. and Union Carbide Co. grew with the ever-expanding market for their products. Finally, in 1917, these two associates joined forces with several other companies to form Union Carbide and Carbon Corp. One was National Carbon Co., which produced the giant electrodes for the smelting furnaces. The interests of all these companies were closely related and stemmed either from electric furnace developments or from the use of electric furnace products.

Now in its 50th year, Electro Metallurgical Co. is a leader in ferroalloy production and development. In addition to calcium carbide, Electromet produces more than 100 alloys and metals to meet the varied requirements of industry. For example, Electromet manufactures 35 different grades of chromium alloys alone, many of which are used in the production of stainless steel to give the steel its characteristic resistance to rust and corrosion. Electromet also produces ferrosilicon, ferromanganese, silicomanganese, and zirconium for use as deoxidizers in the manufacture of steel and cast iron, and a wide variety of alloys of boron, columbium, manganese, silicon, titanium, tungsten, and vanadium, which are important alloying elements in ferrous and nonferrous metals.

Outstanding in Electromet's recent ferroalloy achievements is development of a low-carbon ferrochrome containing a maximum of 0.010% carbon. This extra low-carbon alloy has been a boon to the stainless steel industry, making it easier for the manufacturer to meet the analysis specifications of stainless steel. A huge plant at Marietta, Ohio, has recently been completed to produce this low-carbon ferrochrome.

As part of a long-range expansion program, Electromet has also built facilities at Marietta, Ohio, to produce electrolytic manganese and electrolytic chromium. The electrolytic process turns out manganese which is 99.90% pure on a metallic basis and chromium which is 99.80% pure, also on a metallic basis. Electromet is also building a titanium sponge plant at Ashtabula, Ohio, which for the first time in the United States will utilize the sodium reduction process. Production was expected to start at the new titanium plant in the second quarter of this year.

The heart of both the ferroalloy and calcium carbide processes is the electric furnace, and, since the founding of the company, technical men have been constantly at work seeking methods to improve it. The electric furnaces used in Electromet plants today are submerged-arc furnaces, which are over three stories high and weigh many tons. The three electrodes alone weigh more than 10 tons. The temperature of the arc between the electrodes is in the neighborhood of 6000°F. Under this intense heat, crushed ores, coke, steel scrap, and various fluxing materials, which are banked con-

tinuously at the top of the furnace, are melted down to form ferroalloys. After being tapped from the furnace, the molten alloy is cooled in large slabs or blocks. It is then cleaned, crushed, and screened to sizes varying from lumps weighing 75 lb each to powder having the fineness of granulated sugar.

Like all great American industries, the alloy business did not just grow by itself. Electromet spent much time, effort, and money over the years to build new alloy plants, to improve products and methods of manufacture, and—most important of all—to find markets not only for the alloys, but also for the steels in which they are used.

Behind the scenes, in Electromet's extensive Metals Research Labs. at Niagara Falls, N. Y., where new alloys developed by Electro Metallurgical Co. first see the light of day, research scientists are constantly searching to find even better steels and alloys than are now available. Electromet, more than any one concern, has been responsible for the vast strides made in recent years in the development of stainless steels and high-temperature alloys. To service and improve its new developments in both steels and alloys, Electromet has a group of expert technicians who work hand-in-hand with metal producers, helping in the selection of raw materials and advising on furnace techniques and melting practices, as well as on casting, rolling, and other forming operations. Their service work includes advice to users and fabricators of metal products, helping them to select the proper metal or alloy for products of all kinds.

As Electro Metallurgical Co. embarks on its second half-century of production and development, it faces the future with confidence, not only because of its constant search for new and better alloys and metals and better ways to make them, but also because it is working to help assure an ever-expanding market for the products in which these alloys and metals are used.

Cleveland Meeting, September 30 to October 4, 1956

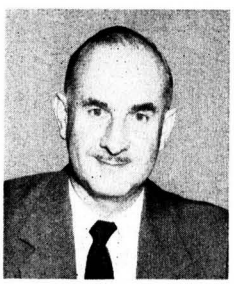

LEO PUCHER

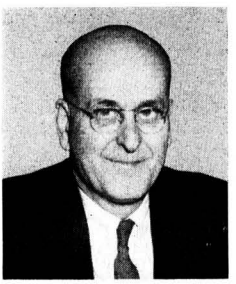

W. H. STOLL

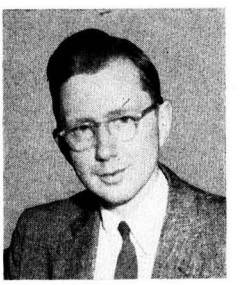

F. C. KELLER

E. B. YEAGER

Electrochemists planning to attend the Society's fall convention in Cleveland, September 30 to October 4, 1956, will find an interesting program of technical papers and discussions, a variety of plant trips and relaxing entertainment. Convention headquarters will be at the Hotel Statler in the heart of the shopping and theater center of Cleveland.

Mr. Leo Pucher is Chairman of the Hotel Committee; General Chairman is Mr. W. H. Stoll; Mr. F. C. Keller is Chairman of the Registration Committee; and the Program Committee is headed by Dr. E. B. Yeager.

Although it has many diversified industries such as steel, paints, electrical, rubber, and chemical, Cleveland has many attractions since it is a center for industrial electrochemical manufacturing and research.

Several large battery manufacturers, among them, National Carbon Co., Willard Storage Battery Co., and General Dry Batteries Co., have extensive laboratories and plants here. National Carbon Co. is now in the process of building new research facilities in a westerly suburb of Cleveland. The Harshaw Chemical Co. and the Clevite Corp. have made Cleveland the center for crystal growing in the nation. Cleveland is also the home of General Electric's famous Nela Park Lighting Institute. Among the larger of the research laboratories interested in electrochemistry are Horizons, Inc., Rand Development Corp., and the Lewis Flight Propulsion Laboratory of the N.A.C.A.

There is a variety of collegiate training available in Cleveland. The largest institution is Western Reserve University with several undergraduate colleges and graduate professional schools. Case Institute of Technology is one of the leading engineering schools in the country. An outstanding cooperative college is Fenn which offers training in several areas including engineering. John Carrol and Baldwin-Wallace provide educational programs of somewhat smaller institutions. John Carrol houses one of the nation's more important seismographs. Oberlin College, alma mater of Charles Hall of aluminum fame, is also not far away.

For diversion there are the nation's first and leading Health Museum, the Thompson Auto and Aviation Museum, Natural History Museum and Planetarium, and Art Museum. The Cleveland Zoo has just completed extensive buildings for housing the larger animals. The bird house is one of the most picturesque in the nation.

Technical Program

The following technical sessions are being planned: Batteries, Corrosion, Electrodeposition, Electronics—Semiconductors, Electrothermics and Metallurgy, Theoretical Electrochemistry Joint Session with Electrodeposition, and Theoretical Electrochemistry.

Employment Posters

Companies which desire to recruit employees at the Cleveland Meeting are invited to prepare posters (not to exceed 8½ in. × 11 in.) to be placed on a bulletin board near the registration desk.

Further details will appear in the August JOURNAL.

Annual Report of the Board of Directors for 1955

During the year 1955, the following awards were made:

Palladium Medal—U. R. Evans, Cambridge University, England.

Young Author's Prize—Milton Stern, Metals Research Labs., Electro Metallurgical Co., Niagara Falls, N. Y., for his two papers: "The Electrochemical Behavior, Including Hydrogen Overvoltage, of Iron in Acid Environments" and "The Effect of Alloying Elements in Iron on Hydrogen Overvoltage and Corrosion Rate in Acid Environments."

Francis Mills Turner Memorial Award, Sponsored by the Reinhold Publishing Corp.—J. G. Jewell, Gulf Research & Development Co., Pittsburgh, Pa., for his paper: "A Theoretical Basis for a New Method of Investigating Corrosion Inhibition."

Honorable Mention—D. E. Kinney and S. S. Brenner.

One of the primary highlights of the year 1955 was the gift of $10,000 by The Electro Metallurgical Co., establishing the F. M. Becket Award. This has been handled through our Electrothermics and Metallurgy Division, primarily by the good offices of Mr. Marvin J. Udy, our immediate past-president.

At the suggestion of the Cleveland Section, a principal change has been made in the handling of membership applications. In the past, the members were elected and then billed for the first year's dues. As of January 1, 1956, all membership applications must be accompanied by the first year's dues. This is a step forward in simplifying office procedures.

During the year 1955, the new designation of Patron Member was approved by the Board of Directors. The Patrons would be those companies or individuals that wish to support the activities of the Society to the extent of a minimum of $1,000 yearly.

On the recommendation of the Ways and Means Committee, the President appointed a Survey Committee, composed of Dr. Ralph Schaefer, Chairman, Dr. Ralph Hunter, and Mr. George Heise, to study the present affairs of the Society, the business operations of the home office of the Society in general, and plan the future of the organization in the years to come.

During the year 1955, the following monographs were published:

"Vacuum Metallurgy," Papers Presented at the Vacuum Metallurgy Symposium of the Electrothermics and Metallurgy Division of The Electrochemical Society, October 6 and 7, 1954, Boston, Mass.

"Electrochemistry in Biology and Medicine," Edited by Theodore Shedlovsky.

"Vapor Plating," by C. F. Powell, I. E. Campbell, B. W. Gonser.

"Abstracts of the Literature on Semiconducting and Luminescent Materials and Their Applications," 1954 issue, compiled by Battelle Memorial Institute.

Annual Report of the Secretary for 1955

During the year 1955, Mr. William J. Holian, Assistant Secretary, resigned. Following the very helpful suggestions of the Survey Committee (appointed at the Cincinnati meeting), a new Assistant Secretary was hired. Mr. Robert K. Shannon, formerly Secretary of the National Paint, Varnish and Lacquer Association, has stepped in and is carrying on, learning the idiosyncrasies of The Electrochemical Society office in remarkably short time. Our office now is functioning on a much more permanent basis, and we feel that stability has been attained. I am sure that any members who are in the New York area would enjoy stopping in at the office and talking to Bob Shannon. The Society is very fortunate to have found a man with his ability to handle this job.

As reported in the Annual Report of the Secretary for 1954, the tabulation of membership is not necessary in this report since it is being published quarterly in the JOURNAL so that all members can follow our progress.

During this past year, the Board of Directors have seen fit to institute a policy in which the Society pays two-thirds of the premium and the employee one-third of the premium on a health insurance policy, thus obviating the Society from obligation to carry physically incapacitated employees on the payroll.

During the year 1955, we acquired five new Sustaining members: American Potash & Chemical Corp., National Carbon Co., Carborundum Co., Michelin Corp., and Corning Glass Works.

Report of Tellers of Election

For President: Hans Thurnauer, 764; 9 write-ins; 42 abstentions

For Vice-President: W. C. Gardiner, 386; John Musgrave, 240; Eugene Willihnganz, 179; 2 write-ins; 8 abstentions

Eleven ballots were declared invalid because more than one candidate was marked for the same office.

Total votes cast as of December 15, 1955, deadline for casting ballots, was 826.

The ballot tabulations have been placed in a sealed envelope in the charge of the Assistant Secretary at The Electrochemical Society office.

(Signed) EMIL SCHMITT, JR., *Chairman*
HENRY T. WOLLMAN
WARREN A. KOSSOWSKY

The Tellers' Report was unanimously accepted and a motion was made declaring the candidates, Hans Thurnauer (President) and W. C. Gardiner (Vice-President), duly elected.

HENRY B. LINFORD, *Secretary*

Treasurer's Report for 1955

Edward Goodrich Acheson Fund

Guaranty Trust Co., Custodian

		Closing Price 12/31/55	1955 Income
Capital Funds Securities—12/31/55			
$2,000	American T & T 2¾% Bond, due 10/1/75	$1,880.00	$55.00
$2,000	Pennsylvania RR 3½% Mortgage Bond, due 1/1/85	1,692.40	62.50
$5,000	USA 3¼% Treasury Bonds, due 6/15/83	5,252.00	162.50
85 shs.	American Can Co. 7% Pfd. Stk.	3,813.95	134.29
14 shs.	Corn Products Ref. 7% Pfd. Stk.	2,457.00	98.00
10 shs.	Eastman Kodak 6% Pfd. Stk.	1,665.00	60.00
10 shs.	Ingersoll Rand 6% Pfd. Stk.	1,640.00	60.00
25 shs.	International Harvester 7% Pfd. Stk.	4,206.25	175.00

20 shs.	National Biscuit 7% Pfd. Stk.	3,495.00	140.00
20 shs.	National Lead Co. 7% Pfd. Stk.	3,515.00	140.00
28 shs.	Pacific Gas & Electric 6% Pfd. Stk.	1,004.36	42.00
60 shs.	Pacific Gas & Electric 5½% Pfd. Stk.	1,972.20	82.48
20 shs.	Pacific T & T 6% Pfd. Stk.	2,910.00	90.00
		35,503.16	1,301.77
Sale Rights Pacific T & T			115.14
Total Income 12/31/55			1,416.91
Income Balance 12/31/54			11,083.32
			12,500.23

Disbursements 12/31/55		
Purchase New Stock	10,080.25	
Brokerage Charges and Taxes	73.47	
Custodian Fees	106.00	10,259.72
Income Balance 12/31/55		$2,240.51

Edward Weston Fellowship Fund

The Hanover Bank, Trustees

Capital Funds Securities 12/31/55	
1160 Units—Hanover Bank Trust Fund A—Value 12/31/55	$14,016.97
$1817.66—Ac 1330, Brook Ave., Bronx, N. Y., N.Y.T. & M. Co., allowed claims	
1—Prudence 422, 34 East 86th St., New York, N. Y., Mortgage Certificate	

Principal Trust Account			
Balance 1/1/55		$72.51	
Income for 1955	$539.60		
Less Custodian Fees	21.59		
Net Income 12/31/55	518.01		
Credit Dividends to Checking Account	518.01	00.00	
Balance 12/31/55			$72.51
Checking Account			
Balance 1/1/55	796.91		
Income from Principal Account for 1955	518.01		
Balance 12/31/55			1,314.92
Total Balance 12/31/55			$1,387.43

Consolidated Fellowship Fund

Capital Funds Securities

Wellington Fund, Inc.,		
The Corporation Trust Co., Agent		
120 Broadway, New York 5, N. Y.		
Total number of shares 1/1/55	352.360	
Credit—Dividend shares	23.860	
Total number of shares 12/31/55	376.220	
Net asset value 12/31/55 @ $26.47 per share		$9,958.54

Fundamental Investors, Inc.

City Bank Farmers Trust Company, Agent		
22 William St., New York 15, N. Y.		
Total number of shares 1/1/55	701.661	
Credit—Dividend shares	20.963	
Total number of shares 12/31/55	722.624	
Net asset value bf 12/31/55 @ $17.50 per share		12,645.92
Total value of Fund Securities 12/31/55		$22,604.46
National City Bank Balance 12/31/55		21.95
		$22,626.41

Corrosion Handbook Fund

Total Corrosion Handbook Fund 1/1/55		$16,501.19
Total Corrosion Handbook Fund 12/31/55		17,174.34
New York Savings Bank		
Balance 1/1/55		$6,029.82
Deposits	$2,030.91	
Interest	68.06	2,098.97
		8,128.79
Withdrawals	75.06	
Interest Income to ECS	359.53	
To Millbury Savings Bank	5,000.00	
Palladium Medal Account	1,100.00	6,534.59
Balance		1,594.20
Millbury Savings Bank		
Deposit	5,000.00	
Interest 12/31/55	108.77	5,108.77
Balance		6,702.97
U. S. Government Bonds (Chemical Corn Exchange Bank)		10,471.37
Total Fund 12/31/55		$17,174.34

Joseph W. Richards Memorial Fund

Central Savings Bank	
Broadway at 73rd St.	
New York, N. Y.	
Balance 1/1/55	$769.72
Interest 12/31/55	21.82
Balance 12/31/55	$791.54

Columbus Convention Fund

Corn Exchange Bank	
102nd St. and Broadway	
New York, N. Y.	
USA Savings Bonds Series F (earmarked in safe deposit box)	$400.00

L. I. Gilbertson, *Treasurer*

Auditor's Report

Balance Sheet

December 31, 1955

Assets

Furniture and Office Equipment	$4,967.52	
Cash	46,358.61	(A)
U. S. Savings Bonds (Cost)	28,860.00	(B)
Inventory—Journals (1954, 1955)	5,181.25	
Accrued Income on Investments	8,710.00	
Guarantee Deposits	400.00	
	$94,477.38	

Liabilities, Reserves, and Surplus

Accounts Payable—Suppliers	$3,003.48

Taxes Withheld From Salaries	516.16
Life Memberships	1,234.21
Prepaid Sustaining Memberships	3,200.00
Prepaid Subscriptions	4,610.93
Reserve for Depreciation	1,315.92
Deferred Income (India Section)	75.96
Surplus (See Notes A and B for Fund Allocation)	80,520.72
	$94,477.38

(A) Includes:

General Funds	
First National City Bank	$21,658.55
Chemical Corn Exchange Bank	416.94
Petty Cash	210.17
	22,285.66
Corrosion Handbook Fund	
New York Savings Bank	1,594.20
Millbury Saving Bank	5,000.00
	6,594.20
Becket Award Fund	
First National City Bank	10,000.00
Electrothermics & Metallurgy Division	
First National City Bank	309.18
General Reserve Fund	
First National City Bank	48.00
Publication Reserve Fund	
First National City Bank	5,166.32
Willard Gibbs Fund	
First National City Bank	40.00
Electrodeposition Division	
First National City Bank	1,795.11
Theoretical Electrochemistry Division	
First National City Bank	120.14
Total	$46,358.61

(B) Includes:

General Funds	$17,988.63
Corrosion Division Funds	10,471.37
Columbus Convention Fund	400.00
Total	$28,860.00

Cash Statement

January 1 to December 31, 1955

First National City Bank

Book balance December 31, 1954		$18,934.98
Receipts—1955 (Gross)	$103,464.09	
Disbursements—1955 (Gross)	93,261.77	
Excess receipts over disbursements		10,202.32
Book balance December 31, 1955		29,137.30
Becket Fund check credited Consd. Fellowship acct.		10,000.00
Adjusted book balance December 31, 1955		39,137.30

Chemical Corn Exchange Bank

Book balance December 31, 1954 (Includes $2,000 in transit)		2,656.23
Receipts—1955 (Gross) (Excludes $2,000 in transit 12/31/54)	48,737.49	
Disbursements—1955 (Gross)	50,976.78	
Excess disbursements over receipts		2,239.29
Book balance December 31, 1955		416.94

New York Savings Bank (Corrosion Handbook Fund)

Book balance December 31, 1954		5,922.20
Interest—1955	175.68	
Deposits—1955	2,030.91	2,206.59
		8,128.79
Withdrawals—1955 (Includes $1,100 to Palladium Medal Exp. Acct.)		6,534.59
Book balance December 31, 1955		1,594.20

Millbury Savings Bank (Corrosion Handbook Fund)

Transferred from New York Savings Bank	5,000.00
Cash on hand—Agent—December 31, 1955	210.17
Total	46,358.61

Total accounted for as follows as of December 31, 1955:

First National City Bank per bank statement	31,874.90	
Less outstanding checks	2,737.60	29,137.30
Chemical Corn Exchange Bank per bank statement	1,332.62	
Less outstanding checks	915.68	416.94
New York Savings Bank		1,594.20
Millbury Savings Bank		5,000.00
Petty Cash		210.17
Becket Fund deposit to be transferred		10,000.00
Total, as above		46,358.61

Analysis of Expenditures

January 1 to December 31, 1955

Furniture and office equipment	$282.21
Journal	30,877.57
Reprints	2,080.24
Salaries, full-time employees	33,894.46
Wages, part-time employees	807.50
Rent	2,400.00
Stationery and supplies	1,623.80
Postage and express	1,616.61
Miscellaneous office expenses	2,740.48
Accident and health insurance	359.53
Conventions	4,299.22
Advertising agent	5,199.96
Volume 101	1,063.64
Audit	175.00
Prizes	100.00
Local Sections:	
Philadelphia	141.50
Cleveland	135.00
Midland	51.00
India	67.00
Ontario-Quebec	75.00
Wash.-Baltimore	116.00
Pacific No. West	57.00
N. Y. Metropolitan	52.00
San Francisco	50.00
Publication Committee	350.94
Corrosion Division	269.50

Emblems	113.14
Advertising	123.30
Federal Insurance Contr. Tax	572.82
Audit Bureau of Circulation	101.70
Vapor Plating royalties	199.56
Electric Insulation Division	50.00
Publication Reserve	2,005.16
Battery Division	41.99
Electronics Division	586.00
Theoretical Division	414.00
Faraday Society	1,264.20
Palladium Medal Expense Account	1,100.00
Total	$95,457.03

Bank interest	175.68
Refund—Consol. Edison deposit	20.00
F. M. Becket Fund	10,000.00
Willard Gibbs Fund	40.00
General Reserve Fund	456.00
Publication Reserve	1,969.05
Battery Division	41.99
Electronics Division	586.00
Theoretical Division	414.00
Faraday Society	1,999.20
DBG Payable	351.00
Total	$114,395.19

ANALYSIS OF INCOME

January 1 to December 31, 1955

Dues:	
1954	$90.00
1955	12,145.03
1956	18,510.51
Bound Volumes:	
1952	97.50
1955	510.00
1956	1,526.40
Publications	636.30
Nonmember subscriptions—Journal	14,443.06
Advertising	14,592.46
Conventions	10,419.09
Reprints	3,999.17
Sustaining Memberships	14,950.00
Corrosion Division	2,465.50
Cathodic Protection	166.45
Abstracts of Literature	257.00
Vapor Plating	266.07
Biology and Medicine	558.34
Modern Electroplating	1,704.11
Electrothermics & Metallurgy Division	309.18
Journal	546.90
10-Year Index	35.00
Thompson Monograph	18.70
Membership Directory	8.00
Emblems	87.50

ANALYSIS OF INVESTMENT IN U. S. SAVINGS BONDS

December 31, 1955

Date of Issue	*Serial No.*	*Face Value*	*Cost*	*Value 12/31/55*
Oct. 1943	M-673354-F	$1,000	$740	$1,000
Oct. 1943	M-673355-F	1,000	740	1,000
Oct. 1943	M-673356-F	1,000	740	1,000
Oct. 1943	M-673532-F	1,000	740	1,000
Oct. 1943	M-673533-F	1,000	740	1,000
Oct. 1943	M-673534-F	1,000	740	1,000
March 1944	M-749592-F	1,000	740	980
March 1944	M-749593-F	1,000	740	980
March 1944	M-749594-F	1,000	740	980
March 1944	M-749595-F	1,000	740	980
March 1944	M-749605-F	1,000	740	980
March 1944	M-749606-F	1,000	740	980
March 1944	M-749607-F	1,000	740	980
March 1944	M-749608-F	1,000	740	980
June 1944	V-54568-F	5,000	3,700	4,900
Dec. 1944	V-58025-F	5,000	3,700	4,810
May 1945	X-62428-F	10,000	7,400	9,450
Jan. 1946	M-1059303-F	1,000	740	914
Jan. 1946	M-1059304-F	1,000	740	914
Jan. 1946	M-1059305-F	1,000	740	914
Jan. 1946	M-1059306-F	1,000	740	914
Jan. 1946	M-1059307-F	1,000	740	914
Total		$39,000	$28,860	$37,570

(Signed) H. K. LEICHT, *Auditor*

DIVISION NEWS

Electronics Division

The Annual Business Meeting of the Electronics Division was held in San Francisco on May 3.

The Chairman reported on the activities of the Division. Among other things:

"The 1953 and 1954 Semiconductor Digests have been published. As of January 1, 1956, the total sales figure of the 1953 issue was 887; for the 1954 issue, 382. The break-even point for the Society on the 1954 issue is approximately 670 copies. Dr. Middleton resigned as Chairman of the Management and Editorial Board. He was succeeded by Dr. E. Paskell, Battelle Memorial Institute."

"Under the chairmanship of Dr. J. H. Schulman, a committee has been investigating the feasibility of establishing reference standards for inorganic phosphors. These would serve as a base for gauging the performance of new phosphors and greatly facilitate the exchange of information. Negotiations have been conducted with the National Bureau of Standards to enlist their services in handling the distribution of samples of the phosphors selected for this purpose. The phosphors will be donated by various phosphor manufacturers, and selected on the basis of their known emission and excitation characteristics, color, and decay rates. It is expected that this operation will be financially self-supporting by means of a nominal fee to defray the cost of rebottling and mailing the samples."

The Bylaws Committee, J. R. Musgrave, Chairman, proposed a change in the Bylaws, whereby the officers of the Division will hold office for two-year terms. This provision is in line with the practice of the other Divisions. The reelection provision for the Secretary-Treasurer has been retained to insure continuity of effort. An affirmative vote was cast for the proposed change. The change takes effect at the spring 1957 convention.

The Division membership, as of April 3, 1956, is 362.

Symposia planned for next year include: Luminescence, Semiconductors, Oxide Cathodes, and Instrumentation. If sufficient interest is shown, a symposium on Screen Applications will also be held. A symposium on Semiconductors is planned for the Cleveland Meeting.

The new officers of the Division

elected at the business meeting are: *Chairman*—A. E. Middleton; *Vice-Chairman (Luminescence)*—Luke Thorington; *Vice-Chairman (General Electronics)*—L. W. Evans; *Vice-Chairman (Semiconductors)*—M. F. Lamorte. The term of the Secretary-Treasurer does not expire at this time.

The fiscal year of the Division continues until May 31. Since the results of this year's sale of abstract booklets are not yet complete, the financial report given below does not include data of those transactions:

Balance reported at Cincinnati meeting	$831.40
Net loss from 1955 booklet	29.65
Balance on 1955 operations	$801.34
Interest on bank balance	8.53
Total assets	$809.87
Total paid out	60.67
Balance carried forward	$749.20

M. F. QUAELY, *Secretary-Treasurer*

SECTION NEWS

Council of Local Sections

The new officers of the Council, elected at the San Francisco Meeting of the Society in May, are:

Chairman—L. O. Case, University of Michigan, Ann Arbor, Mich.

Vice-Chairman—R. R. Rogers, Dept. of Mines & Technical Surveys, Ottawa, Ont., Canada

Secretary—H. T. Francis, Armour Research Foundation, Chicago, Ill.

Director, 2-year term—F. W. Koerker, 4103 Dyckman, Midland, Mich.

Director (continuing), 1-year term—R. A. Woofter, Jones & Laughlin Steel Corp., Pittsburgh, Pa.

Boston Section

The second meeting of the Boston Section was held on April 17 at the M. I. T. Graduate House. The dinner portion of the meeting was attended by Dr. H. H. Uhlig, our National President. Dr. Uhlig gave a short after-dinner talk on Society affairs.

A technical program, "Transistors and Semiconductors," was presented by three speakers from the Raytheon Manufacturing Co. Dr. Worden Waring spoke on "Transistors—Their Growth and Diseases." A wide variety of materials show semiconducting properties: elements such as diamond, silicon germanium, gray tin, selenium, tellurium, some intermetallic compounds, some oxides, sulfides, selenides, and even some organic crystals. Germanium which has been "doped" with a pentavalent element such as arsenic has free conduction electrons from the fifth, nonbonded, valence electron. "Doping" with a trivalent element such as boron or indium introduces electron vacancies, or "holes," which conduct current. Germanium is usually purified to one part in several hundred million, and impurities of 1 ppm introduced. If impurities are introduced into a single crystal lattice so as to form a fairly sharp boundary between the regions of free electrons (donor, *n*-type) and free holes (acceptor, *p*-type), a space charge forms at the boundary and acts to rectify current passing across this junction. A transistor consists of two such junctions, back to back; it can be used to amplify current very effectively. In order to get acceptable performance at high frequencies, it is necessary to obtain flat, parallel, close junctions. Cleaning of germanium transistors is accomplished by electropolishing in potassium hydroxide solution. Anodic solution occurs by hole reaction, so the *p*-type dissolves smoothly but the *n*-type resists anodic action. Some diseases which affect transistors are curvature and irregularity of junctions, leakage of current on the surface, low amplification factor, falling off of amplification with increasing current, deterioration on aging. Cures for some of these are known; prognosis is favorable for curing the remainder. Surface phenomena are at present least understood and cause the most difficulty.

Dr. Warren Ericksen presented "Current-Carrying Mechanisms in Semiconductors." The three types of current conduction in germanium transistors are bulk conduction, inversion layer conduction, and surface conduction. There are marked differences between the inversion layer type and excess (surface layer) type. The ionic conduction theory is refuted in that currents continue after all the impurity items should be plated out. Experiments have been conducted to obtain ambient saturation with organic vapors during transistor operation. No correlation could be obtained between the dielectric constant of the organic material and electrical characteristics of the germanium. Operating germanium transistors in an oxygen atmosphere saturated with an organic vapor yielded lower currents than in a similarly saturated nitrogen atmosphere.

Dr. Sumner P. Wolsky discussed "Adsorption and Structure on Germanium Surfaces." Two sets of surface energy levels exist, one at the germanium-oxide interface and the other at the oxide-air interface, or within the oxide. Three types of surfaces were investigated: etched, "clean," and clean. In etching from a sodium hydroxide or other alkaline solution, an oxide layer 10 Å thick is obtained, which causes a continuous drift in electrical properties for many hours. Radioactive tracer methods using Na^{24} show that fractions of micrograms of sodium are retained around the *n-p* junction. The "clean" surface is obtained by heating in high vacuum, or by argon bombardment and annealing. Carbon monoxide, carbon dioxide, and nitrogen are adsorbed at 300°K, hydrogen at lower temperatures. An experimental apparatus which involves a quartz microbalance in high vacuum has been set up to detect pressure changes. Sensitivity of balance is 0.1 to 0.2 μg. The oven can be operated from liquid nitrogen temperatures to near the melting point of germanium. A binocular comparator is incorporated into the system for observation. Preliminary results indicate that an etched surface continues to oxidize at a lower rate; further oxidation depends on many variables.

At the Annual Business Meeting the Bylaws were voted upon and approved as submitted, subject to recognition by the Society Board of Directors. Annual Reports were presented by the Officers and Committee Chairmen. The following slate of officers, as submitted by the Nominating Committee, was approved by unanimous vote:

Chairman—F. C. Benner

Vice-Chairman—L. B. Rogers

Secretary-Treasurer—Charles Levy, 61 Central St., Auburndale 66, Mass.

Representatives on Council of Local Sections—C. W. Jerome (2 yr) and Herbert Bandes (1 yr)

CHARLES LEVY, *Secretary*

Detroit Section

A joint dinner meeting was held with the National Association of Corrosion Engineers on February 23 at the Engineering Society of Detroit building. A talk on the use of statistical methods as applied to experimental design and interpretation was given by David N.

Collins of Chrysler Corp., Detroit, under the title, "Pulling Moses from the Statistical Bullrushes."

Mathematical statistics is useful to engineers when the artificial manipulations of statistics can be made to correspond with variations among important physical properties of the system under examination. The results of the analysis can then be expressed numerically as probabilities of real differences among the variables analyzed. By application of statistics, results of ordinary precision can be obtained with less laboratory work, or precision can be increased at little or no cost in extra laboratory time.

The three operations of statistics most commonly used in the laboratory are the analysis of variance, calculation of the probability of a difference between two averages, and correlation measurements. Using the analysis of variance, the effects of measured variables are separated from uncontrolled experimental error; the resulting parts can then be evaluated separately. The difference between two averages is expressed as a function (Student's t) of the combined variance of the original data. Correlation makes quantitative the straight-line relationship (if any) between two variables, or measures the contribution of each of several independent variables on the end result.

Although statistics, as applied above, makes possible the condensation of a series of measurements into a single quantitative result, its applications are most effective before laboratory work begins. In the design of experiments, the statistician acts as a referee, advising and arbitrating between the man who will do the laboratory work and the man who asked the question which the work must answer.

Before a statistical design can be selected, it must be agreed that the question asked has been expressed in terms that the laboratory worker can understand. In addition, the statistician must be furnished with a numerical value for the reliability of the test method, and a value for the least difference in results which will be of practical value to the user. The outcome of a design conference should be the selection of a type of test program and the preparation of a detailed schedule of testing.

The following have been elected to office in the Detroit Section for the year 1956–57:

Chairman—G. V. Kingsley
1st Vice-Chairman—Manuel Ben
2nd Vice-Chairman—Sam Piken
Secretary-Treasurer—Manuel Shaw, Chrysler Engineering, Dept. 487, 12800 Oakland, Highland Park 3, Mich.
Representative on Council of Local Sections—Frank Passal

M. Shaw, *Secretary-Treasurer*

Philadelphia Section

The Philadelphia Section held its annual spring meeting at the Morris Arboretum of the University of Pennsylvania, in Chestnut Hill, on May 12. Members, guests, and their wives gathered in this beautiful setting late in the afternoon and enjoyed guided tours arranged by Dr. John A. Fogg, Director of the Arboretum, and his staff. Several of the ladies supplied canapés for the cocktail hour and are greatly to be commended for the excellence of their work. Dinner followed, and then the group was treated to a most interesting talk by Dr. Fogg. The speaker had traveled extensively in India, Burma, and Thailand surveying the resources of medicinal plants, in particular *rauwolfia serpentina*. His talk was profusely illustrated with some of the finest color photography it has been our pleasure to see. The group of some 50 persons was unanimous in its enthusiasm and voted its deep appreciation to Dr. Fogg and the university for making this meeting such an enjoyable affair.

The following officers were re-elected for the 1956–57 season:

Chairman—E. L. Eckfeldt
Vice-Chairman—G. F. Temple
Treasurer—A. A. Ware
Secretary—G. W. Bodamer, Rohm & Haas Co., 5000 Richmond St., Philadelphia 37, Pa.

G. W. Bodamer, *Secretary*

Washington-Baltimore Section

Corrosion was the subject of the joint meeting of the Section with the National Association of Corrosion Engineers, and the Baltimore-Washington Section of the American Electroplaters' Society held on April 10 at the National Bureau of Standards.

William H. Metzger, President of the Baltimore-Washington Section of AES introduced Dr. William Blum, 1944 Acheson Medalist, who described the corrosion research promoted by the American Electroplaters' Society. Dr. Fielding Ogburn, Chairman of the Washington-Baltimore Section of ECS introduced Dr. M. C. Bloom, Naval Research Lab., who outlined the work of the Corrosion Division of The Electrochemical Society. Ben J. Philibert, Chairman of the Baltimore Section of NACE introduced George Best, a Director of the Association, who spoke on the extensive activities of the organization.

The principal speaker of the evening, Frank LaQue, was introduced by Ken Huston of Armco Steel Corp., Program Chairman for this meeting. Mr. LaQue's topic was "Planning and Interpretation of Corrosion Tests." Enlivened with dry humor, the intricacies and anomalies of accelerated and long-term tests for corrosion resistance of metals were set forth. The designing and interpreting of corrosion tests involve many factors including pitting and crevice corrosion, and the effects of heat treatment, galvanic action, stress, and velocity.

The attendance of more than 125 was

DECEMBER 1956 DISCUSSION SECTION

A Discussion Section, covering papers published in the January–June 1956 Journals, is scheduled for publication in the December 1956 issue. Any discussion which did not reach the Editor in time for inclusion in the June 1956 Discussion Section will be included in the December 1956 issue. Those who plan to contribute remarks for this Discussion Section should submit their comments or questions in triplicate to the Managing Editor of the Journal, 216 W. 102nd St., New York 25, N. Y., *not later than September 1, 1956*. All discussions will be forwarded to the author, or authors, for reply before being printed in the Journal.

a tribute to the speaker and his topic as well as to Ken Huston for arranging this most interesting program.

JEANNE BURBANK, *Secretary*

NEW MEMBERS

In May 1956 the following were approved for membership in The Electrochemical Society by the Admissions Committee:

Active Members

PIERRE V. ANDREAE, Cramet, Inc.; Mail add: 2530 Avalon Circle, Chattanooga 5, Tenn. (Electrothermics & Metallurgy)

ABRAHAM ARAD, Vulcan Battery Works Ltd.; Mail add: 13 Hermon St., Haifa, Israel (Battery)

THEODORE BAURER, Sylvania Electric Products Inc.; Mail add: 69-21 266 St., Floral Park, L. I., N. Y. (Electrothermics & Metallurgy)

ROBERT R. BROOKSHIRE, Hughes Aircraft Co.; Mail add: 7009 Quartz Ave., Canoga Park, Calif. (Corrosion, Electrodeposition)

ORVAL M. BROWN, Hughes Aircraft Co.; Mail add: 4320 Stewart Ave., Los Angeles 66, Calif. (Electrodeposition, Electrothermics & Metallurgy, Theoretical Electrochemistry)

MELVIN CUTLER, Hughes Aircraft Co.; Mail add: 10636 Bradbury Rd., Los Angeles 64, Calif. (Electronics)

ROBERT F. EHRSAM, Manning, Maxwell & Moore, Inc.; Mail add: 110 Parkwood Rd., Stratford, Conn. (Electrodeposition)

MARION E. ELMORE, Associated Lead & Zinc Co.; Mail add: 2700-16th Ave. S.W., Seattle 4, Wash. (Battery)

CHARLES GEORGE, W. H. & L. D. Betz; Mail add: Southampton Rd. & Endicott St., Philadelphia 16, Pa. (Corrosion)

GIAMPAOLO BOLOGNESI, University of Ferrara; Mail add: Via Scandiana 25, Ferrara, Italy (Corrosion, Electrodeposition)

RICHARD F. HAREN, Standard Telephones & Cables Pty. Ltd., 252 Botany Rd., Alexandria, Sydney, Australia (Electric Insulation, Electrodeposition, Electronics)

WILLIAM W. HAPP, Beckman Instruments; Mail add: 11442 Alford Ave., Mountain View, Calif. (Electronics)

HENRY W. HENDRICKS, International Business Machines Corp.; Mail add: 560 E. San Carlos St., San Jose 12, Calif. (Battery, Corrosion, Electrodeposition, Electronics, Electro-Organic, Electrothermics & Metallurgy, Theoretical Electrochemistry)

JOHN P. JASIONIS, Sylvania Electric Products Inc.; Mail add: 43 Pine St., Belmont 78, Mass. (Electronics)

HUGH H. JOHNSTON, Hart Battery Div., The Dominion Linseed Oil Co., Ltd.; Mail add: 1 Severn Ave., Montreal 6, P. Q., Canada (Battery)

GEORGE T. KERR, Research Div., Aircraft-Marine Products, Inc., 2100 Paxton St., Harrisburg, Pa. (Corrosion, Electro-Organic)

YOSHIHIDE KOTERA, Government Chemical Industrial Research Institute; Mail add: 1219, Oharamachi, Setagaya-ku, Tokyo-to, Japan (Electronics)

PAUL R. KRUESI, Heavy Minerals Co.; Mail add: 836 So. Michigan Ave., Chicago, Ill. (Electrothermics & Metallurgy)

GEORGE A. LARCHIAN, Hughes Aircraft Co.; Mail add: 2515 No. Lincoln St., Burbank, Calif. (Electrodeposition, Electronics)

LEO MISSEL, Lockheed Missile Systems Div.; Mail add: 6547 Troost Ave., No. Hollywood, Calif. (Electrodeposition)

AURAND L. MUNN, JR., General Electric Co., 235 Montgomery St., San Francisco, Calif. (Industrial Electrolytic)

ALAN D. PRINGLE, Olin Mathieson Chemical Corp.; Mail add: 4819 University Court, Niagara Falls, N. Y. (Industrial Electrolytic)

KENNETH J. RADIMER, M. W. Kellogg Co.; Mail add: 12 Martin Place, Little Falls, N. J. (Electrodeposition)

CHARLES F. RYAN, Rohm & Haas Co.; Mail add: 4710 Ashville St., Philadelphia 36, Pa. (Electronics)

CHARLES SHEER, Vitro Labs., 200 Pleasant Valley Way, West Orange, N. J. (Electrothermics & Metallurgy)

JOHN L. SHELDON, Corning Glass Works, Mail add: 179 Dodge Ave., Corning, N. Y. (Electronics)

WILLIAM K. SNEAD, Wayne University; Mail add: 620 Merrick, Detroit 2, Mich. (Theoretical Electrochemistry)

ELIZABETH H. TARRANTS, Wright Air Development Center; Mail add: 791 Wagon Wheel Drive, Dayton 3, Ohio (Electronics)

Student Associate Members

(Awarded by the Cleveland Section)

LEWIS M. ELTON, Fenn College; Mail add: 3456 Scranton Rd., Cleveland 9, Ohio (Electrothermics & Metallurgy)

ORA P. FERGUSON, Hiram College; Mail add: Box 421, Hiram, Ohio

ROBERT E. HAGMAN, Case Institute of Technology; Mail add: 2117 Abington Rd., Cleveland 6, Ohio (Electrodeposition)

STEWART J. STRICKLER, College of Wooster, Kenarden VII, Wooster, Ohio (Electronics)

JAMES J. ZWOLENIK, Adelbert College of Western Reserve University; Mail add: 3003 Lennox Ave., Cleveland 29, Ohio

Reinstatements to Active Membership

GARTH L. PUTNAM, Self-employed Professional Engineer and Consultant; Mail add: 1628 No. 167 St., Seattle 33, Wash. (Corrosion)

WILFORD H. THOMAS, Ethyl Corp.; Mail add: 1764 Carl Ave., Baton Rouge, La. (Industrial Electrolytic)

VICTOR ZENTNER, Hughes Aircraft Co.; Mail add: 611 Erskine Drive, Pacific Palisades, Calif. (Corrosion, Electrodeposition, Theoretical Electrochemistry)

By action of the Board of Directors of the Society, commencing January 1, 1956, all prospective members must include first year's dues with their applications for membership.

Also, please note that, if sponsors sign the application form itself, processing can be expedited considerably.

NEWS ITEMS

New Sustaining Member

Hercules Powder Co., Wilmington, Del., recently became a Sustaining Member of the Society.

Palladium Medal Award for 1957

The fourth Palladium Medal of The Electrochemical Society will be awarded at the Fall Meeting of the Society in Buffalo, N. Y., October 6-10, 1957. The medal was established in 1951 by the Corrosion Division for distinguished contributions to fundamental knowledge of theoretical electrochemistry and of corrosion processes. It is awarded biennially to a candidate selected by a committee appointed by the Society's Board of Directors. This year the Committee members are H. A. Laitinen, J. P. Fugassi, E. B. Yeager, P. Delahay,

T. P. May, and N. Hackerman, Chairman.

The Committee requests Sections, Divisions, and members of the Society to send suggestions for candidates, accompanied by supporting information, to *Norman Hackerman, Dept. of Chemistry, University of Texas, Austin 12, Texas.* Candidates may be citizens of any country and need not be members of the Society. Previous medallists are Carl Wagner, Massachusetts Institute of Technology; N. H. Furman, Princeton University; and U. R. Evans, Cambridge University.

Science Grants

The American-Scandinavian Foundation, 127 East 73 St., New York, N. Y., has announced the following Fellowship grants in science for 1956–57:

To Robert G. Greenler, Ph.D. candidate at Johns Hopkins, to study chemistry in Sweden.

To Arthur B. Komar, Ph.D. candidate at Princeton, to study physics in Denmark.

The Foundation invites applications for its Fellowships.

Investment in Education

The best paying investment a country can make is the education of its people in chemistry and the physical sciences, stated Carnegie Tech President, Dr. J. C. Warner, who spoke on April 26 in observance of Chemical Progress Week at the William Penn Hotel, Pittsburgh, Pa.

Among the audience were the senior high school winners of the 17th Annual Buhl Planetarium School Science Fair and their teachers.

Dr. Warner, who is also President of the American Chemical Society, a Past President of The Electrochemical Society, and who has been elected to the National Academy of Sciences, surprised his audience by quoting from the defunct *North American Review* to support his statement.

"Competition today between the nations is essentially in the science and application of chemistry.

"The country that has the best chemists will in the long run be the most prosperous and the most powerful. It will have at the lowest cost the best food, the best manufactured materials, the fewest wastes and unutilized forms of matter, the best guns and strongest explosives, the most resistant armour.

"Its inhabitants will make best use of their country's resources; they will oppose the least resistance to favorable evolution; they will be the most thrifty and the least dependent on other nations."

Dr. Warner concluded, "That quotation was written in 1896 and it is still true today!"

John B. Merrill Memorial Scholarship

The John B. Merrill Memorial Scholarship in Science has been established by the Sylvania Foundation through grants to the Bradford County, Pa., Board of Education, it was announced by Marion E. Pettegrew, General Manager of the Tungsten and Chemical Division of Sylvania Electric Products Inc., Towanda, Pa.

The Bradford County Board of Education will administer the Merrill Scholarship program and will select the scholarship recipients who will be chosen among high school students of Bradford County. Under the terms of the scholarship program, each award will total $5000.

At the time of his death last fall, Mr. Merrill was a Sylvania vice-president, whose responsibilities included the operation of the Tungsten and Chemical Division.

Titanium Price Cut

Titanium Metals Corp. of America, New York, N. Y., has announced a reduction of 20¢ per lb in the price of titanium sponge metal, bringing the price down to $3.25. This is the fourth price cut initiated by TMCA, in a 14-month period, and is part of an aggressive program to make this new engineering metal fully competitive with certain steels, aluminum, and magnesium.

1956 Directory

The 1956 Directory of Members of The Electrochemical Society should be available the latter part of July. The Directory contains an alphabetical and geographical list of members of the Society as of March 1, 1956, and a list of Patron and Sustaining Members, Past Presidents, and winners of Society prizes and awards.

Members who wish to receive the Directory are requested to send their order, accompanied by a check for $2.00, to Society Headquarters, 216 West 102 St., New York 25, N. Y.

At the same time, the prices of all mill products—sheet, strip, billet, bar, extrusions, and wire—are lowered about 6%, with reductions ranging from 65¢ per lb to $1.00 per lb for products such as sheet or strip. On April 1, November 1, and November 23, 1955, reductions were announced totaling 23% for sponge and more than 19% for mill products.

A. E. C. Zirconium Supply Contracts

The use of nuclear reactors to generate electric light and power for the homes and factories of the U. S. A. is one step closer, and the high corrosion-resistant powers of a formerly "rare" metal will be economically available to the U. S. chemical industry as a result of a $22,750,000 five-year zirconium supply contract between the NRC Metals Corp., a wholly owned subsidiary of the National Research Corp. of Cambridge, Mass., and the Atomic Energy Commission, it has been announced by Mr. Richard S. Morse, President of both corporations. The contract will result in the construction of a plant larger than any now existing for the production of metallic zirconium. A new process plus proximity to raw materials will produce metallic zirconium at nearly one-half the current market price.

Plans are well under way for the construction of a new NRC Metals Corp. plant near Pensacola, Fla.

The contract with the Atomic Energy Commission is for the annual supply of 700,000 lb of hafnium-free reactor grade zirconium.

The Carborundum Co. will increase its capacity for production of zirconium to over 1½ million lb/yr with the construction of a new plant in Parkersburg, W. Va. The Parkersburg plant will be operated by Carborundum Metals Co., Inc., a Carborundum subsidiary, according to an announcement by General Clinton F. Robinson, President of the parent firm in Niagara Falls, N. Y.

Announcement of the new plant came immediately after confirmation that the Atomic Energy Commission had awarded a new contract to Carborundum Metals to supply an additional 500,000 lb of zirconium annually.

At present the company is producing 325,000 lb annually for A.E.C. The new contract increases the company's firm A.E.C. commitments to 825,000 lb of zirconium per year. The new contract also gives A.E.C. priority on an additional 400,000 lb of Carborundum

Metals zirconium production, making the company's total firm and conditional commitments 1,225,000 lb of zirconium per year for A.E.C.

The capacity of the new Parkersburg plant, coupled with production at Akron, N. Y., makes it possible for Carborundum Metals to meet its A.E.C. contracts and also give firm commitments now for delivery of zirconium in 1957 and 1958 to commercial users both in the domestic and foreign markets.

Construction has started and the plant is scheduled for operation in early 1957.

Engineers and constructors of U. S. Industrial Chemicals Co.'s new zirconium sponge plant will be the Bechtel Corp. of San Francisco, Calif., it was announced by Dr. Robert E. Hulse, Vice-President of National Distillers Products Corp. and General Manager of the U. S. I. Division.

U. S. I. earlier announced its plans to construct a zirconium sponge plant in Ashtabula, Ohio, to produce 1,500,000 lb/yr of reactor grade (hafnium free) zirconium sponge; 1,000,000 lb/yr have been contracted for by the Atomic Energy Commission, and the remaining 500,000 lb/yr will be available for direct sale to industry.

Engineering and design work on the plant is already under way and construction is scheduled to start at Ashtabula by midsummer.

Sylvania Semiconductor Program

Sylvania Electric Products Inc. has purchased a modern plant in Hillsboro, N. H., to expand the company's manufacture of transistors and crystal diodes.

C. W. Hosterman, General Manager of the company's Electronics Division, said acquisition of the new plant was "another step in Sylvania's multi-million-dollar program to meet growing demand for semiconductor devices."

Both germanium and silicon types of diodes and transistors will be manufactured at Sylvania's new plant. Operations were expected to start on June 1.

Solvay Expansion

Plans for expansion of its mercury cell chlorine-caustic soda plant, now under construction at Brunswick, Ga., have been announced by Solvay Process Division, Allied Chemical & Dye Corp.

Carlton Bates, S lvay's President, stated that capacity of the plant will be doubled. Construction of the initial facilities is expected to be completed late this year. It is hoped to have the second step ready for operation in the fall of 1957.

Increase in capacity of the plant has been decided upon so that Solvay will be in a position to supply the growing needs of the chlorine-caustic soda consuming industries in the Southeast.

Lithium Metal Dispersions

Lithium Corp. of America, Inc., Minneapolis, Minn., has announced the successful production of dispersions of Lithium Metal. Interest in the possibilities of these dispersions has been heightened by recent reports on their use as catalysts in the production of the new "natural" rubber.

The company's Product Research & Development Dept. is making available instruction sheets describing methods for laboratory preparation of these lithium metal dispersions in such dispersing mediums as mineral oil, petrolatum, and wax. Particle sizes in the range of 5 to 20μ are possible by use of these techniques. It is expected that some time in the near future prepared dispersions in selected media will be available for sale through the company's Sales Dept.

Bart Mfg. Corp. Appoints Exclusive Distributor

The Michigan Pipe Co., Ferndale, Mich., has been appointed exclusive distributor, in the United States and Canada, for Bart Lectro-Clad, nickel plated pipe and fittings, according to an announcement from S. G. Bart, President of Bart Manufacturing Corp., Belleville, N. J.

Used extensively in the process industries for more than a decade, Bart Lectro-Clad manufacturing will be centralized at a new, specially designed plant in North Newark, N. J. Sales headquarters will be: Bart Lectro-Clad Sales Division, Michigan Pipe Co., 2415 Burdette Ave., Ferndale, Mich.

Liaison between the two companies will be maintained by W. A. Hopkins, who was recently appointed General Manager of the Lectro-Clad Division, Bart Manufacturing Corp.

Foote Offers Lithium Metal

Lithium metal is now available in commercial quantities from Foote Mineral Co.'s new metal cell located at their Exton, Pa., plant. The metal is offered in 1 lb ingots packed under oil in sealed steel cans and typically analyzes 99.8% Li.

While the company is not currently in commercial production on lithium metal derivatives, development size quantities of a number of derivatives are expected in the near future.

Electromet Producing Titanium Metal

The first heat of titanium metal sponge at the new Ashtabula plant of Electro Metallurgical Co., a Division of Union Carbide & Carbon Corp., was completed on April 26. This heat produced by the sodium-reduction process marks the entry of Electromet into the titanium metal sponge field on a commercial scale.

The plant which has a capacity of about 7,500 tons of titanium metal sponge a year is the largest built to date and was privately financed by the company. The new plant is located on the Lake Erie site of Electromet's plant for the production of ferroalloys and calcium carbide at Ashtabula.

This is the first commercial production of titanium sponge in the United States by a method other than the magnesium-reduction process. In Electromet's process, sodium is used to reduce titanium tetrachloride, resulting in metal of high quality.

New Fluorine Chemical

Through a production process on which patents are pending, the Pennsylvania Salt Manufacturing Co. will become the first commerical supplier of perchloryl fluoride. This new compound, a powerful oxidizing agent, was discovered in 1952. Studies on the properties and applications of the company's newest fluorine compound are being continued at the Whitemarsh Labs. by Dr. John Gall, director of Inorganic Research, and a group led by Dr. Gerhard Barth-Wehrenalp.

Production of Alloy Plate Steel

A closed-circuit television installation, which enables attendants to "peer" around corners for remote observation and control of processing operations, is speeding production of alloy plate steel at the Lukens Steel Co., Coatesville, Pa.

Incorporating nine separate RCA industrial television cameras, the installation makes possible one-man control of a huge furnace line and also enables a single operator to control a complete plate-finishing shearing operation.

Chlorine and Caustic Soda Production

Olin Mathieson Chemical Corp. has announced that arrangements have been completed for the purchase of a large tract of land from Brunswick Pulp and Paper Co., Brunswick, Ga. The land purchased lies adjacent to the Brunswick paper mill and the Turtle River.

Olin Mathieson also announced its intention to proceed immediately with construction of equipment and facilities initially costing in excess of $1 million for rail and water movement of chlorine and caustic soda at Brunswick. Rail and water movement of chlorine and caustic soda is expected to begin early in 1957. Pipelines for the direct delivery of chemicals to Brunswick Pulp and Paper Co.'s mill will be included in the construction.

Olin Mathieson further indicated that engineering studies will be completed soon for the production at Brunswick of various chemicals required by the pulp and paper industry, in addition to chlorine and caustic soda.

BOOK REVIEWS

INDUSTRIAL AND MANUFACTURING CHEMISTRY, Part I, Organic, by Geoffrey Martin as revised by Edward I. Cooke. Published by Philosophical Library, Inc., New York, 1955. Seventh Edition. 752 pages.

INDUSTRIAL AND MANUFACTURING CHEMISTRY, Part II, Vol. I, Inorganic, by Geoffrey Martin as revised by Wilfrid Francis. Published by Philosophical Library, Inc., New York, 1955, Sixth Edition. XXIII + 600 pages.

It is stated in the preface that this sixth edition, like the earlier editions, was written to satisfy the continued demand which has existed for Martin's "Industrial Chemistry" ever since the first edition appeared in 1916. The main object therefore has been to bring the book up to date, at the same time preserving the original character of the text. This has been done, particularly in the sections on fuels, fuel utilization, and power generation, in keeping with the special background in these fields of Dr. Francis. Actually about one-third of the entire text is devoted to a thorough description of these topics.

The remaining two-thirds of this volume is devoted to descriptions of water technology and the heavy chemical industries, such as sulfur, sulfuric acid and related materials, hydrochloric acid, salt, salt cake, soda ash, caustic soda, and the alkali industry, potash, gypsum, ammonia, nitric acid, and industrial gases other than fuels. The other industrial inorganics such as cements, electrothermal products, silicates, glass, clay, refractories, metals, and others not covered in this volume are treated in Vol. II of this series.

Descriptions and diagrams of equipment are very good. Many diagrams are quite detailed and informative. This is especially true of the numerous isometrics and the pictoral type illustrations, so that the reader cannot help but obtain a clear understanding of the physical appearance and method of operation. This reviewer was most favorably impressed with the number and quality of these illustrations, as well as the clarity of the text descriptions.

A point which should be noted, however, is the scarcity of flow diagrams of the various chemical processes. These flow diagrams have so proved their worth in describing complex chemical operations that it was a bit disappointing not to see much wider use made of them in this otherwise fine collection.

So far as the actual material which the authors present is concerned, the descriptions reflect mostly English and European practice, which in some instances differs from American practice. Emphasis also seems to be divided differently between older and newer processes than is the case in certain other well-known texts on this subject. Part of the author's purpose has been to present a number of older, obsolete processes for their historical or educational value to students and manufacturers to illustrate changes which have occurred in the process of development of an industry. This purpose is fulfilled quite well, but at the expense of adding a certain amount of bulk to the text. No difficulty is encountered because of this inclusion, since newer practice is clearly differentiated from classical methods.

In summary, therefore, this volume will supply the student of industrial inorganic chemistry with a modern European viewpoint, and provide a ready source of catalogued information on the process industries, their equipment, and characteristics.

WILLIAM H. KAPFER

INDUSTRIAL AND MANUFACTURING CHEMISTRY, Part II, Vol. II, Inorganic, by Geoffrey Martin as revised by Wilfrid Francis, assisted by N. Berkowitz, M. Francis, and A. B. Searle. Published by Philosophical Library, Inc., New York, 1955. Sixth Edition. 491 pages. (Set of three volumes sells for $50.00)

TITANIUM, Metallurgy of the Rarer Metals, No. 4, by A. D. McQuillan and M. K. McQuillan. Published by Academic Press Inc., New York, 1956. 466 pages, $10.00.

In the Foreword to the first book of this series, which now includes volumes on chromium, zirconium, manganese, and titanium, the General Editor, Dr. H. M. Finniston, wrote that "the aim is to provide a readable reference; a textbook which students will find not unattractive; which research workers will find informative, and from which they will gain incentive to do further work to fill in the gaps in our knowledge; and in which scientists and technologists whose work requires metallurgical facts and figures will find the background and data they seek." The reviewer's opinion is that this aim has been well met in the present book, as it has also in the previous volumes.

The metals so far included in the series are rare in the sense that they were not produced in high purity form until recent years. Titanium is the fourth most abundant structural metal in the earth's crust, although it is only comparatively rarely found in concentrations of commercial interest and is difficult to recover from the ore and produce in massive form. Annual world production now exceeds 10,000 tons and is expected to be several times that in the near future.

The book is well organized for reference, with an adequate index and with an outline table of contents running 13 pages. Reference to isolated specific sections is possible with a minimum of reading of other sections.

Approximately half of the book deals with problems related to the reactivity of titanium, much of this applicable for others of the reactive metals now achieving widespread use. Of this half, major attention is divided between recovery, purification, and melting, and an equal section on fabrication in the broadest sense. There is a shorter section on reaction with gases and corrosion, and a section on metallographic techniques.

The other half of the book lists physical properties, with special attention to mechanical properties, discusses deformation and transformations, and has a very large section (130 pages) on constitutional diagrams of titanium alloys, all binary. Higher alloy systems are included only in the bibliography.

There are nearly 600 references, arranged at the end of each chapter. These are reasonably complete through 1954.

ROBERT B. GREEN

REFLECTIONS OF A PHYSICIST by P. W. Bridgman. Published by Philosophical Library, Inc., New York, 1955. Second Edition. 576 pages, $6.00. Professor Bridgman's nontechnical writings, brought up to date.

ANNOUNCEMENTS FROM PUBLISHERS

A HYDROGEN EFFUSION METHOD FOR THE DETERMINATION OF CORROSION RATES IN AQUEOUS SYSTEMS AT ELEVATED TEMPERATURE AND PRESSURE by M. C. Bloom and M. Krulfeld, Naval Research Laboratory. Published November 1955. Available as Report PB 111772.* 18 pages, 50 cents.

INVESTIGATION OF THE EFFECTS OF CORROSION ON THE SERVICE LIFE OF BALL BEARINGS by James C. Hanson, Rock Island Arsenal Laboratory. Published June 1955. Available as Report PB 111829.* 44 pages, $1.25.

ZIRCONIUM—TECHNOLOGY AND ECONOMICS. Published by the Atomic Industrial Forum, Inc., 260 Madison Ave., New York 16, N. Y. Report based on the proceedings of a two-day meeting held under the sponsorship of the Subcommittee on Process Metallurgy and Fabrication of the Forum's Industrial Committee on Reactor Materials. 125 pages, $3.00.

* Order from Office of Technical Services, U. S. Dept. of Commerce, Washington 25, D. C.

EMPLOYMENT SITUATIONS

Please address replies to box shown, % The Electrochemical Society, Inc., 216 W. 102nd St., New York 25, N. Y.

Positions Available

METALLURGISTS

Company engaged in basic process and pyrometallurgy requires several men for Production, Development, and Quality Control who have some experience in one or more of the following: Smelting and Refining, Steelmaking, or Electric Furnace Operation. Excellent opportunities for qualified men. Hospitalization, insurance, and pension plan provided by Company. Plants located midwest, north, and south. All replies held strictly confidential. *Submit detailed resumé to Box A-265.*

ELECTRO OR INORGANIC CHEMIST

Chemist or Chemical Engineer, bachelor's degree or equivalent, for customer service and development work in laboratory of New England manufacturer of electroplating specialties and metal cleaning compounds. Metal finishing experience desirable but not necessary.

We offer a challenging position in a well-established and expanding company. Liberal vacation, insurance, and profit sharing benefits. Small city or rural living. *Reply to Box A-266.*

Positions Wanted

CHEMIST, 36, 11 years' experience, including batteries, electroplating, general physical and chemical commerical testing, seeks New Jersey, Philadelphia, New York City position. *Reply to Box 357.*

CHEMICAL ENGINEER, 40, B.S. degree, 14 years' experience, including materials engineering and research, electrodeposition processes, product engineering and development work involving capacitors. *Reply to Box 358.*

CHEMICAL ENGINEER, experience in high temperature process development, including fused salt electrolysis, electric furnaces, metals extraction, B.Ch.E. 1939, married, age 38, seeking challenging, mature position. *Reply to Box 359.*

ADVERTISERS' INDEX

The Electrochemical Society

INSTRUCTIONS TO AUTHORS OF PAPERS

Address all correspondence to the Editor, JOURNAL OF THE ELECTROCHEMICAL SOCIETY, 216 W. 102nd St., New York 25, N. Y.

FORM

Manuscripts submitted for publication should be in triplicate to expedite review. They should be typewritten, double-spaced, with 2½–4 cm (1–1½ in.) margins.

Title should be brief, followed by the author's name and his business or university connection.

Abstract of about 100 words should state the scope of the paper and give a brief summary of results.

ILLUSTRATIONS

Drawings will be reduced to column width, 8 cm (3⅛ in.), and after reduction should have lettering at least 0.15 cm ($\frac{1}{16}$ in.) high. Original drawings in India ink on tracing cloth or white paper are preferred. Curves may be drawn on coordinate paper only if the paper is ruled in blue. All lettering must be of lettering-guide quality. See sample drawing on reverse page.

Photographs must be glossy prints and mounted flat.

Captions for all figures must be included on a separate sheet. Captions and figure numbers should not appear in the body of the figure.

General—Figures should be used only when necessary. Omit drawings or photographs of familiar equipment. Figures from other publications are to be used only when the publication is not readily available, and should always be accompanied with written permission for reprinting.

REFERENCES

Literature and patent references should be listed at the end of the paper on a separate sheet, in the order in which they are cited. They should be given in the style adopted by *Chemical Abstracts*. For example:

R. Freas, *Trans. Electrochem. Soc.*, **40**, 109 (1921).

H. T. S. Britton, "Hydrogen Ions," Vol. **1**, p. 309, D. Van Nostrand Co., New York (1943).

H. F. Weiss (To Wood Conversion Co.), U. S. Pat. 1,695,445, Dec. 18, 1928.

UNITS OF MEASUREMENT

Metric units should be used throughout but, where desirable, English units may be given in parentheses.

Corrosion rates in the metric system should preferably be expressed as milligrams per square decimeter per day (mdd), and in the English system as inches penetration per year (ipy).

As regards algebraic signs of potentials, the standard electrode potential for $Zn \rightarrow Zn^{++} + 2e$ is negative; for $Cu \rightarrow Cu^{++} + 2e$, positive.

ABBREVIATIONS

Abbreviations should conform with the American Standards Association's list of "Abbreviations for Scientific and Engineering Terms."

GENERAL

Authors should be as brief as is consistent with clarity, and must omit all material which can be regarded as familiar to specialists in the particular field.

The use of proprietary names, trade-marks, and trade names should be avoided if possible. If used, these should be capitalized so that the owner's legal rights are not jeopardized.

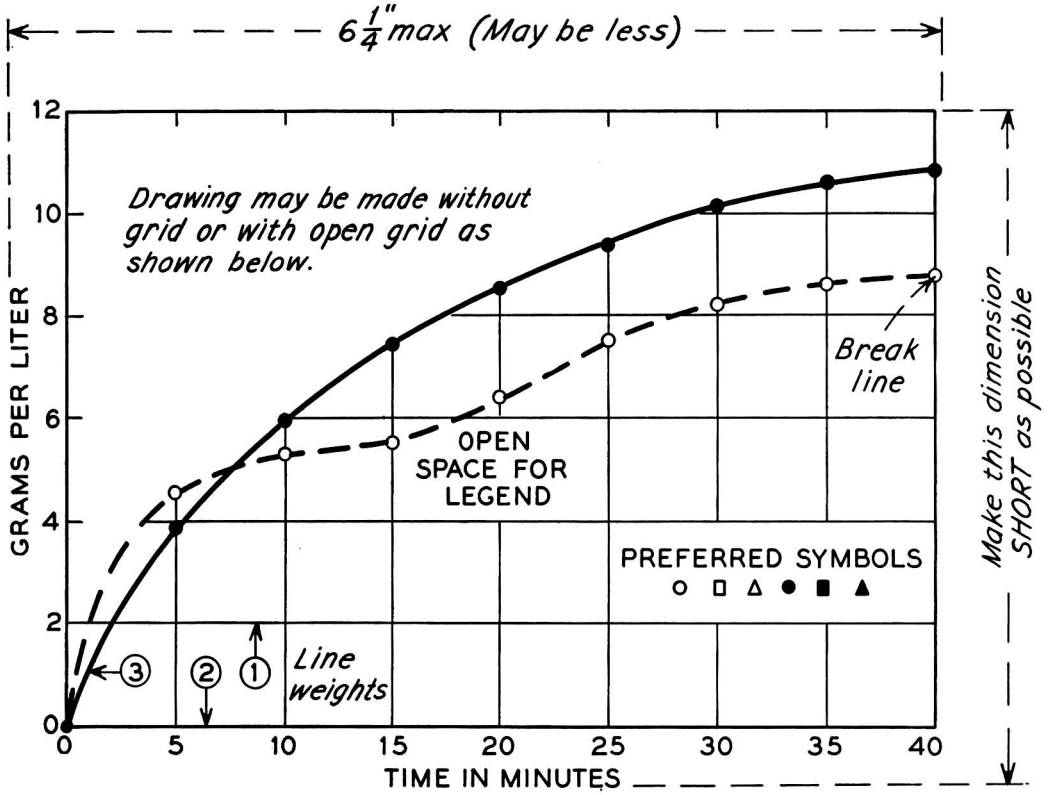

Remarks: Line weight ② is used for borders and zero lines. When several curves are shown, each may be numbered and described in the caption. Lettering is approx. 1/8".

SAMPLE CURVE DRAWING FOR REDUCTION TO $\frac{1}{2}$ SIZE

The Electrochemical Society

Patron Member

International Nickel Co., Inc., New York, N. Y.

Sustaining Members

Air Reduction Co., Inc., New York, N. Y.
Ajax Electro Metallurgical Corp., Philadelphia, Pa.
Allied Chemical & Dye Corp.
General Chemical Div., New York, N. Y.
Solvay Process Div., Syracuse, N. Y. (3 memberships)
Alloy Steel Products Co., Inc., Linden, N. J.
Aluminum Co. of America, New Kensington, Pa.
Aluminum Co. of Canada, Ltd., Montreal, Que., Canada
American Machine & Foundry Co., Raleigh, N. C.
American Platinum Works, Newark, N. J. (2 memberships)
American Potash & Chemical Corp., Los Angeles, Calif.
American Potash & Chemical Corp. (Nevada), Henderson, Nev.
American Zinc, Lead & Smelting Co., St. Louis, Mo.
Auto City Plating Co. Foundation, Detroit, Mich.
Bart Manufacturing Co., Bellville, N. J.
Bell Telephone Laboratories, Inc., New York, N. Y.
Bethlehem Steel Co., Bethlehem, Pa. (2 memberships)
Burgess Battery Co., Freeport, Ill. (4 memberships)
Canadian Industries (1954) Ltd., Montreal, Que., Canada
Carborundum Co., Niagara Falls, N. Y.
Chrysler Corp., Detroit, Mich.
Columbia-Southern Chemical Corp., Pittsburgh, Pa.
Consolidated Mining & Smelting Co. of Canada, Ltd., Trail, B. C., Canada (2 memberships)
Corning Glass Works, Corning, N. Y.
Crane Co., Chicago, Ill.
Diamond Alkali Co., Cleveland, Ohio (2 memberships)
Dow Chemical Co., Midland, Mich.
Wilbur B. Driver Co., Newark, N. J.
E. I. du Pont de Nemours & Co., Inc., Wilmington, Del.
Eagle-Picher Co., Joplin, Mo.
Eaton Manufacturing Co.
Stamping Div., Cleveland, Ohio
Electric Auto-Lite Co., Toledo, Ohio
Electric Storage Battery Co., Philadelphia, Pa.
The Eppley Laboratory, Newport, R. I.
Food Machinery & Chemical Corp.
Becco Chemical Div., Buffalo, N. Y.
Ford Motor Co., Dearborn, Mich.
General Electric Co., Schenectady, N. Y.
General Motors Corp.
Research Laboratories Div., Detroit, Mich.
Gould-National Batteries, Inc., Depew, N. Y.
Graham, Crowley & Associates, Inc., Chicago, Ill.
Great Lakes Carbon Corp., Niagara Falls, N. Y.
Hanson-Van Winkle-Munning Co., Matawan, N. J. (3 memberships)
Harshaw Chemical Co., Cleveland, Ohio (2 memberships)
Hercules Powder Co., Wilmington, Del.
Hooker Electrochemical Co., Niagara Falls, N. Y. (3 memberships)
Houdaille-Hershey Corp., Detroit, Mich.
Kaiser Aluminum & Chemical Corp.
Div. of Metallurgical Research, Spokane, Wash.
McGean Chemical Co., Cleveland, Ohio
Merck & Co., Inc., Rahway, N. J.
Metal & Thermit Corp., New York, N. Y.
Michelin Tire Manufacturing Co., Clermont-Ferrand, Puy-de-Dome, France
Monsanto Chemical Co., St. Louis, Mo.
National Cash Register Co., Dayton, Ohio
National Lead Co., New York, N. Y.
National Research Corp., Cambridge, Mass.
Norton Co., Worcester, Mass.
Olin Mathieson Chemical Corp., Niagara Falls, N. Y. (4 memberships)
Pennsylvania Salt Manufacturing Co., Philadelphia, Pa.
Philco Corp., Lansdale, Pa.
Philips Laboratories, Inc., Irvington-on-Hudson, N. Y.
Poor & Co.
Promat Div., Waukegan, Ill.
Potash Co. of America, Carlsbad, N. Mex.
Radio Corp. of America
RCA Victor Div., Harrison, N. J.
Ray-O-Vac Co., Madison, Wis.
Rockwell Spring & Axle Co.
Standard Steel Spring Div., Coraopolis, Pa.
Shawinigan Chemicals Ltd., Montreal, Que., Canada
Speer Carbon Co.
International Graphite & Electrode Div., St. Marys, Pa. (2 memberships)
Stackpole Carbon Co., St. Marys, Pa.
Stauffer Chemical Co., San Francisco, Calif.
Sylvania Electric Products Inc., Bayside, N. Y. (2 memberships)
Sarkes Tarzian, Inc., Bloomington, Ind.
Tennessee Products & Chemical Corp., Nashville, Tenn.
Udylite Corp., Detroit, Mich. (4 memberships)
Union Carbide & Carbon Corp.
Electro Metallurgical Co., New York, N. Y.
National Carbon Div., New York, N. Y. (2 memberships)
United Chromium, Inc., New York, N. Y.
Vanadium Corp., of America, New York, N. Y.
Victor Chemical Works, Chicago, Ill.
Wagner Brothers, Inc., Detroit, Mich.
Western Electric Co., Inc., Chicago, Ill.
Westinghouse Electric Corp., E. Pittsburgh, Pa.
Wyandotte Chemicals Corp., Wyandotte, Mich.
Yardney Electric Corp., New York, N. Y.

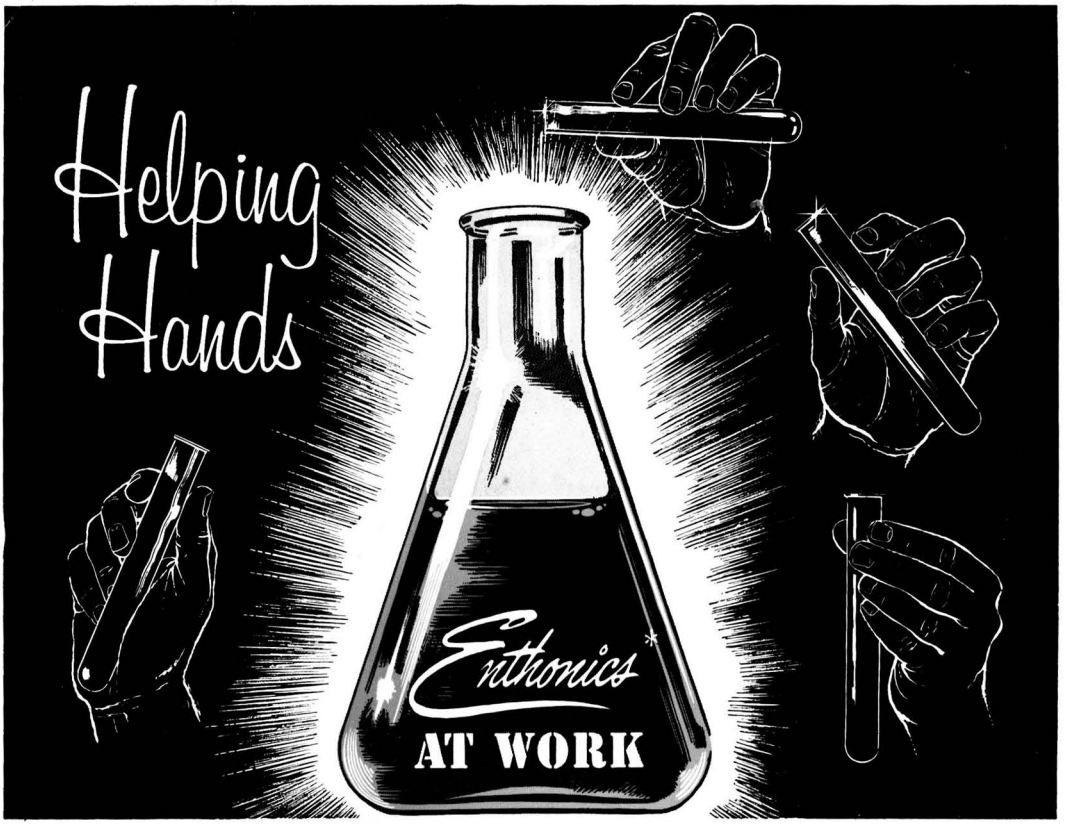

FROM THOUSANDS of TESTS . . .

. . . *come the solutions to your metal finishing problems.*

If *you* are looking for creative chemistry to supply new methods for the improvement of metal finishing, look to the leader – ENTHONE. Write for the answers to these problems, identifying them by number. If your specific problem is not listed, Enthone will gladly help to find the answer.

1. HOW TO BLACKEN copper, brass, zinc, steel and other metals to meet U.S. Government specifications.
2. HOW TO STRIP NICKEL from steel without etching the steel.
3. HOW TO STRIP NICKEL from copper and brass without attacking the part.
4. HOW TO SHED WATER from metals to prevent staining or spotting during drying.
5. HOW TO TRAP FUMES from hot sulfuric acid pickles.
6. HOW TO STRIP SYNTHETIC ENAMELS from aluminum and other metals without attacking the metal.
7. HOW TO CLEAN AND REMOVE RUST AND OXIDES from steel in one operation without acids.
8. HOW TO RINSE AND DRY STEEL WITHOUT RUSTING, using cold or hot water.
9. HOW TO SHORTEN ALKALI CLEANING TIME for steel to 15 seconds.
10. HOW TO REMOVE SOLID DIRT AND OIL from metals.
11. HOW TO STRIP LEAD, TIN or soft solder from copper and brass with no etching.
12. HOW TO PLATE METALS upon aluminum.
13. HOW TO REMOVE EXCESS SILVER SOLDER chemically from silver brazed steel parts.
14. HOW TO MAKE PAINT STICK to brass and zinc.
15. HOW TO SOLVENT-CLEAN parts and assemblies with cold non-hazardous solvent.
16. HOW TO OVERCOME CHROMIC ACID CONTAMINATION in cleaners.
17. HOW TO PREVENT STAINING of chromium plate.
18. HOW TO GIVE ZINC AND CADMIUM high salt spray resistance.
19. HOW TO COLOR ALUMINUM in one operation.
20. HOW TO STRIP METAL COATINGS from zinc die castings.

* *The Scientific Solution of Metal Finishing Problems.*

ENTHONE
INCORPORATED

442 ELM STREET, NEW HAVEN 11, CONNECTICUT

ELECTROPLATING CHEMICALS • METAL FINISHING PROCESSES

Service Representatives and Stock Points in Principal Cities of U.S.A. and Canada, Mexico, Brazil, England, France, Sweden and Germany.